ISSN: 2151-1950 (Print), 2151-1969 (Online) Vol. 2, No. 3, July 2010

Journal of Geographic Information System

www.scirp.org/journal/jgis

Journal Editorial Board

ISSN: 2151-1950 (Print) ISSN: 2151-1969 (Online)

http://www.scirp.org/journal/jgis

Journal of Geographic Information System(JGIS) is a comprehensive international journal published by Research Center for GIS Software and Application Engineering, Ministry of Education, Zondy Cyber and SRP(Scientific Research publishing).

Journal of Geographic Information System, **2010, 2, 129-184**
Published Online July 2010 in SciRes (http://www.SciRP.org/journal/jgis/)

TABLE OF CONTENTS

Volume 2 Number 3 July 2010

Journal of Geographic Information System

Journal Information

SUBSCRIPTIONS

The *Journal of Geographic Information System* (Online at Scientific Research Publishing, www.SciRP.org) is published quarterly by Scientific Research Publishing, Inc., USA.

Subscription rates:

Print: $50 per issue.
To subscribe, please contact Journals Subscriptions Department, E-mail: sub@scirp.org

SERVICES

Advertisements
Advertisement Sales Department, E-mail: service@scirp.org

Reprints (minimum quantity 100 copies)
Reprints Co-ordinator, Scientific Research Publishing, Inc., USA.
E-mail: sub@scirp.org

COPYRIGHT

PRODUCTION INFORMATION

For manuscripts that have been accepted for publication, please contact:
E-mail: jgis@scirp.org

Journal of Geographic Information System, **2010, 2, 129-146**
doi:10.4236/jgis.2010.23020 Published Online July 2010 (http://www.SciRP.org/journal/jgis)

An Information System for Risk-Vulnerability Assessment to Flood

Subhankar Karmakar[1], Slobodan P. Simonovic[2], Angela Peck[2], Jordan Black[2]
[1]*Centre for Environmental Science and Engineering, Indian Institute of Technology Bombay, Mumbai, India*
[2]*Department of Civil and Environmental Engineering, The University of Western Ontario, London, Canada*
E-mail: *skarmakar@iitb.ac.in, simonovic@uwo.ca*
Received May 18, 2010; *revised June* 20, 2010; *accepted June* 25, 2010

Abstract

An exhaustive knowledge of flood risk in different spatial locations is essential for developing an effective flood mitigation strategy for a watershed. In the present study, a risk-vulnerability analysis to flood is performed. Four components of vulnerability to flood: 1) physical, 2) economic, 3) infrastructure and 4) social; are evaluated individually using a Geographic Information System (GIS) environment. The proposed methodology estimates the impact on infrastructure vulnerability due to inundation of critical facilities, emergency service stations and bridges. The components of vulnerability are combined to determine an overall vulnerability to flood. The exposures of land use/land cover and soil type (permeability) to flood are also considered to include their effects on severity of flood. The values of probability of occurrence of flood, vulnerability to flood, and exposures of land use and soil type to flood are used to finally compute flood risk at different locations in a watershed. The proposed methodology is implemented for six major damage centers in the Upper Thames River watershed, located in the South-Western Ontario, Canada to assess the flood risk. An information system is developed for systematic presentation of the flood risk, probability of occurrence of flood, vulnerability to flood, and exposures of land use and soil type to flood by postal code regions or Forward Sortation Areas (FSAs). The flood information system is designed to provide support for different users, *i.e.*, general public, decision-makers and water management professionals. An interactive analysis tool is developed within the information system to assist in evaluation of the flood risk in response to a change in land use pattern.

Keywords: Flood Management, Flood Risk, Geographic Information System, Risk Management, Vulnerability Analysis, Information System

1. Introduction

Records of loss of life and damage caused by floods worldwide show that these have continued to rise steadily during recent years. Understandably, the response has been to call for increased efforts to protect life and property. The sustainable and effective management of floods demands a holistic approach—linking socio-economic development with the protection of natural ecosystems and appropriate management links between land and water uses. It is recognized that a watershed is a dynamic system in which there are many interactions between human population, land use and water bodies. Assessment and mapping of "flood risk" [1-7] and "vulnerability to flood", and dissemination of the appropriate information to different stakeholders is a very important part of the flood management process. The general public may use the information in purchasing a house, or in selecting a site to start a business. Knowledge of flood risk could aid decision-makers in: developing land development plans and land use zoning; planning emergency response strategies; waste disposal site selections; preparing infrastructure budgetary decisions; developing guidelines for operation of existing infrastructure; and general policy development at all levels. Water management professionals can utilize the flood risk information in planning, design, construction, and operation & maintenance of flood protection infrastructure (e.g., reservoirs, dikes, drainage pipes, etc). Flood risk mapping has been performed extensively for effective flood management, starting with the pioneering work of Garrett [8]. The risk of flooding to towns and villages along 200 km of the River Thames

and its tributaries are assessed using a mathematical model developed for Thames Water Rivers Division, UK. The River Thames Strategic Flood Defence Initiative examines the vulnerability of floodplain development along the river. The achievements of the Flood Risk Mapping Program, New Brunswick, Canada, are summarized by Burrell and Keefe [9]. The procedures used to produce flood risk maps are outlined very clearly along with an assessment of the accuracy achieved. Floyd [1] performs a flood risk assessment on the city of Bombay (Mumbai), India. The results provide an initial indication of the cost-effectiveness of different remedial measures. Morris and Flavin [10] present maps of England and Wales showing the built-up areas that would be at flood risk. Shrubsole [11] mentions government responsibilities in flood management of the Saguenay and Red River valley and provides alternative flood management strategies considering ecosystem management, partnerships and the role of science. Hall *et al*. [12] represents the processes of fluvial and coastal flooding over linear flood defence systems in sufficient detail to test alternative policy options for investment in flood management. Potential economic and social impacts of flooding are assessed using national databases of floodplain properties and demography. A case study of the river Parrett catchment and adjoining sea defences in Bridgwater Bay in England demonstrates the application of the method and presentation of results using Geographic Information System (GIS). Barredo *et al*. [13] aims to illustrate a framework for flood risk mapping at pan-European scale produced by the Weather-Driven Natural Hazards (WDNH). The threatening natural event is represented as the hazard component, and furthermore, exposure and vulnerability are considered as anthropogenic factors that contribute also to flood risk. The flood risk is considered on the light of exposure, vulnerability and hazard, and mathematically considered as product of hazard, exposure and vulnerability.

Vulnerability assessments have been undertaken to understand the "potential for loss", traditionally they focused on the nature of the hazard and who and what are exposed [14]. More recently, vulnerability assessments have explored the social, economic, and political conditions that are likely to affect the capacity of individuals or communities to cope with or adapt to hazards [15]. Bender [16] discusses the development and use of natural hazard vulnerability assessment techniques in the Americas. He emphasizes how and why a thorough vulnerability analysis is required for physical, economic and social planning in a watershed. There are numerous studies that have addressed contemporary vulnerability of different communities worldwide to flooding from the natural hazards perspective of understanding exposure and the number of people and structures affected [17,18] but few that explore the socio-economic aspects of flooding vulnerability [19-22]. Recently, the conceptualization on social vulnerability has gained prominence in the literature. It is related to characteristics that influence an individual's or group's ability or inability to anticipate, cope with, resist, and recover from or adapt to any external stress such as the impact of flooding [23-25]. Cutter *et al*. [26] present a method for assessing vulnerability in spatial terms using both biophysical and social indicators. Their results suggest that the most biophysically vulnerable places do not always spatially interact with the most vulnerable populations. Flax *et al*. [27] develop a risk-vulnerability assessment methodology named as Community Vulnerability Assessment Tool (CVAT), which assists emergency managers in their efforts to reduce vulnerabilities through hazard mitigation, comprehensive land use and development planning. Cutter *et al*. [28] list factors that have gained consensus among social scientists as contributing to social vulnerability to environmental hazards. Blong [29] introduces a new damage index for estimating the replacement cost of damaged buildings in vulnerability analysis. Carter [30] analyzes flood risk as a combination of threat, consequence, and vulnerability. He discusses the federal role in investment decisions for flood control infrastructure. Chakraborty *et al*. [31] develop two new quantitative indicators, *i.e*., a geophysical risk index, based on National Hurricane Center and National Flood Insurance Program data, and a social vulnerability index, based on census information. Rygel *et al*. [32] focus on constructing a social vulnerability index and its application to a case study of hurricane storm hazard. They demonstrate a method of aggregating vulnerability indices for different indicators using Pareto ranking that results in a composite index of vulnerability, which avoids the problems associated with assigning weights. Werritty *et al*. [33] discuss the social impacts of flood events in Scotland including attitude and behavior toward flooding events, warnings, evacuations and consequences. The study suggests ways for enhancing social resilience for sustainable flood management in Scotland.

GIS is considered as a key tool by many researchers [34-38] to map the spatial distribution of flood risk and vulnerability to flood. A GIS facilitates the input, storage, management, analysis, integration, and output of spatial data which can aid with real time decision making and strategic planning for effective risk management and hazard preparedness [39]. GIS can improve warning, evacuation, and emergency response systems by helping route emergency response vehicles and locating emergency response facilities [39-40]. Exposures of soil and geology to flood, urban infrastructure, and socioeconomic data, can be input and stored in a GIS and then analyzed to identify areas prone to flood, identify vulnerable populations, and forecast flood events, and aid in land use zoning decisions to improve flood mitigation and management [17,39].

The flood risk mapping and analysis on various flood prone watersheds have been performed by many researchers throughout the world. In a recent study on Romanian national strategy, Varga *et al*. [41] provide basic information for preliminary flood risk assessments and flood hazard mapping in all areas with a significant flood risk, according to the Flood Directive. The technical and scientific approach and the main steps in setting up the plan for flood prevention, protection and mitigation at the river basin level are presented. Apel *et al*. [7] perform flood risk analyses in Eilenburg, Germany, especially in urban areas and tested a number of combinations of models of different complexity both on the hazard (probability of occurrence) and on the vulnerability. Chang *et al*. [42] examine the anthropogenic and natural causes of flood risks in six representative cities in the Gangwon Province of Korea. Tran *et al*. [43] explore the impacts of floods on the economy, environment and society; and tries to clarify the rural community's coping mechanism to flood disasters in Central Viet Nam. They reveal that flooding is an essential element for a coastal population, whose livelihood depends on productive functions of cyclical floods. Forster *et al*. [44] assess flood risk for a rural detention area, alongside the Elbe River in Germany. They find that the losses in agricultural areas exhibit a strong seasonal pattern, and the flooding probability also has a seasonal variation. The flood risk is assessed for a planned detention area based on loss and probability estimation approaches of different time frames, namely a monthly and an annual approach.

The present research study is motivated by the Hotspots project [45,46] completed by the Center for Hazards and Risk Research (CHRR) at Columbia University and the World Bank's Disaster Management Facility [DMF), now the Hazard Management Unit (HMU). In the Hotspots project, the risk levels are estimated by combining hazard or probability of occurrence with historical vulnerability for two indicators of risk—population and Gross Domestic Product (GDP) per unit area—for six major natural hazards: earthquakes, volcanoes, landslides, floods, droughts, and cyclones. The relative risks for each grid cell, rather than country as a whole, is calculated at sub-national scales. Such information can inform a range of disaster prevention and preparedness measures, and development of long-term land-use plans and multi-hazard risk management strategies. Hotspots global analysis and case studies stimulate additional research, particularly at national and local levels. The present study develops an information system for risk-vulnerability analyses to flood and facilitates vulnerability mitigation by providing various flood information to different users. The information system is designed to provide selective access to information on the bases of user needs. This reduces the misuse of data and promotes data security. A set of suitable vulnerability indicators and the procedure for their integration into an overall vulnerability index with high spatial density represent the major analysis tool within the information system. The additional innovations of the information system include: 1) the computation of selected flood risk-vulnerability indicators organized into themes from four components of vulnerability to flood, *i.e.*, physical, economic, infrastructure, and social vulnerability [15], 2) the spatial infrastructure vulnerability analysis to flood due to inundation of main communication routes and road bridges, 3) the spatial flood impacts due to inundation of critical facilities (schools, hospitals, and fire stations) and 4) quantification of exposures of land use/land cover and soil permeability to flood. The postal codes or Forward Sortation Areas (FSA) are considered for spatial discretization of the region and flood risk evaluation. An interactive analysis tool is also developed for calculation of flood risk as a function of change in land use. The proposed information system is implemented to six major damage centers in the Upper Thames River watershed, located in the South-Western Ontario, Canada. The study focuses only on floods which are caused by the overflow of river banks that are characteristics for the region of interest.

As a prerequisite, some relevant technical definitions are provided in the next section. The third section contains a detailed description of the study area—the Upper Thames River basin in South-Western Ontario, Canada. The fourth, fifth and sixth sections provide the details on determination of probability of occurrence, vulnerability and exposures of land use and soil permeability to flood, respectively; and summarize the results obtained. The seventh section describes the features of developed information system for risk-vulnerability analyses to flood. The eighth section summarizes the conclusions from the study.

2. General Definitions

The most common approach to define "flood risk" is the definition of risk as the product of "hazard", *i.e.*, the physical and statistical aspects of the actual flooding (e.g., return period of the flood, extent and depth of inundation), and the "vulnerability", *i.e.*, the exposure of people and assets to floods and the susceptibility of the elements at risk to suffer from flood damage [7,47,48]. This definition is adopted in the Flood Directive [49]. According to Forster *et al*. [44], flood risk is a combination of potential damage and probability of flooding. More precisely, risk is considered as the product of hazard and vulnerability of a region [47]. However, in this study flood risk is the product of probability of occurrence (p_e), vulnerability to flood (V), and exposures of land use (E^{Land}) and soil permeability (E^{Soil}) to flood, following

the concept of Kron [50] and Barredo *et al*. [13], where flood risk is expressed as a function of the hazard, vulnerability and exposed values:

$$Flood\ Risk = (p_e) \times (V) \times (E^{Land}\ and\ E^{Soil}) \quad (1)$$

Hazard may be defined as a threatening event, or the "probability of occurrence (p_e)" of a potentially damaging phenomenon within a given time period and area [31, 47]. It frequently encompasses hydrological and hydraulic analyses and the mapping of flood lines on floodplain. Vulnerability to flood (V) is defined as a measure of a regions' or population susceptibility to flood damages [51-53]. Exposures of land use (E^{Land}) and soil permeability (E^{Soil}) to flood quantify their effect on the severity of flood. When the exposures of land use/land cover and soil permeability to flood are considered, these denote how land use and soil permeability affects the severity of flood. For example, urbanized land use pattern results in an impervious soil layer increasing the severity of flood and thus the exposure of land use pattern to flood in an urban area is high. The exposure of soil permeability to flood is also directly related to flood flow. The more permeable soil has more infiltration capacity and therefore reduces surface runoff, whereas less permeable soil has less infiltration capacity and is more prone to water logging [54].

In the present study, all the information on the above mentioned three components of flood risk are effectively presented and processed using GIS. The layout for collecting and integrating the data, along with the sequential procedural steps for data processing and representation are outlined in **Figure 1**. The vulnerability section in **Figure 1**, illustrates the concept of layering data using a GIS, as well as combining vulnerability components to assess the overall vulnerability to flood. The next section presents the detailed characteristics and geography of the study area.

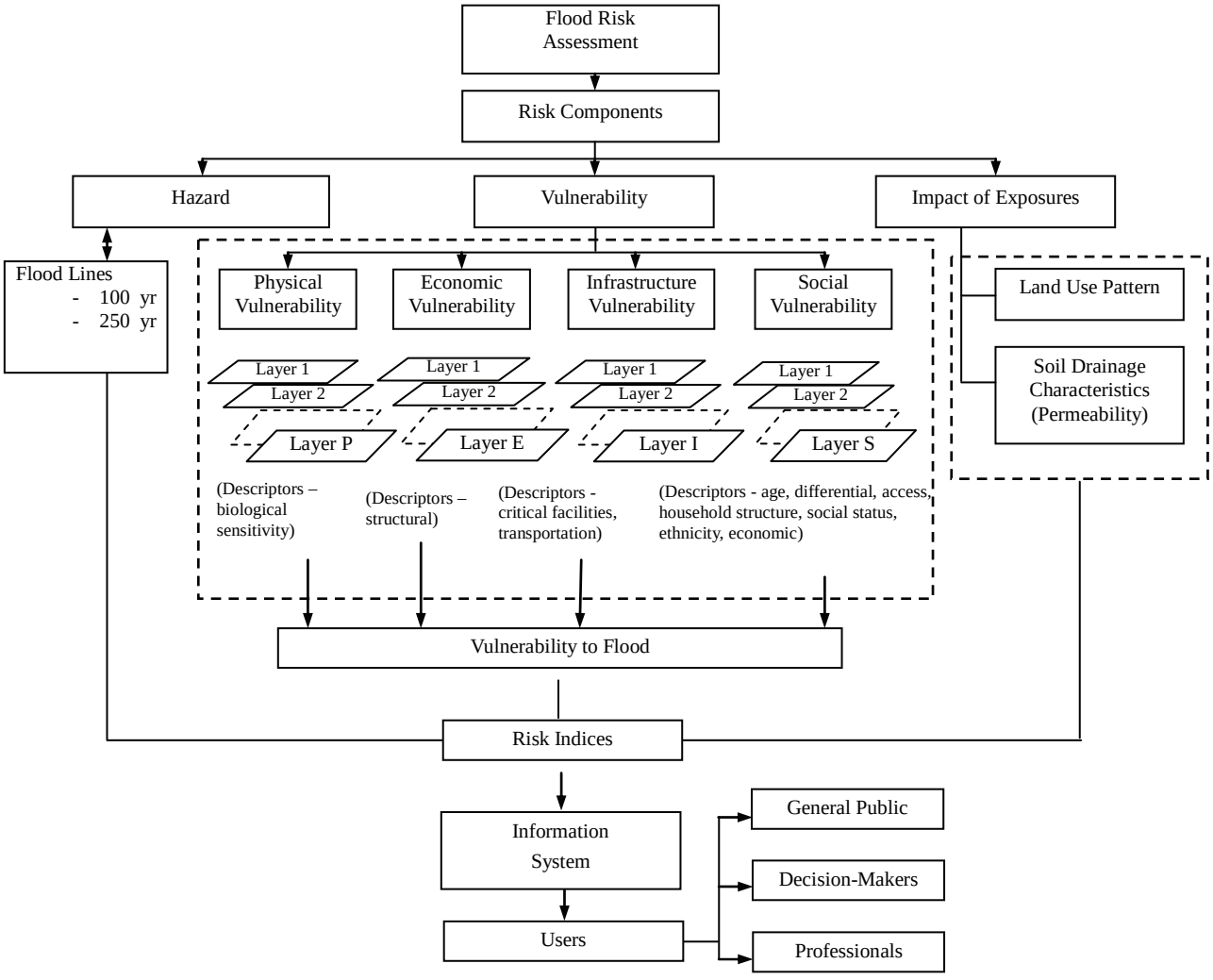

Figure 1. Organization of the flood information system.

3. Study Area

The Upper Thames river basin lies in the middle of south western Ontario; drains an area of 3,500 km^2; and is populated by approximately 422,000 people. The basin is nested between the Great Lakes Huron and Erie. The basin has a well documented history of flooding events dating back to the 1700s. A detailed map of the Upper Thames River watershed in Ontario, Canada with a location map (inset) is shown in **Figure 2**. Two main tributaries of the Thames River, referred to as the North (1,750 km^2) and South (1,360 km^2) branches, join at a location in London known as "The Forks" (**Figure 2**). The Forks region has served as a historical landmark for London, and is characterized by both commercial and residential structures. Major flood damage centers in the watershed include communities of London, St. Marys, Ingersoll, Mitchell, Stratford and Woodstock. The Upper Thames river basin is an area of special importance for the sustainable socio-economic development of Ontario. This is a large and fertile area, and plays an important role in agriculture production from, fishing and aquaculture to perennial fruit trees. The flooding in the Upper Thames river watershed has the great effect on the fertility of soil and increase in the natural aquatic production. It is also the most dangerous natural disaster hazard affecting the socio-economic development and the life of the people in the area. Several studies have already been done to estimate the economic damage in the watershed due to flooding [55].

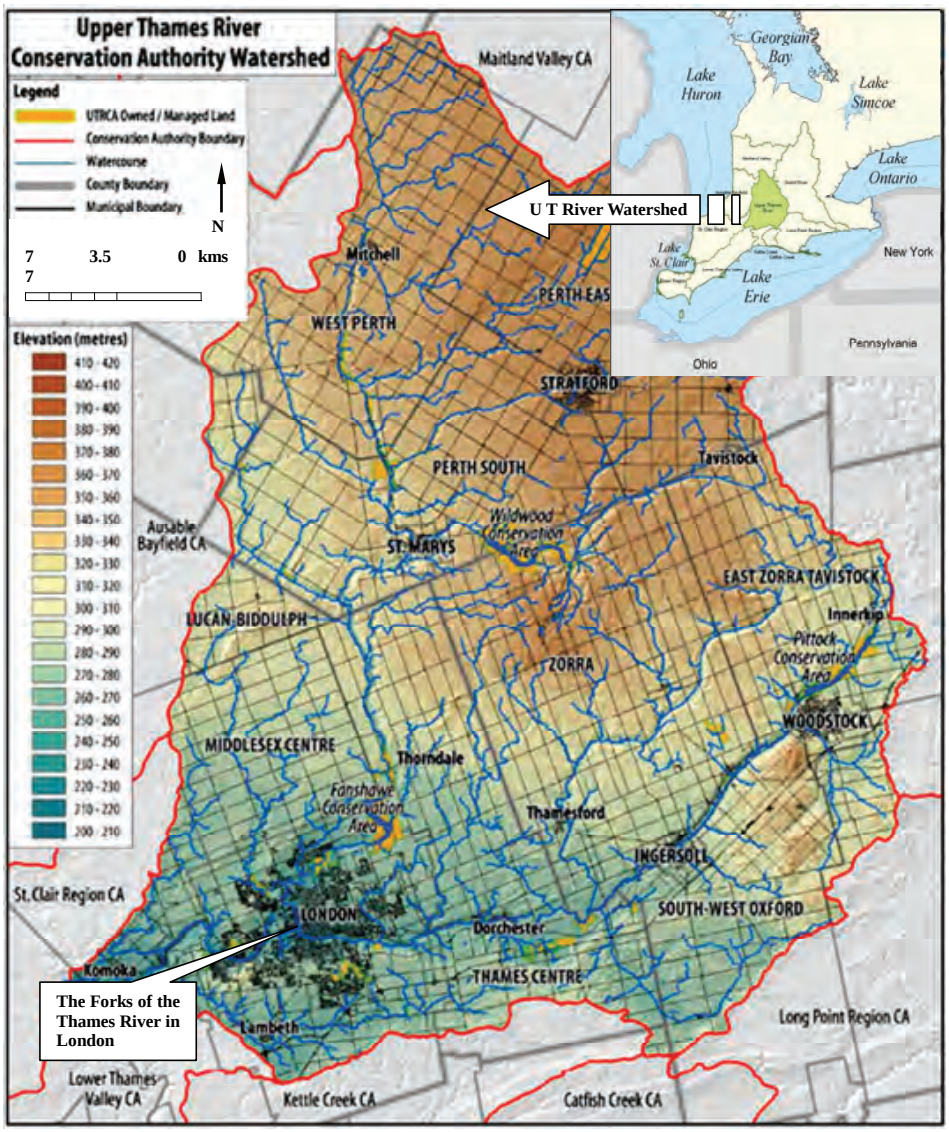

Figure 2. Detailed map and location map (inset) of the Upper Thames River watershed (Source: <http://www.thames-river.on.ca/About_Us/images/UTRCA_Watershed.jpg>).

The study area consists of a number of major postal code regions, some of which extend beyond the watershed bo- undaries. The Forward Sortation Areas (FSAs) are distinguished by the first three characters of their postal code designation. The regions which historically experience more frequent flooding events are selected as areas of particular significance and the FSAs of these regions are selected for analysis. A total of 25 FSAs from these cities have been considered in the study, and are listed in **Table 1**. These FSAs are the smallest spatial geographic units considered in this study. The cities of important FSAs include London (17 FSAs), Woodstock (3 FSAs), Mitchell (1 FSA), St. Marys (1 FSA), Ingersoll (1 FSA) and Stratford (2 FSAs); with a particular emphasis on the city of London. **Table 1** shows that the largest FSA by area in London is N6P; with an area of 103 km^2 and in the entire study area is N0K; with an area of 1510.0 km^2. The smallest FSA by area in London is N6B; with an area of 3.2 km^2, and in the entire study area is N4Z; with an area of 0.5 km^2. The average area of an FSA in London is 29.5 km^2 and the average area of all FSAs in the study area is 122.2 km^2.

Numerical data necessary for the development of a flood information system has been collected from Statistics Canada, which provides updated national statistics consistently every five years following a Census of the population. Data is available for areas of various sizes, including FSAs as small census divisions which remain relatively stable over many years. Various layers and datasets compatible with the GIS software are collected from Statistics Canada, The Ontario Fundamental Dataset, Upper Thames River Conservation Authority (UTRCA), Surficial Geology of Southern Ontario (SGSO) dataset, and Route Logistics (RL). These datasets are available online or obtained from the Serge A. Sawyer map library and the Internet Data Library System (IDLS) at the University of Western Ontario (UWO), London, Canada. **Table 2** presents the detailed information on different data layers with their formats and sources used in the present case study. All three components of the flood risk are assessed and represented in the information system separately in dissimilar ways. Each component is represented graphically, numerically, or using a combination of both. Next two sections describe the methodologies for determination of probability of occurrence and vulnerability to flood.

Table 1. List of the municipalities and FSAs (PSEPC* 2005).

Municipality	FSA	Area (in km^2)	Municipality	FSA	Area (in km^2)
London	N5V	46.7	London	N6L	38.0
	N5W	15.7		N6M	28.7
	N5X	27.0		N6N	70.0
	N5Y	10.0		N6P	103.0
	N5Z	11.0	Mitchell	N0K	1510.0
	N6A	7.1	Wood-Stock	N4S	326.0
	N6B	3.2		N4T	4.1
	N6C	13.5		N4V	2.1
	N6E	20.6	St. Marys	N4X	327.0
	N6G	25.8	Stratford	N4Z	0.5
	N6H	41.5		N5A	233.0
	N6J	12.0	Ingersoll	N5C	149.0
	N6K	28.4			

*Public Safety and Emergency Preparedness Canada.

Table 2. Information on data layers used in GIS.

Indicator	Source*	Layer	Type
Wetlands	OFD	wetlands_unit	Polygon
Roads	OFD	road	Line
Railways	OFD	transport_line	Line
Unpaved roads	OFD	road	Line
Intersections	RL	ren	Point
Critical facilities	OFD	building_symbol	Point
Bridges	RL	rll	Line
Land use	RL	ONland_use	Polygon
Soil permeability	SGSO	sgu_poly	Polygon
100-year flood line	UTRCA	--	Line
250-year flood line	UTRCA	--	Line
Grid	BM	obmindex	Polygon
FSAs	RL	zip	Polygon

*OFD—Ontario Fundamental Dataset (OGDE-Alymer_Guelph.mdb) from the Serge A. Sauer Map Library at UWO; RL—CanMaps Route Logistics, 2006 dataset from the UWO IDLS; SGSO—Surficial Geology of Southern Ontario, 2003 cd-rom dataset from Serge A. Sauer Map Library aUWO; UTRCA—the layers obtained from the Upper Thames River Conservation Authority in 2007; BM—Ontario Base Map Sheet, 2001 from the UWO IDLS.

4. Probability of Occurrence

Probability of occurrence of flood (p_e) [31] describes a physical threat from a flood occurring and a region becoming inundated. The consideration of probability of occurrence as a flood risk component is essential, since flood risk of a highly vulnerable population to flood is negligent if there is less probability or chance of occurrence of flood. The probability of occurrence (*i.e.*, the extreme events and associated probability) of flood is also termed as "flood hazard" by many researchers [7,13,47,50,56]. In the present study however, the available results on p_e performed by the UTRCA are used. Already available 100-year and 250-year flood lines are used for risk-vulnerability analysis.

The probability or likelihood of occurrence of flooding is described as the chance that a location will be flooded in any one year. For example, 1.3% chance of flooding each year implies 1 in 75 chance of flooding at that location in any year. Exceedance probability (p_e) of a flood is represented as [31,57]:

$$P[X \geq x] = p_e = 1 - F(x) \quad (2)$$

where $F(x)$ denotes the value of Cumulative Distribution Function (CDF) of river flow x. The return period (T_x) of flood flow x is the reciprocal of exceedance probability, which is mathematically represented as [57]:

$$T_x = 1/P[X \geq x] = 1/[1 - F(x)] \quad (3)$$

A flood line of a particular return period is the extreme boundary of the region exposed to a flood of the same return period. It represents the spatial extent of threat from the flood of a particular return period. The flood lines for a particular return period are evaluated by using physical, hydraulic and hydrologic characteristics of a particular location in the watershed. The present study utilizes 250-year flood line data for all FSAs being considered and 100-year flood line data for FSAs within the City of London, as per the availability. A flood hazard map with 100 and 250-years flood lines is used as one of risk components depicting spatial extent of flooding with exceedance probability of 0.01 and 0.004, respectively. The following procedural steps are followed in GIS for incorporating the information on probability of occurrence in this study: 1) the FSA, 100 and 250-years flood line shapefile layers are imported into ArcMap [58]; 2) the FSA layer and 100-yr flood line layers are turned "on" so that they are displayed in the Data Viewing window; 3) twenty five FSAs of interest in this study are highlighted using the selection tool and then converted into their own layer (FSA layer of interest); 4) these map features are then observed in the "layout" view where it is possible to insert map elements such as north arrows, legends and scale bars using the Insert Map Elements feature; 5) the map is then exported to ".jpeg" format. The same procedure is repeated for the 250-year flood line layer.

5. Vulnerability to Flood

Vulnerability to flood is defined as measure of a region's susceptibility to flood damage [51-53]. It also includes population susceptibility to physical, mental or emotional damage due to flooding. Vulnerability could be influenced by individual emotions, seriousness of the current situation, and previous experiences with natural disasters. Traditionally, vulnerability has considered only biophysical factors. More recently, social factors have also been incorporated into assessment of vulnerability to disasters [31].

In this study, vulnerability to flood has been defined as a combination of four distinctive types of vulnerabilities: physical, economic, infrastructure and social [15]. The *physical vulnerability* generally incorporates only those indicators susceptible to biological sensitivity. Wetlands are for example, considered regions of physical vulnerability in this study. Wetlands are among the most productive ecosystems on earth. The richness of these transitional ecosystems relates mostly to the diversity of ecological niches created by the variability of seasonal and interannual cycles. Modifications in the hydrologic regime that disturb these cycles have been found to be the main stress factor threatening shoreline wetlands in all the world's major rivers [59]. The regulation of water levels has also caused the shrinkage of wetlands, and an incidental reduction in the diversity of plant communities and the number of plant species [60]. These regions have high biodiversity and sensitive life, which would experience higher damages, longer, slower recovery times due to flooding. *Economic vulnerability* includes flood damage indicators which can be expressed in monetary terms. *Infrastructure vulnerability* includes civil structure such as road networks, railways, and road bridges. Infrastructure components are important to movement of population, communications, and safety. Their inundation impedes traffic and hinders communications, increasing stress in the exposed population. Inundation may also block important emergency routes and cause physical damage to roads. *Social vulnerability* focuses on the reaction, response, and resistance of a population to a disastrous event. Vulnerable population may require special attention in an evacuation situation for example. The indicators are chosen based on a review of existing literature assessing vulnerability to current hazards [25-27, 31,32,51].

The vulnerability index (VI_i) corresponding to each indicator for i^{th} FSA is calculated using the following equation, which standardizes [61] each vulnerability index value ranging from 0.0 to 1.0 as done by Wu *et al.* [51]:

$$VI_i = \frac{V_i - V^{\min}}{V^{\max} - V^{\min}} \quad (4)$$

where V^{min} and V^{max} are the minimum and maximum values of the indicator for all FSAs, respectively, and V_i is the actual value of the indicator for i^{th} FSA. All physical, economic, infrastructure (including the numbers of critical facilities and road bridges) and social vulnerability indices are directly calculated using (4). For example, vulnerability index for i^{th} FSA of the social vulnerability indicator "Population under 20yrs of age" is calculated from the data set of 25 values (for 25 FSAs) on population under 20yrs of age using (4). The GIS is not used for determination of economic and social vulnerability indices, as they are directly calculated in the spreadsheet using Statistics Canada Census data. The economic and so-

cial vulnerability maps are created in ArcMap on the basis of calculated values of vulnerability indices. The following procedure is followed for calculating the sum of the length of roadways/railways: 1) roads/railways layer is imported into GIS; 2) the length of each road/railway is contained in the attributes table; 3) those road/railway segments from the attribute table are selected which fall within and intersect a particular FSA; 4) the "statistics" option from the "length" field in the attribute table options is selected; 5) the program calculates the sum of lengths and display them in that particular FSA; 6) the values are stored in a table and finally 4) is used for determining the vulnerability indices—"length of roads" and "length of railways". The similar procedure is followed for the vulnerability index—"unpaved roads", but the unpaved, dirt and gravel roads are selected for each FSA individually using the "Select by Location" or "Select by Attributes" tool.

This calculation of vulnerability index using 4) [61] offers an improvement over the traditional calculation [26,31,51] of vulnerability index, *i.e.*, dividing all values by the maximum value, $VI_i = (V_i / V^{\max})$, as it considers both the maximum and minimum values and ensures that the vulnerability indices are within [0, 1] interval and always non-negative. It is not necessary to use the scale [0, 1] for standardization. Montz and Evans [25], Grosshans *et al*. [54] and Odeh *et al*. [62] standardize the values of vulnerability and plotted the maps considering [0, 10], [0, 5] and [0, 100] scales, respectively. In the assessment of infrastructure vulnerability, the present study considers: a) the impact of flooding of critical facilities (schools, hospitals, and fire stations) and b) the spatial impact of flooding of main communication routes and road bridges. The developed methodologies for considering these impacts are discussed in next two subsections. The main objectives of the analysis presented in these two subsections are: 1) to model the impact of inundation of critical facilities (e.g., schools, hospitals and fire stations) of an FSA on its total infrastructure vulnerability, which is achieved by considering the "number of critical facilities (*i.e.*, number of schools or hospitals within an FSA)" as vulnerability indicators [determined by using 4), as done for physical, economic, social and other infrastructure vulnerability indicators]; and 2) to model the impact of inundation of an FSA (which may contain one or more than one critical facilities) on its surrounding FSAs, which is modeled using a grid system. There are numerous studies that have addressed the impact of inundation of critical facilities on infrastructure vulnerability based on the number of critical facilities within an FSA [27,51,62], but none that explore the impact on surrounding FSAs, because people dwelling outside the flooded FSA also may depend on the critical facilities situated within the flooded FSA. This impact on infrastructure vulnerability of surrounding FSAs is modeled using a grid system.

5.1. Infrastructure Vulnerability Due to Inundation of Critical Facilities

Vulnerability of critical facilities is an indicator of infrastructure vulnerability [27,51,62]. Emergency shelters, nursing homes, public buildings, schools, hospitals, fire and rescue stations, police stations, water treatment or sewage processing plants, utilities, railroad stations, airports and government facilities are identified as critical facilities by Odeh *et al*. [62] and Flax *et al*. [27]. Critical facilities are those that play an integral role in public safety, health, and provision of aid [27]. As per the availability of data, the critical facilities considered in this study include schools, fire stations and hospitals, and are given special attention in vulnerability analysis in order to provide a more accurate estimate of flood risk.

Schools can be used for both education and as a place of refuge and a center for aid distribution during a flood. Fire stations provide the source of response to an emergency in the area near the station, and aid in disaster relief. Flooding of a fire station causes the population in close proximity to be more vulnerable. Hospitals represent another type of critical facilities that require special attention during flooding. Hospitals may have patients that need special attention in the case of an emergency. Procedure for assessment of infrastructure vulnerability due to inundation of critical facilities includes the use of a GIS tool. As per the availability of data, the FSAs of London are considered for the demonstration of the methodology. The impact of inundation of critical facilities of an FSA on its total infrastructure vulnerability is determined by considering the "number of critical facilities (*i.e.*, number of schools or hospitals within an FSA)" as vulnerability indicators [determined by using 4), as done for physical, economic, social and other infrastructure vulnerability indicators]. To model the impact of inundation of an FSA (which may contain one or more than one critical facilities) on its surrounding FSAs, a 6x6 grid layer is placed over the FSAs of London, which breaks the entire city into 36 cells, as illustrated in **Figure 3(a)**. The size of each grid cell is 25 km^2 (5 km × 5 km). The cell area for each FSA is calculated using area calculation function provided by the GIS tool. The layer containing the information on critical facilities is placed onto the grid layer and FSA layer to determine areas more susceptible to damage. The process used in assigning infrastructure vulnerability due to the inundation of critical facilities is based on the assumption that the people closest to the facility are its primary users. Thus, the spatial shape, termed as "vulnerability shape" in this study, is square as shown in **Figure 3(b)**. There are four different color designations (red, orange, yellow and white) representing assigned Degree of Importance (DI).

The presence of just one of these is sufficient to classify the cell as important. All "important" cells are equally important. The DI values indicating vulnerability levels decrease equally in all directions with the distance from the inundated cell. Procedure implemented using GIS tool is as follows:

1) Divide the area under consideration into a grid—the grid should be regular in shape. In this analysis, a 6 × 6 square grid is used for demonstration purpose.

2) Use the DI to quantify the importance of a critical facility for each FSA. Red, orange, yellow and white color codes correspond to 1.0, 0.75, 0.2 and 0.0 DI values, respectively. The colors are reflecting the DI of each cell: red (high), orange (medium), yellow (low), white (no influence), which indicates the importance of the presence of critical facilities. The grid cells within an FSA that contain one or more critical facilities are identified. These grid cells are assigned red color, the highest DI of 1, assuming that the people closest to the facility are its primary users.

3) Assign a white color, indicating "zero" DI value to the remaining grid cells. The result is a square-shaped representation of vulnerability, which decreases with distance from the red (center) cell.

4) Following the previous three steps, assign DI values for all grid cells separately for each case of a grid cell with red color. For example, if 10 (ten) grid cells contain critical facilities, the grids cells would be assigned appropriate DI values 10 times. Finally, the Overall DI (ODI) for a grid cell is calculated by averaging these ten DI values.

5) The vulnerability for an FSA—area shown in bold solid line in **Figure 3(c)** —is calculated as:

$$Vul_{e_i} \text{ of i}^{\text{th}} \text{ FSA} = \sum_{j=1}^{k} (ODI_k \times A_k) \Big/ \sum_{j=1}^{k} A_k \qquad (5)$$

where ODI_k is overall DI for kth grid cell, A_k is the area of ith FSA.

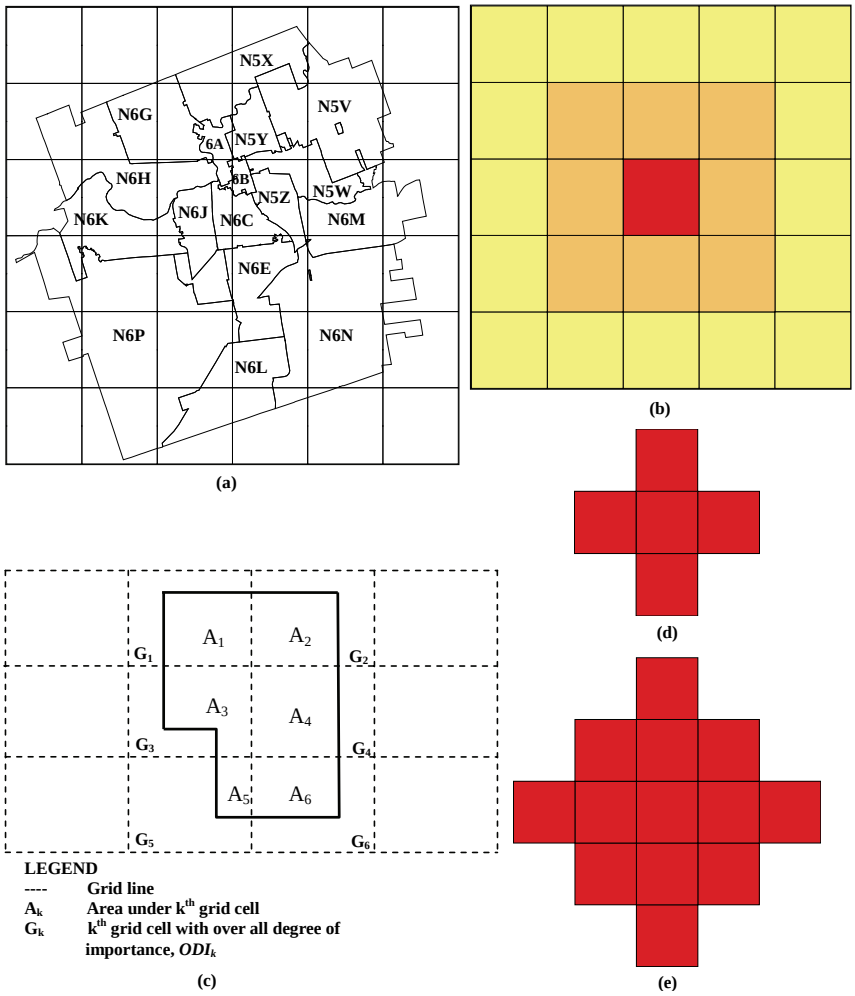

Figure 3. Determination of the vulnerability due to inundation of critical facilities and bridges. (a) 6 × 6-grid layered over the FSAs of London; (b) square vulnerability shape; (c) example FSA region divided in grid cells; (d) vulnerability shapes for cells with 1-5 bridges; (e) with 6-10 bridges (not to scale).

6) Determine the standardized vulnerability index value using:

$$Vul_{e_i}^{std} = \frac{Vul_{e_i} - Vul_e^{\min}}{Vul_e^{\max} - Vul_e^{\min}} \quad (6)$$

where Vul_e^{max} and Vul_e^{min} are the maximum and minimum vulnerability values of critical facilities, Vul_{e_i} is the value of vulnerability for critical facilities pertaining to the i[th] FSA. Thus the standardized infrastructure vulnerability values are obtained at FSA level.

5.2. Infrastructure Vulnerability Due to Inundation of Road Bridges

The infrastructure vulnerability is also affected by the inundation of road bridges. Vulnerability of an area due to the inundation of a bridge includes the interruption of traffic and formation of communication barriers between different locations in the affected region. Inundation of, or damage to a particular bridge affects not only the FSA in which it is located, but also all other FSAs that depend on the use of the bridge. In this study, only bridges over the water bodies are considered significant, because these bridges have limited alternate routes associated with them, and are necessary for safe crossing of the water body. They are frequently used as means for transporting commercial goods, a route to and from the workplace, and as emergency routes in case of a disaster.

The impact of inundation of road bridges of an FSA on its total infrastructure vulnerability is modeled by considering the "number of road bridges" as vulnerability indicator [determined by using 4), as done for physical, economic, social and other infrastructure vulnerability indicators]. To model the impact of inundation of an FSA (which may contain one or more than one road bridges) on its surrounding FSAs, the same procedure (steps 1 through 6) as described in previous subsection is followed, with the use of the new vulnerability shapes as shown in **Figures 3(d)** and **(e)**. Again, 6 × 6 grid is used in the assessment of vulnerability as shown in **Figure 3(a)**. However, the shape used in assessing vulnerability due to the inundation of road bridges is not a box, but rather cross-like. The shape varies with the number of bridges in any particular grid cell. **Figures 3(d)** and **(e)** illustrate the shapes of vulnerability for cells containing 1-5 and 6-10 road bridges, respectively. The number of bridges over water that is contained in each cell determines the shape that would be used in assessment of vulnerability. As the number of bridges increases, the more likely it is that inundation of that cell would affect more people. The vulnerability shape due to inundation of bridges is mainly based on a basic assumption: the need for crossing any given bridge decreases with distance from the bridge (*i.e.*, the need for crossing the bridge is highest in areas that are closest to the bridge), because people further away from a particular bridge may have other alternatives for crossing the water body with equal convenience. The proposed method assumes that the whole cell being considered is flooded, and that bridges in that cell are unavailable for use. The cells are assigned a DI based on the vulnerability mapping in proximity to the inundated cell. The DI assignment is similar to the one used in assessing the infrastructure vulnerability due to inundation of critical facilities. However, the road bridges scenario designates a DI as either red/high (1.0) or yellow/low (0.2) for demonstration of the proposed methodology. In both analyses it was assumed that the whole grid cell is equally affected by the flooding, thus damage is assumed to be uniform across the cell area. The population density within a portion of the FSA covered by a grid cell is not known. Therefore a uniform distribution of population is assumed throughout each FSA.

The following procedural steps are followed in GIS for incorporating the information on infrastructure vulnerability due to inundation of critical facilities: 1) the "buildings" layer is imported; 2) in the attribute table the type of building is specified. In the options for the attribute table "select by attribute" is used and then the category (e.g., school/hospital/fire station) is used to select only those buildings which are schools/hospitals/fire stations; 3) these buildings are saved as a separate layer for referencing in the critical facilities analysis of the study. The same procedure is followed for road bridges but the "bridge" layer is imported.

The calculation of the vulnerability indices following the procedures described in this section provides input for mapping each category of vulnerability in GIS. **Table 3** shows the values of four components of vulnerability in the Upper Thames River basin. The seventh column of **Table 3** indicates the standardized average vulnerability values of four vulnerability components (presented in columns 3-6) for all FSAs. In physical vulnerability, the FSA-N0K in Michell is identified as the most vulnerable due to large wetland areas in the region. The FSAs with "zero" values in the column of physical vulnerability indicate absence of wetlands. The FSA–N4S in Woodstock is the most vulnerable in economic sense due to the presence of large number of older houses in this region. The FSA–N0K in Michell is also identified as the most vulnerable in regards to infrastructure component due to its largest land area, which includes the longest road and railway networks. It is also identified that the FSA–N4Z in Stratford is the least vulnerable due to the absence of railway and minimum length of paved and unpaved roads. The column for social vulnerability shows high values for most of the FSAs within the city of London due to high population in these FSAs. The FSA–N5Y is the most vulnerable in social sense due to high values of indicators such as "differential access to resources", "so-

cial status" and "ethnicity".

The present study incorporates a unique consideration of inundation of road bridges and critical facilities in assessing infrastructure vulnerability.

Figure 4 displays the difference in infrastructure vulnerability due to inundation of critical facilities and road bridges. In most cases, the standardized values of infrastructure vulnerability of the FSA increase with the addition of impacts due to the inundation of road bridges and critical facilities. The GIS generated map may be produced for each component of vulnerability values as presented in **Table 3** for identifying spatial variability of vulnerabilities to flood. More details of the processed numerical data and graphical results of the present vulnerability analysis to flood can be obtained from Peck *et al.* [63].

5.3. Calculation of the Vulnerability to Flood

Although maps of individual component of vulnerability can be useful, it is easiest to assess vulnerability throughout the watershed if the multidimensional components can be integrated into a single measure [32]. In the present study, the simplest way to combine the four components of vulnerability into a single measure would be to average the values of indices [31,51] for each component [as given in the seventh column of **Table 3**]. **Figure 5** shows the GIS generated map of vulnerability to flood obtained by averaging and standardizing the four components of vulnerability. The darker color indicates larger vulnerability. Map in **Figure 5** provides for easy comparison of vulnerability between different FSA regions of six major damage centers, and insight into the spatial

Table 3. Vulnerability analysis to flood of the Upper Thames River basin.

Damage Center	FSA	Components of Vulnerability to Flood				Overall vul*	Rank
		Phy.	*Eco.*	*Infras.*	*Soc.*		
London	N6A	0.000	0.264	0.432	0.383	0.296	15
	N6B	0.000	0.282	0.467	0.399	0.316	12
	N6C	0.014	0.613	0.477	0.794	0.498	6
	N6E	0.000	0.128	0.256	0.767	0.303	13
	N6G	0.000	0.495	0.556	0.703	0.471	9
	N6H	0.015	0.828	0.356	0.784	0.503	5
	N6J	0.000	0.876	0.447	0.732	0.296	14
	N6K	0.004	0.457	0.299	0.613	0.527	4
	N6L	0.000	0.000	0.022	0.000	0.353	11
	N6M	0.009	0.234	0.172	0.012	0.000	25
	N6N	0.044	0.004	0.055	0.020	0.110	19
	N6P	0.005	0.084	0.089	0.072	0.032	22
	N5V	0.002	0.815	0.305	0.813	0.061	20
	N5W	0.000	0.515	0.421	0.608	0.486	8
	N5X	0.034	0.288	0.293	0.390	0.405	10
	N5Y	0.001	0.707	0.461	1.000	0.268	16
	N5Z	0.005	0.539	0.502	0.736	0.562	3
Michell	N0K	1.000	0.749	1.000	0.632	1.000	1
Wood-stock	N4S	0.000	1.000	0.510	0.715	0.572	2
	N4T	0.000	0.110	0.011	0.082	0.041	21
	N4V	0.004	0.027	0.008	0.030	0.010	23
St. Marys	N4X	0.002	0.266	0.299	0.181	0.200	18
Stratford	N4Z	0.000	0.048	0.000	0.021	0.009	24
	N5A	0.134	0.673	0.384	0.690	0.494	7
Ingersoll	N5C	0.092	0.293	0.275	0.261	0.249	17

*Overall vulnerability: standardized average values

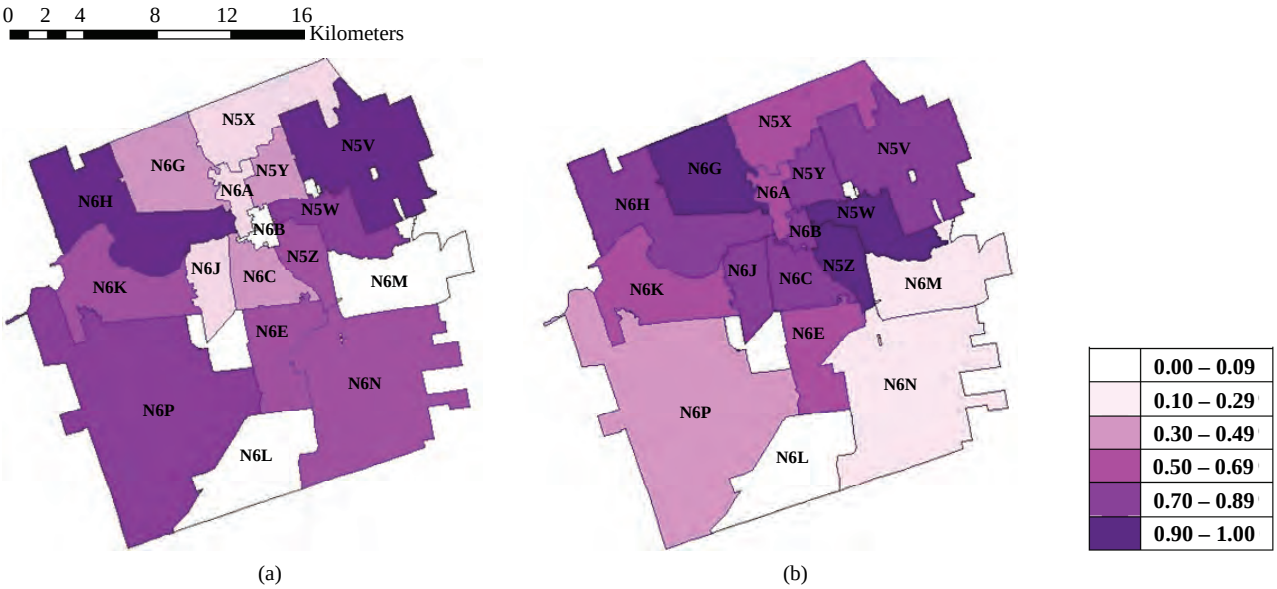

(a) (b)

Figure 4. Infrastructure vulnerability for the FSAs of London. (a) infrastructure vulnerability not considering the impact of critical facilities and bridges; (b) infrastructure vulnerability including the critical facilities and bridges.

variability of vulnerability. It is identified from **Table 3** and **Figure 5** that FSA–N0K in Michell is the most vulnerable in the basin, as the area under this postal code is much larger than other FSAs and consequently it contains a number of wetlands and more infrastructure. It is found that the vulnerability values for FSAs in London vary between 0 and 0.562. The FSA–N5Z is identified as the most vulnerable, whereas N6M is identified as the least vulnerable within the city of London. The **Table 3** and **Figure 5** give a general description of region's vulnerability, and can be used for emergency flood management, disaster mitigation activities and planning future disaster protection infrastructure.

It should be noted for clarification that, there may be some correlation among vulnerability indicators under different components of vulnerability. In this study the chance of involving correlated indicators is very less, as the indicators are chosen based on a review of existing literature [25-27,31,32,51]. If the number of indicators is too high Principal Components Analysis (PCA) [32] can be applied to select the set of uncorrelated indicators. The basic aim of a PCA is to reduce a complex set of many correlated variables into a set of fewer, uncorrelated components.

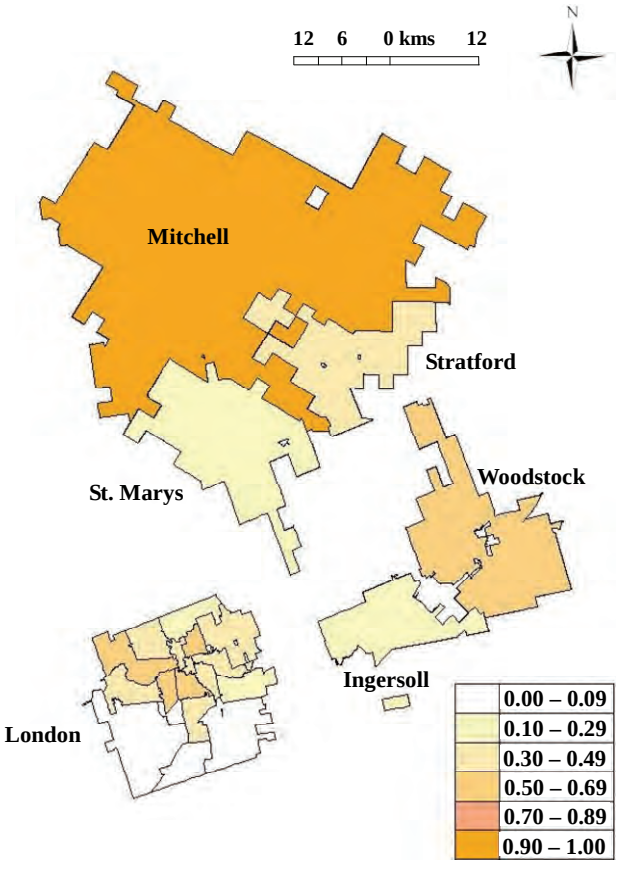

Figure 5. GIS generated map of standardized average vulnerability to flood.

6. Exposures of Land Use and Soil Permeability to Flood

The present study utilizes 250-year flood line data for all FSAs and 100-year flood line data for FSAs within the City of London, as obtained from UTRCA, Canada, for considering the values of probability of occurrence in the calculation of flood risk. The impacts of land use and soil type are not considered during generation of the flood lines and probability of occurrences. To incorporate the impact of exposures of land use and soil permeability into the analysis a separate component of the flood risk is considered as expressed in (1), following Kron [50] and Barredo *et al*. [13]. The indices of vulnerability to flood, as discussed in previous section, have no influence on flood flow and river channel characteristics. The exposures of land use and soil permeability are two physical watershed characteristics which affect the flood flow [64], and are considered as the important characteristics of flood risk in the Upper Thames River watershed. This study considers the impact of exposures of land use and soil permeability only for those FSAs within the municipality of London as per the availability of data. An exposure value of 1 is assigned to the regions outside of the City of London.

6.1. Land Use

The land use map used in the present study is obtained from the UWO Internet Data Library System (IDLS). Their CanMap Route Logistics 2006 dataset contains the Ontario land use GIS layer. This layer is designated as "ONland_use" and is of type "polygon" as mentioned in **Table 2**. The available land use data include seven different categories of use: open space, commercial, residential, parks and recreational, government and institutional, resource and industrial, and water body. Each of these land use categories has been assigned a DI value. These values, while estimated by the research team, can be changed by decision-makers with more extensive knowledge on how different land use influences flood runoff characteristics. Overdeveloped and highly commercialized areas include more pavement and impervious surfaces. They increase runoff quantity and shorten the time of concentration. On the other side, open land (including agricultural land) is exposed to direct infiltration of rainfall which decreases runoff quantity and lengthens the time of concentration. With this knowledge, the DI values are assigned to each category of land use, which are as follows: water body (0.1), parks & recreational (0.2), open area (0.3), Government and institutional (0.7), commercial (0.8), residential (0.8), resources & industrial (0.8).

Area under each land use type is expressed as a fraction of the FSAs total area. Summation of the fraction of

each type multiplied by its DI provides an exposure value representative of the land use for an FSA. Therefore, mathematically the exposures of land use to flood for i[th] FSA is expressed as:

$$E_i^{Land} = \sum_{l=1}^{n} [DI_l \times (A_i^l / A_i)] \quad (7)$$

where E_i^{Land} is the exposure of land use to flood, DI_l is the DI of land use type "l". "l" may be any of the land use types. Area under each land use type l is expressed as A_i^l for i[th] FSA. Total area of the i[th] FSA is denoted as A_i.

6.2. Soil Permeability

Soil permeability refers to the hydrological drainage characteristic of soil to allow water movement through its pores, which is inversely proportional to soil density. The more permeable the soil is, the more water can be transmitted through it. A soil with low permeability, such as clay, doesn't permit much water flow. This could cause "puddling" of water and thus higher accumulation of water on the soil surface. Regions which are composed primarily of these types of soils are prone to a higher flood risk because the water requires a longer time to drain or infiltrate into the ground [54]. Using a GIS dataset known as Surficial Geology of Southern Ontario, it was possible to spatially assess the soil permeability characteristics of the region. The data is available with different designations of permeability: low, medium-low, high or variable. A DI is assigned to each permeability category based on the ability of soil to infiltrate water, facilitate its transmission, and decrease flooding. DI values assigned to each category of soil permeability are as follows: low (0.8), low-medium (0.6), variable (0.5), high (0.3).

Area under each permeability category is expressed as a fraction of the FSAs total area. Summation of the fraction of each category multiplied by its DI provides an exposure value representative of soil permeability for an FSA. Therefore, mathematically the exposure of soil permeability to flood for i[th] FSA is expressed as:

$$E_i^{Soil} = \sum_{p=1}^{m} [DI_p \times (A_i^p / A_i)] \quad (8)$$

where E_i^{Soil} is the exposure of soil permeability to flood, DI_P is the DI of permeability category "p". "p" may be low, medium-low, variable and high. Area under each permeability category (p) is expressed as A_i^p for i[th] FSA. Total area of the i[th] FSA is denoted as A_i. The standardization is being performed following the equation similar to (4) and (6), expressed as:

$$E_i^{std} = \frac{E_i - E^{\min}}{E^{\max} - E^{\min}} \quad (9)$$

where E^{max} and E^{min} are the maximum and minimum exposure values pertaining to land use/soil permeability, E_i is the value of exposure of land use/soil permeability pertaining to the i[th] FSA. The following procedural steps are followed in GIS for incorporating the information on exposures of soil permeability and land use to flood: 1) the Ontario Surficial Geology dataset for Zone 17 in Ontario is imported into ArcMap; 2) the layer features are symbolized by categorical attributes; 3) to symbolize each soil type with its own colour, the Layer Properties dialogue box is opened, "Symbology" and "Categories" tabs are selected from the left menu, and "unique values" is highlighted; 4) in the Value Field, "SINGLE_PRI" is selected, which represents the single primary material of the soil composition. A colour scheme is selected and then each soil is represented by its own colour in the ArcMap data viewer; 5) the "Select by Location" tool of GIS is used to isolate those soils which fall within a particular FSA; 6) an area calculation is then performed on these "soils of interest" which provides the area of each soil type and the FSA boundaries that the soil area is within. An additional field is entered into the layers attribute table; the name of the field (column) and its type (floating point, integer etc.) are specified. All values are initialized to 0. The calculator option is then selected to compute the areas of the selected attributes. An advanced Visual Basics Application (VBA) area statement is used to calculate the required areas; 7) the type of each soil can be found in the layers attribute table along with the soils characteristic permeability which varied from "low" to "high"; 8) the results are summarized in a table. A similar procedure is followed for land use, but "category" is symbolized by: Commercial, Government & Institutional, Open area, Parks and Recreational, Residential, Resource and Industrial, and Water body. The impacts of exposures of land use and soil permeability to flood for FSAs of London are tabulated in **Table 4**. All

Table 4. Impact of exposures of land use and soil permeability to flood.

FSA	Impact of Exposures (standardized value)	
	Based on land use	*Based on soil permeability*
N6A	0.7362	0.2139
N6B	1.0000	0.0000
N6C	0.7562	0.9403
N6E	0.4311	0.9497
N6G	0.3954	0.5836
N6H	0.2481	0.5144
N6J	0.7067	0.8668
N6K	0.3339	0.4643
N6L	0.0000	1.0000
N6M	0.0386	0.7239
N6N	0.0125	0.9149
N6P	0.0122	0.7982
N5V	0.3049	0.3906
N5W	0.7427	0.1372
N5X	0.2357	0.3267
N5Y	0.8250	0.2760
N5Z	0.7938	0.4290

the values are standardized with in [0, 1] to produce an indicator scores. **Table 4** indicates that the exposure of land use for FSA-N6B, which is located in the central part of London, has maximum impact to flood due to presence of more commercial, residential and industrial areas; whereas the exposure of soil permeability has minimum impact to flood, as N6B has high permeable soil with high drainage capacity. The table also indicates that the exposure of land use for FSA-N6L, which is located in the southern part of London, has minimum impact to flood due to presence of more open and recreational areas; whereas the exposure of soil permeability has more impact to flood, as N6L has low permeable soil with less drainage capacity.

7. Development of the Information System

Providing a website for people to access flood risk information is an effective way of informing the public about the susceptibility to flooding that they may otherwise not be aware of. The study of Barredo *et al*. [13] is a contribution to the discussion about the need for communication tools between the natural hazard scientific com- munity and the political & decision making players in this field. The website can serve as an information center and may provide analysis tools for interactive processing of available flood information. It also provides the opportunity to tailor the presentation of the same information to different types of users according to their needs. According to the program evaluation glossary of USEPA [65], an information system is an organized collection, storage, and presentation system of data and other knowledge for decision making, progress reporting, and for planning and evaluation of programs. It can be either manual or computerized, or a combination of both. The information from the present risk-vulnerability analysis to flood is systematically kept in a computerized information system for more efficient use. The Adobe Dreamweaver Creative Sweet 3 software (http://www.adobe.com/ap/products/dreamweaver) is used for creating the flood information system. The whole website is based off the Cascading Style Sheets (CSS) template provided in Adobe CS3. The developed information system is easy to navigate. The process starts by providing access to different FSAs of 6 damage centers in the Upper Thames watershed. After selecting the damage center, typing in the first three digits of an FSA will direct the user to information about that FSA. Selected three digits of the FSA activate the search engine that is created using a search engine composer. Information page is available for every FSA region. The information that is displayed for all the users; includes maps, numerical data, and an analysis tool in Microsoft excel spreadsheet format for calculation of flood risk as a function of change in land use. After typing the first three digits of an FSA in an identified cell of the spreadsheet, the user will be directed to the information on flood risk of the FSA, considering the present land use pattern and area under different categories of land use. Area under each land use type can be changed by the user to find out the flood risk under future scenario of land use pattern. It will calculate risk by using (1).

The prototype information system created for this risk-vulnerability analysis to flood targets 3 different user categories: 1) general public, 2) decision-makers and 3) water management professionals. The general public has access to a simple explanation of flood risk terminology, tables providing values of vulnerability to flood and a description of what they mean, 100-year and 250-year flood lines, as well as a simple analysis tool for flood risk calculation. Decision-makers are provided with a more detailed description of flood risk terminology and the implications of flooding. They have access to the same flood hazard maps as the general public. Decision-makers are provided with a more detailed and flexible analysis tool which allows the user to change the land use and compare the present level of flood risk with the one obtained under changed land use scenario. This may assist in the analyses of different land development initiatives and their consequences on flood risk. Water management professionals are presented with the most detailed descriptions and the most technical flood related information. They are provided a very detailed numerical breakdown of vulnerability and exposures of land use and soil permeability, including a list of all indicators used in the analyses. They also have access to the flood hazard maps similar to those provided to the general public and the decision-makers. The analysis tool available to professionals is the same as one provided to the decision-makers. The professionals are the only user with access to a "raw data" containing all of the numerical data used for the flood risk analyses. Screenshots of the opening page of prototype information system and analysis tool are shown in **Figures 6(a)** and **(b)**. The information system is user-friendly and the details can be found in Black *et al.* [66].

8. Conclusions

The present study analyzes flood risk and vulnerability to flood in the Upper Thames River basin, Ontario, Canada. It deals with a large region as a case study with six major damage centers in the watershed for flood risk mapping considering probability of occurrence, four components of vulnerability and exposures of land use and soil permeability to flood. The impact of inundation of critical facilities and road bridges on infrastructure vulnerability is analyzed. New indices are introduced in the infrastructure vulnerability to flood, for example—length of railway, length of road, number of major intersections,

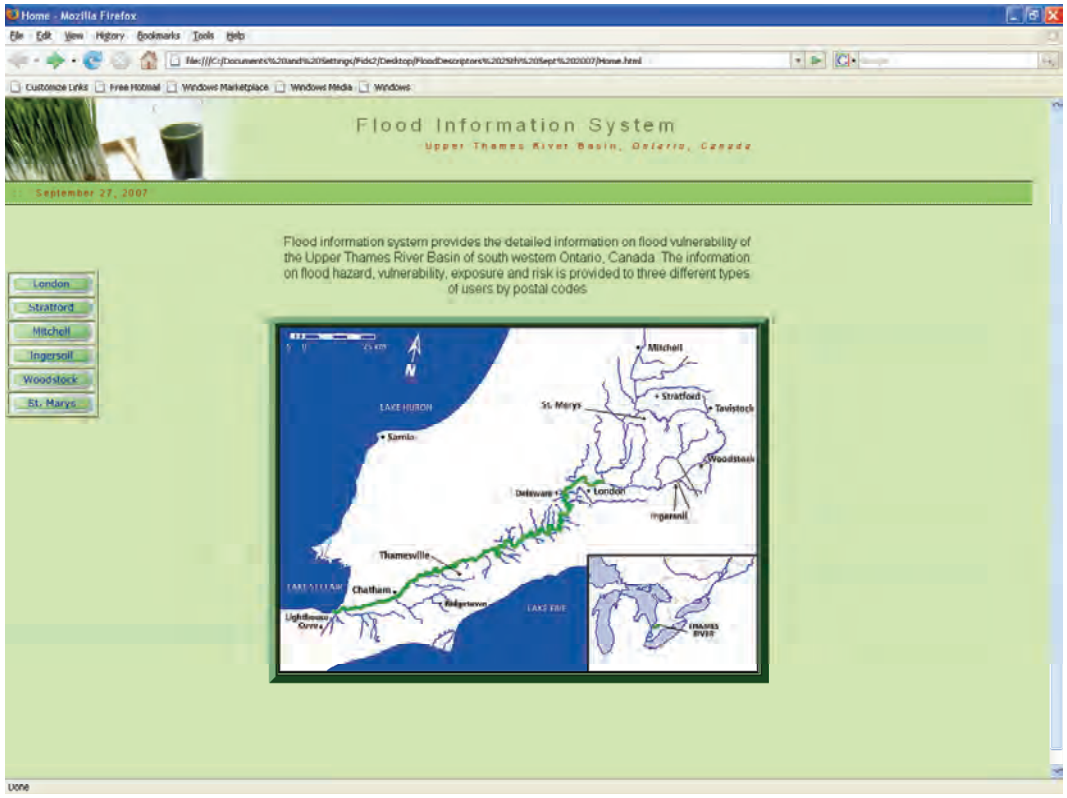

(a)

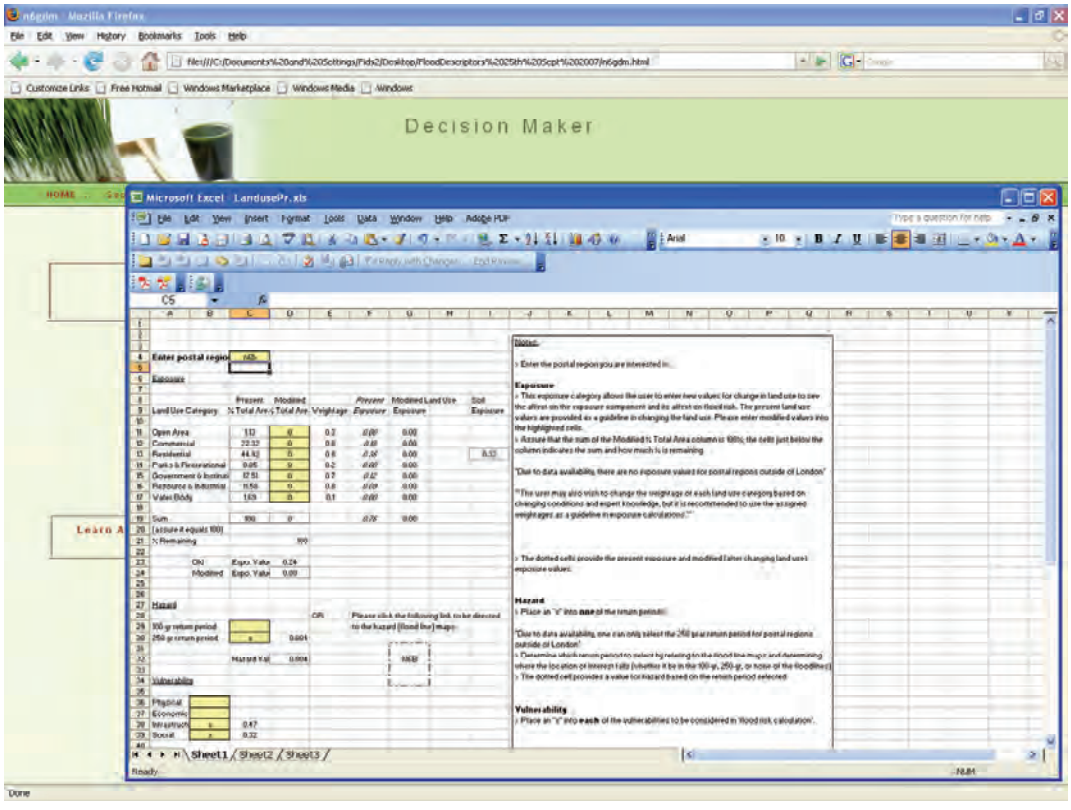

(b)

Figure 6. (a) Opening page of the information system; (b) analysis tool for decision makers.

number of critical facilities and road bridges. Typically, exposures of land use and soil permeability have been included as a component of risk. The minimum and maximum values of vulnerability are considered in the standardization process instead of using the conventional formula for standardization. A user-friendly information system is designed to systematically represent all flood information. The study provides an "analysis tool" for estimation of flood risk as a consequence of change in land use.

The present study has some limitations and offers some benefits for future development. In the flood information system all the indices of infrastructure vulnerability for critical facilities are not considered due to unavailability of data. For example, emergency shelters, nursing homes, public buildings, police stations, water treatment or sewage processing plants, utilities, railroad stations, airports and government facilities; which are identified critical facilities [27,62]. The assignment of Degree of Importance (DI) for calculation of impact inundation of important service buildings, emergency service stations and road bridges across the river on infrastructure vulnerability, and in calculation for exposures of land use and soil permeability is dependent on the perspective of decision-makers or floodplain planners, which introduces some uncertainty due to vagueness or imprecision in the model. This uncertainty due to imprecision in the assignment of DI may be addressed in the flood risk calculation. In the present system only two flood lines are available, e.g., 100- and 250-years flood lines, which limit the calculation of flood risk. The impact of critical facilities and road bridges across the river on infrastructure vulnerability is calculated only for the City of London as per the availability of data. The same analysis may be performed for other damage centers in the watershed. In future studies, different shapes and sizes of "vulnerability shapes" with finer grid system and actual population density can be considered for determining the impact of inundation of critical facilities and road bridges. The impact of climate change is not considered in the current version of the system. The hazard maps or the position of flood lines will change if the climate change impacts are taken into consideration [67]. The values of flood risk for different postal codes may be easily updated to include the impact of climate change. No hydrologic calculation is performed in the present study to find out current position of flood lines. A sophisticated hydrologic modeling may be implemented for finding out the current positions of flood lines and result in more accurate calculation of flood risk. The proposed methodologies of flood risk mapping are not limited to the present case study and may be easily applied to other watersheds.

9. Acknowledgements

The authors sincerely thank the Upper Thames River Conservation Authority, Statistics Canada, Canadian Homebuyers Guide, Serge A. Sawyer map library & the IDLS library at The University of Western Ontario for providing data used in this study. Work presented in this paper has been conducted under the research grant by the Natural Sciences and Engineering Research Council of Canada.

10. References

[1] P. J. Floyd, "Reducing Flood Risks," *Floods and Flood Management*, 1992, pp. 419-435.

[2] E. J. Plate, "Flood Risk and Flood Management," *Journal of Hydrology*, Vol. 267, No. 1-2, 2002, pp. 2-11.

[3] A. Becker and U. Grünewald, "Disaster Management: Flood Risk in Central Europe," *Science*, Vol. 300, No. 5622, 2003, p. 1099.

[4] D. P. Loucks, J. R. Stedinger, D. W. Davis and E. Z. Stakhiv, "Private and Public Responses to Flood Risks," *International Journal of Water Resources Development*, Vol. 24, No. 4, 2008, pp. 541-553.

[5] M. J. Purvis, P. D. Bates and C. M. Hayes, "A Probabilistic Methodology to Estimate Future Coastal Flood Risk Due to Sea Level Rise," *Coastal Engineering*, Vol. 55, No. 12, 2008, pp. 1062-1073.

[6] R. J. Dawson, L. Speight, J. W. Hall, S. Djordjevic, D. Savic and J. Leandro, "Attribution of Flood Risk in Urban Areas," *Journal of Hydroinformatics*, Vol. 10, No. 4, 2008, pp. 275-288.

[7] H. Apel, G. T. Aronica, H. Kreibich and A. H. Thieken, "Flood Risk Analyses—How Detailed do We Need to be?" *Natural Hazards*, Vol. 49, No. 1, 2009, pp. 79-98.

[8] P. Garrett, "Assessing Flood Risk," *Water Bull*, Vol. 355, 1989, p. 9.

[9] B. Burrell and J. Keefe, "Flood Risk Mapping in New Brunswick: A Decade Review," *Canadian Water Resources Journal*, Vol. 14, No. 1, 1989, pp. 66-77.

[10] D. G. Morris and R. W. Flavin, "Flood Risk Map for England and Wales," *Report - UK Institute of Hydrology*, 1996, p. 130.

[11] D. D. Shrubsole, "Flood Management in Canada at the Crossroads," *Global Environmental Change Part B*: *Environmental Hazards*, Vol. 2, No. 2, 2000, pp. 63-75.

[12] J. W. Hall, R. J. Dawson, P. B. Sayers, C. Rosu, J. B. Chatterton and R. Deakin, "A Methodology for National-scale Flood Risk Assessment," *Proceedings of the Institution of Civil Engineers: Water and Maritime Engineering*, Vol. 156, No. 3, 2003, pp. 235-247.

[13] J. I. Barredo, A. de Roo and C. Lavalle, "Flood Risk Mapping at European Scale," *Water Science and Technology*, Vol. 56, No. 4, 2007, pp. 11-17.

[14] S. L. Cutter, (Ed.) "American Hazardscapes: The Regionalization of Hazards and Disasters," Joseph Henry Press, Washington, D.C., 2001, p. 211.

[15] S. L. Cutter, "Vulnerability to Environmental Hazards," *Progress in Human Geography*, Vol. 20, No. 4, 1996, pp. 529-539.

[16] S. Bender, "Development and Use of Natural Hazard Vulnerability-Assessment Techniques in the Americas," *Natural Hazards Review*, American Society of Civil Engineers, 2002, pp. 136-138.

[17] L. Roy, R. Leconte, F. Brissette and C. Marche, "The Impact of Climate Change on Seasonal Floods of a Southern Quebec River Basin," *Hydrological Processes*, Vol. 15, No. 3, 2001, pp. 3167-3179.

[18] N. Nirupama and S. Simonovic, "Increase in Flood Risk Due to Urbanization: A Canadian Example," *Natural Hazards*, Vol. 40, No. 1, 2007, pp. 25-41.

[19] M. Morris-Oswald and S. Simonovic, "Assessment of the Social Impacts of Flooding for Use in Flood Management in the Red River Basin," Report Submitted to the International Red River Basin Task Force, International Joint Commission, Winnipeg, Manitoba, 1997. http://www.ijc.org/php/publications/html/assess.html

[20] E. Enarson, "Women, Work, and Family in the 1997 Red River Valley Flood: Ten Lessons Learned," Disaster Preparedness Resources Centre, University of British Columbia, British Columbia, Canada, 1999.

[21] E. Enarson and J. Scanlon, "Gender Patterns in Flood Evacuation: A Case Study in Canada's Red River Valley," *Applied Behavioural Science Review*, Vol. 7, No. 2, 1999, pp. 103-124.

[22] Natural Hazard Center, "Evaluation of a Literature Review of the Social Impacts of the 1997 Red River Flood," Report Submitted to the International Red River Basin Task Force, International Joint Commission. University of Colorado, Boulder, Colorado, USA, 1999, p. 11.

[23] P. Blaikie, R. Cannon, I. Davis and B. Wisner, "At Risk: Natural Hazards, People's Vulnerability, and Disasters," Routledge, New York, 1994, p. 284.

[24] P. M. Kelly and W. N. Adger, "Theory and Practice in Assessing Vulnerability to Climate Change and Facilitating Adaptation," *Climatic Change*, Vol. 47, No. 4, 2000, pp. 325-352.

[25] B. Montz and T. Evans, "GIS and Social Vulnerability Analysis," In: E. Gruntfest and J. Handmer, Eds., *Coping with Flash Floods*, Kluwer Academic Publishers, Netherlands, 2001, pp. 37-48.

[26] S. L. Cutter, J .T. Mitchell and M. S. Scott, "Revealing the Vulnerability of People and Places: A Case Study of Georgetown County, South Carolina," *Annals of the Association of American Geographers*, Vol. 90, No. 4, 2000, pp. 713-737.

[27] L. K. Flax, R. W. Jackson and D. N. Stein, "Community Vulnerability Assessment Tool Methodology," *Natural Hazards Review*, American Society of Civil Engineers, Vol. 3, No. 4, 2002, pp. 163-176.

[28] S. L. Cutter, B. J. Boruff and W. L. Shirley, "Social Vulnerability to Environmental Hazards," *Social Science Quarterly*, Vol. 84, No. 2, 2003, pp. 242-261.

[29] R. Blong, "A New Damage Index," *Natural Hazards*, Vol. 30, No. 1, 2003, pp. 1-23.

[30] N. T. Carter, "Flood Risk Management: Federal Role in Infrastructure," CRS Report for Congress, 2005, http://fpc. state.gov/documents/organization/56095.pdf

[31] J. Chakraborty, G. A. Tobin and B. E. Montz, "Population Evacuation: Assessing Spatial Variability in Geophysical Risk and Social Vulnerability to Natural Hazards," *Natural Hazards Review*, American Society of Civil Engineers, Vol. 6, No. 1, 2005, pp. 23-33.

[32] L. Rygel, D. O'Sullivan and B. Yarnal, "A Method for Constructing a Social Vulnerability Index: An Application to Hurricane Storm Surges in a Developed Country," *Mitigation and Adaptation Strategies for Global Change*, Vol. 11, No. 3, 2006, pp. 741-764.

[33] A. Werritty, D. Housto, T. Ball, A. Tavendale and A. Black, "Exploring the Social Impacts of Flood Risk and Flooding in Scotland," Scottish Executive Social Research, Edinburgh, 2007.

[34] S. K. Sinnakaudan, A. Ab Ghani, M. S. S. Ahmad, and N. A. Zakaria, "Flood Risk Mapping For Pari River Incorporating Sediment Transport," *Environmental Modelling and Software*, Vol. 18, No. 2, 2003, pp. 119-130.

[35] J. Bai, C. Wang, Z. Niu, S. Qi and G. Li, "Utilizing Remote Sensed TM Images and Meteorological Data to Plan Flood Risk Area," *Proceedings of The International Society for Optical Engineering*, Vol. 5232, 2006, pp. 370-377.

[36] F. Forte, L. Pennetta and R. O. Strobl, "Historic Records and GIS Applications for Flood Risk Analysis in the Salento Peninsula (Southern Italy)," *Natural Hazards and Earth System Science*, Vol. 5, No. 6, 2005, pp. 833-844.

[37] R. Abdalla, C. V. Tao, H. Wu and I. A. Maqsood, "GIS-Supported 3D Approach for Flood Risk Assessment of the Qu'Appelle River, Southern Saskatchewan," *International Journal of Risk Assessment and Management*, Vol. 6, No. 4-6, 2006, pp. 440-455.

[38] D. G. Hadjimitsis, "The Use of Satellite Remote Sensing and GIS for Assisting Flood Risk Assessment—A case study of Agriokalamin Catchment Area in Paphos-Cyprus," *Proceedings of The International Society for Optical Engineering*, Vol. 6742, No. 67420Z, 2007.

[39] K. Smith, "Environmental Hazards: Assessing Risk and Reducing Hazards," 3rd Edition, Routledge (Taylor & Francis Group), New York, 2001, p. 392.

[40] J. Lowry, H. Miller and G. Hepner, "A GIS-Based Sensitivity Analysis of Community Vulnerability to Hazardous Contaminants on the Mexico/U.S. Border," *Photogrammetric Engineering & Remote Sensing*, Vol. 61, No. 11, 2005, pp. 1347-1359.

[41] L. A. Varga, D. Radulescu and R. Drobot, "Romanian National Strategy for Flood Risk Management," IAHS-AISH Publication, Vol. 323, 2008, pp. 75-86.

[42] H. Chang, J. Franczyk and C. Kim, "What is Responsible for Increasing Flood Risks? The Case of Gangwon Province, Korea," *Natural Hazards*, Vol. 48, No. 3, 2009, pp. 339-354.

[43] P. Tran, F. Marincioni, R. Shaw, M. Sarti and A. L. Van, "A Flood Risk Management in Central Viet Nam: Challenges and Potentials," *Natural Hazards*, Vol. 46, No. 1, 2008, pp. 119-138.

[44] S. Forster, B. Kuhlmann, K. E. Lindenschmidt and A. Bronstert, "Assessing Flood Risk for a Rural Detention Area," *Natural Hazards and Earth System Science*, Vol. 8, No. 2, 2008, pp. 311-322.

[45] M. Dilley, R. S. Chen, U. Deichmann, A. L. Lerner-Lam, M. Arnold, J. Agwe, P. Buys, O. Kjekstad, B. Lyon and G. Yetman, "Natural Disasters Hotspots: A Global Risk Analysis," Synthesis Report, The World Bank, Washington, D.C., 2005.

[46] M. Arnold, R. Chen, U. Deichmann, M. Dilley, A. Lerner-Lam, R. Pullen and Z. Trohanis, "Natural Disaster Hotspots: Case Studies," Disaster Risk Management Series, No. 6, The World Bank, Washington, D.C., 2006.

[47] UN, "Internationally Agreed Glossary of Basic Terms Related to Disaster Management," United Nations Department of Humanitarian Affairs, Geneva, 1992.

[48] B. Merz and A. H. Thieken, "Flood Risk Analysis: Concepts and Challenges," *O¨sterreichische Wasser und Abfallwirtschaft*, Vol. 56, No. 3-4, 2004, pp. 27-34.

[49] EU, "European Flood Directive: Richtlinie 2007/60/EG des Europäischen Parlaments und des Rates vom 23. Oktober 2007 über die Bewertung und das Management von Hochwasserrisiken," Amtsblatt der Europäischen Union, L288, pp. 27-34.

[50] W. Kron, "Flood Risk = Hazard•Values•Vulnerability," *Water International*, Vol. 30, No. 1, 2005, pp. 58-68.

[51] S. Y. Wu, B. Yarnal and A. Fisher, "Vulnerability of Coastal Communities to Sea-Level Rise: A Case Study of Cape May County, New Jersey, USA," *Climate Research*, Vol. 22, No. 4, 2002, pp. 255-270.

[52] Y. Huang, Y. Zou, G. Huang, I. Maqsood and A. Chakma, "Flood Vulnerability to Climate Change through Hydrological Modeling: A Case Study of the Swift Current Creek Watershed in Western Canada," *Water International*, Vol. 30, No. 1, 2005, pp. 31-39.

[53] A. Hebb and L. Mortsch, "Floods: Mapping Vulnerability in the Upper Thames Watershed under a Changing Climate," Project Report XI, University of Waterloo, 2007, pp. 1-53.

[54] R. Grosshans, H. Venema and S. Barg, "Geographical Analysis of Cumulative Threats to Prairie Water Resources: Mapping Water Availability, Water Quality, and Water Use Stresses," International Institute for Sustainable Development, Winnipeg, Manitoba, 2005, p. 40.

[55] M. Helsten and D. Davidge, "Flood Damage Estimation in the Upper Thames River Watershed CFCAS Project: Assessment of Water Resources Risk and Vulnerability to Changing Climatic Conditions," Project Report VII, Upper Thames River Conservation Authority, 2005, pp. 1-46.

[56] H. Apel, A. H. Thieken, B. Merz and G. A. Blo¨schl, "Probabilistic Modelling System for Assessing Flood Risks," *Natural Hazards*, Vol. 38, No. 1-2, 2006, pp. 79-100.

[57] W. Feller, "An Introduction to Probability Theory and its Applications," 3rd Edition, John Wiley and Sons, New York, Vol. I, 1968.

[58] Environmental Systems Research Institute (ESRI), "Arc 9.2. ESRI," Redlands, California, 2006.

[59] S. E. Mustow, R. F. Burgess and N. Walker, "Practical Methodology for Determining the Significance of Impacts on the Water Environment," *Water and Environment Journal*, Vol. 19, No. 2, 2005, pp. 100-108.

[60] P. A. Keddy and A. A. Reznicek, "Great Lakes Vegetation Dynamics: The Role of Fluctuating Water Levels and Buried Seeds," *Journal of Great Lakes Research*, Vol. 12, No. 1, 1986, pp. 25-36.

[61] S. Efromovich, "Nonparametric Curve Estimation: Methods, Theory and Applications," Springer-Verlag, New York, 1999.

[62] D. Odeh, "Natural Hazards Vulnerability Assessment for Statewide Mitigation Planning in Rhode Island," *Natural Hazards Review*, ASCE, Vol. 3, No. 4, 2002, pp. 177-187.

[63] A. Peck, S. Karmakar and S. P. Simonovic, "Physical, Economical, Infrastructural and Social Flood Risk—Vulnerability Analyses in GIS," Water Resources Research Report No. 057, Facility for Intelligent Decision Support, Department of Civil and Environmental Engineering, London, Ontario, Canada, 2007.

[64] A. Sullivan, J. L. Ternan and A. G. Williams, "Land Use Change and Hydrological Response in the Camel Catchment, Cornwall," *Applied Geography*, Vol. 24, No. 2, 2004, pp. 119-137.

[65] U. S. Environmental Protection Agency (USEPA), "Program Evaluation Glossary". http://www.epa.gov/evaluate/glossary/i-esd.htm

[66] J. Black, S. Karmakar and S. P. Simonovic, "A Web-Based Flood Information System," Water Resources Research Report No. 056, Facility for Intelligent Decision Support, Department of Civil and Environmental Engineering, London, Ontario, Canada, 2007.

[67] P. Prodanovic and S. P. Simonovic, "Inverse Flood Risk Modelling of the Upper Thames River Basin," Water Resources Research Report No. 052, University of Western Ontario, London, Ontario, Canada, 2006.

Journal of Geographic Information System, **2010, 2, 147-151**
doi:10.4236/jgis.2010.23021 Published Online July 2010 (http://www.SciRP.org/journal/jgis)

GPS- vs. DEM-Derived Elevation Estimates from a Hardwood Dominated Forest Watershed

L. Chris Kiser, J. Michael Kelly
Virginia Polytechnic Institute and State University, Blacksburg, USA
E-mail: {*lckiser, jmkelly*}*@vt.edu*
Received April 28, 2010; *revised May* 29, 2010; *accepted June* 3, 2010

Abstract

Topographic attributes are often used as explanatory variables when providing spatial estimates of various environmental attribute response variables. Elevation of sampling locations can be derived from global positioning systems (GPS) or digital elevation models (DEM). Given the potential for differences in elevation among these two data sources, especially in response to forest canopy cover, our objective was to compare GPS and DEM-derived elevation values during the dormant season. A non-parametric Wilcoxon test indicated GPS elevation was higher than DEM elevation with a mean difference of 6 m. Linear regression analysis indicated that GPS and DEM elevation were well correlated ($R^2 = 0.71$, $r = 0.84$, $p < 0.0001$). Although elevation among the two data sources differed, the strong linear relationship allows for correction of elevation values in a predictable manner.

Keywords: Forest Canopy Cover, Linear Regression, Spatial Estimates

1. Introduction

Global positioning systems (GPS) are widely used in environmental research to identify locations of permanent sampling locations. Horizontal accuracy is suggested to be influenced primarily by GPS grade and canopy cover [1-4]. Spatial estimates of various environmental attribute response variables are widely developed using digital elevation model (DEM) derived topographic attributes as explanatory variables. Elevation derived from a DEM is an attribute typically used in this methodology. Alternatively, elevation determined by GPS may also be used in this type of analysis. Given the potential for differences in elevation among these two data sources, our objective was to compare GPS and DEM-derived elevation in a statistically rigorous manner on a typical hardwood forest site. GPS data for this analysis were collected in part in support of a recently published study on forest soil C and N [5] and are reanalyzed here. The utility of this analysis results from a lack of studies that compare elevation derived from these two data sources.

2. Methods

2.1. Site Description

The Camp Branch Experimental Watershed is located in Fall Creek Falls State Park on the Cumberland Plateau in Central Tennessee ($35^0 38'$ N lat.; $85^0 18'$ W long.). The watershed is a 94 ha mixed hardwood forest. Permanent data points (**Figure 1**) were marked with steel posts as part of an earlier study [6]. GPS data were collected after leaf fall in November 2006 and canopy coverage was

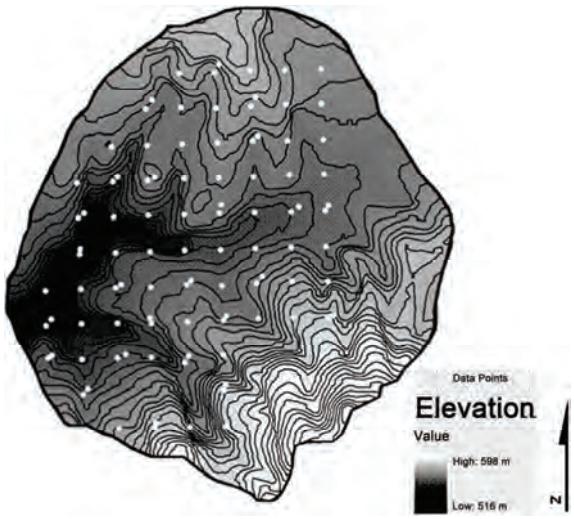

Figure 1. Elevation map of the 94 ha Camp Branch Experimental Watershed. Also shown are the 95 data points for which coordinates and elevation were determined.

estimated to range from 15% to 25% during the GPS data collection period. Mean GPS elevation is 554 m and ranges from 532 m to 584 m. Mean DEM-derived elevation is 548 m and ranges from 528 m to 567 m.

2.2. GPS Data

Coordinates (UTM zone 16N; horizontal datum NAD83) and elevation of the 95 data points were collected in November 2006 with a mapping-grade Trimble GeoXT receiver (Trimble Navigation Ltd., Sunnyvale, CA, USA). Elevation of the data points was recorded as height above mean sea level (MSL) using the EGM96 geoid model. Data were post-processed with TerraSync v.2.52 (Trimble Navigation Ltd., Sunnyvale, CA, USA) using a continuously operating reference station (CORS) in Hartsville, TN located approximately 68 miles from the study area. After post-processing, a shapefile of the 95 data points was generated. Mean and standard deviation of the number of positional fixes was 15.0 and 9.8, respectively. Mean and standard deviation of maximum positional dilution of precision (PDOP) was 4.4 and 0.65, respectively. Mean and standard deviation of horizontal precision was 1.3 m and 0.2 m, respectively.

2.3. Digital Elevation Model

A level 2, 10-m resolution DEM of the watershed taken from the 7.5 minute Sampson, TN quadrangle was obtained from the U.S. Geological Survey's National Elevation Dataset (EROS, Sioux Falls, SD, USA). The horizontal datum of the DEM is NAD27 and the vertical datum is NAVD88.

2.4. ArcGIS

Both the GPS data point shapefile and the DEM were imported into ArcGIS v.9.2 (ESRI Inc., Redlands, CA, USA) and projected in UTM zone 16N and NAD83 (**Figure 1**). Elevations of the 95 data points derived from the DEM were extracted for comparison with GPS elevations. The spatial analyst function was used to generate 10 m contour lines to aid in visualizing topographic features.

2.5. Statistical Analysis

Due to a non-normal mean difference, a non-parametric Wilcoxon procedure was used to test for differences among GPS and DEM-derived elevation (PROC NPAR-1WAY, SAS v.9.1, SAS Institute Inc., Cary, NC, USA). The relationship of GPS to DEM-derived elevation was examined using simple linear regression (PROC REG, SAS v.9.1, SAS Institute Inc., Cary, NC, USA).

3. Results and Discussion

The Wilcoxon test indicated GPS elevations were larger than DEM-derived elevations ($Z = 4.18$, $p < 0.0001$). Mean and standard deviation of the difference in elevation was 6 m and 5 m, respectively. The difference in elevation ranged from 21 m to –5 m (**Table 1**) and was not related to maximum PDOP, the number of positional fixes, and horizontal precision. Regression analysis indicated that GPS and DEM-derived elevation were well correlated ($y = 123.74 + 0.7665x$, $F = 226.2$, $R^2 = 0.71$, $r = 0.84$, $p < 0.0001$) (**Figure 2**). Out of 95 data points, 4 fell outside the 95% prediction interval for the regression (**Figure 2**). Results indicate DEM-derived elevation of other data points within the study area can be adjusted with confidence when GPS-derived elevation is considered more representative of actual elevation thereby minimizing error propagation effects on accuracy of spatial estimates of environmental attribute response variables.

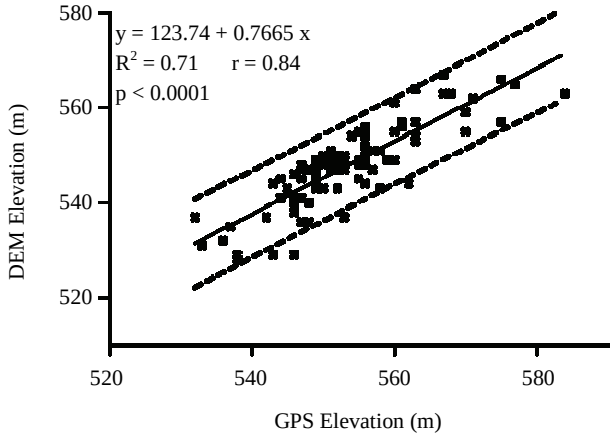

Figure 2. Scatterplot depicting DEM elevation as a function of GPS elevation. Linear regression equation, R^2, r, p-value, and 95% prediction interval are also shown.

Table 1. GPS data collection parameters, GPS elevation, DEM elevation, and elevation difference for each of the 95 permanent data points on the Camp Branch Experimental Watershed.

Maximum PDOP	Positional Fixes	Horizontal Precision	GPS Elevation	DEM Elevation	Elevation Difference
4.8	17	1.1	584	563	21
3.3	14	1.2	575	557	18
3.9	6	1.7	562	544	18
4.3	10	1.3	546	529	17
5.2	15	1.2	553	537	16
5.8	28	1.1	570	555	15
4.9	12	1.3	558	543	15
3.3	13	1.0	543	529	14
4.6	11	1.3	548	536	12
4.7	6	1.3	577	565	12
4.4	15	1.4	556	544	12
5.1	10	1.5	560	549	11
5.0	11	1.4	547	536	11
5.7	14	1.3	570	559	11
3.9	7	1.5	555	545	10
4.4	15	1.4	538	528	10
4.4	19	1.4	557	547	10
4.6	17	1.0	559	549	10
3.9	64	1.0	563	553	10
5.1	11	1.6	563	554	9
4.9	10	1.2	575	566	9
4.5	4	1.8	571	562	9
4.8	10	1.3	552	543	9
3.3	6	1.3	538	529	9
4.9	15	1.1	548	540	8
4.9	10	1.2	556	548	8
4.1	32	1.4	546	538	8
4.3	18	1.5	550	543	7
5.4	16	1.2	555	548	7
4.2	10	1.6	555	548	7
4.6	11	1.1	558	551	7
5.0	16	1.4	556	549	7
4.1	12	1.3	553	547	7
4.7	10	1.6	563	557	6
3.3	12	1.1	549	543	6
4.9	15	1.1	547	541	6
4.5	17	1.0	557	551	6
4.2	15	1.3	555	549	6
3.1	17	1.1	546	540	6
3.8	8	1.0	549	543	6
3.3	16	1.5	552	547	5
2.5	11	0.9	560	555	5
5.2	13	1.1	546	541	5
4.8	12	1.2	556	551	5
3.9	4	1.1	561	556	5
4.0	10	1.1	552	547	5
4.8	66	1.1	549	544	5
3.9	10	1.2	568	563	5
4.7	26	1.3	542	537	5
3.4	10	1.3	551	547	4
4.7	12	1.3	556	552	4

Table 1 continued

Maximum PDOP	Positional Fixes	Horizontal Precision	GPS Elevation	DEM Elevation	Elevation Difference
4.9	12	0.9	561	557	4
3.2	10	1.2	552	548	4
2.5	12	1.1	553	549	4
4.1	12	1.1	536	532	4
4.9	11	1.3	553	549	4
4.7	10	1.2	567	563	4
4.0	14	1.1	553	549	4
5.4	12	1.4	553	550	3
5.0	19	1.6	553	550	3
4.6	11	1.2	549	546	3
4.4	7	1.4	544	541	3
4.7	12	1.1	551	548	3
3.8	12	1.3	551	548	3
4.2	10	1.6	553	550	3
4.2	13	1.2	550	548	2
4.8	22	1.0	545	543	2
4.6	43	1.2	547	545	2
4.4	20	1.2	551	549	2
4.0	13	1.4	549	547	2
5.2	7	1.4	537	535	2
4.7	13	1.6	552	550	2
4.1	12	1.4	550	548	2
4.9	13	1.4	552	550	2
4.8	10	1.0	556	554	2
3.3	15	1.2	533	531	2
4.7	10	1.1	548	547	1
4.1	15	1.4	548	547	1
4.7	16	1.2	556	555	1
4.2	21	1.4	551	551	0
4.9	12	1.7	549	549	0
3.4	14	1.2	554	554	0
4.2	14	0.9	555	555	0
5.3	10	1.8	547	547	0
4.9	12	1.2	551	551	0
4.8	14	1.4	546	546	0
4.8	22	1.4	567	567	0
3.8	9	1.4	550	550	0
4.5	23	1.4	556	556	0
4.1	10	1.3	543	544	-1
3.6	10	1.3	544	545	-1
4.4	46	1.8	563	564	-1
4.9	15	1.4	547	548	-1
5.5	12	1.0	560	561	-1
4.8	23	1.3	532	537	-5

In a study that compared elevations from five mapping-grade Trimble GPS receivers with surveyed benchmark elevations [7], average absolute vertical errors of post-processed data among the receivers ranged from 0.8 m to 1.9 m. The greatest effect on vertical error was canopy coverage. Vertical error of post-processed data was 0.2 m under open sky, 0.4 m under 50% canopy, and 3.3 m under 100% canopy. While the vertical error in our study was larger at 6 m, the two studies are not directly comparable.

4. Conclusions

Results indicate that, under conditions specific to this study,

although GPS elevation was overestimated compared to DEM-derived elevation, the relationship among these data sources was predictable and followed a well defined linear relationship. While the magnitude of the elevation difference among the two data sources was large for some of the data points, the strong linear relationship allows for correction of elevation values in a predictable manner. More generically, the results of this analysis indicate that potential differences in GPS and DEM derived elevation estimates will need to be considered when elevation related environmental attributes are analyzed and extrapolated spatially.

5. References

[1] M. G. Wing, A. Eklund and L. D. Kellogg, "Consumer-Grade Global Positioning System (GPS) Accuracy and Reliability," *Journal of Forestry*, Vol. 103, No. 4, June 2005, pp. 169-173.

[2] M. G. Wing and R. Karsky, "Standard and Real-Time Accuracy and Reliability of a Mapping-Grade GPS in a Coniferous Western Oregon Forest," *Western Journal of Applied Forestry*, Vol. 21, No. 4, October 2006, pp. 222-227.

[3] M. G. Wing and A. Eklund, "Performance Comparison of a Low-Cost Mapping Grade Global Positioning Systems (GPS) Receiver and Consumer Grade GPS Receiver under Dense Forest Canopy," *Journal of Forestry*, Vol. 105, No. 1, January/February 2007, pp. 9-14.

[4] M. G. Wing, A. Eklund, J. Sessions and R. Karsky, "Horizontal Measurement Performance of Five Mapping-Grade Global Positioning System Receiver Configurations in Several Forested Setting," *Western Journal of Applied Forestry*, Vol. 23, No. 3, July 2008, pp. 166-171.

[5] L. C. Kiser, J. M. Kelly and P. A. Mays, "Changes in FoRest Soil Carbon and Nitrogen after a Thirty-Year Interval," *Soil Science Society of America Journal*, Vol. 73, No. 1, February 2009, pp. 647-653.

[6] J. M. Kelly, "Camp Branch and Cross Creek Experimental Watershed Projects," Report Nos. TVA/ONR-79/04, EPA-600/7-79- 053, 1979.

[7] M. G. Wing and A. Eklund, "Vertical Measurement Accuracy of Mapping-Grade Global Positioning Systems Receivers in Three Forest Setting," *Western Journal of Applied Forestry*, Vol. 23, No. 2, April 2008, pp. 83-88.

Journal of Geographic Information System, **2010, 2, 152-162**
doi:10.4236/jgis.2010.23022 Published Online July 2010 (http://www.SciRP.org/journal/jgis)

A Hybrid Approach towards the Assessment of Groundwater Quality for Potability: A Fuzzy Logic and GIS Based Case Study of Tiruchirappalli City, India

Natarajan Venkat Kumar, Samson Mathew, Ganapathiram Swaminathan
Civil Engineering Department, National Institute of Technology, Tiruchirappalli, India
E-mail: *venkatkumar.nit@gmail.com*
Received February 28, 2010; *revised April* 7, 2010; *accepted April* 15, 2010

Abstract

The present study aims to develop a new hybrid Fuzzy Simulink model to assess the groundwater quality levels in Tiruchirappalli city, South India. Water quality management is an important issue in the modern times. The data collected for Tiruchirappalli city have been utilized to develop the approach. This is illustrated with seventy nine groundwater samples collected from Tiruchirappalli city Corporation, South India. The characteristics of the groundwater for this plain were monitored during the years 2006 and 2008. The quality of groundwater at several established stations within the plain were assessed using Fuzzy Logic (FL) and GIS maps. The results of the calculated FL and GIS maps with the monitoring study have yielded good agreement. Groundwater quality for potability indicated high to moderate water pollution levels at Srirangam, Ariyamangalam, Golden Rock and K. Abisekapurm zones of the study area, depending on factors such as depth to groundwater, constituents of groundwater and vulnerability of groundwater to pollution. Fuzzy logic simulation approach has shown to be a practical, simple and useful tool to assess groundwater quality assessment for potability. This approach is capable of showing and updating the water quality assessment for drinking.

Keywords: Groundwater quality, Fuzzy Logic Model, GIS, Potability, Tiruchirappalli City

1. Introduction

Over few decades, competition for economic development, associated with rapid growth in population and urbanization, has brought in significant changes in land use, resulting in more demand of water for domestic activities. Groundwater is one among the Nation's most important natural resources. Very large quanta of ground water are pumped each day for industrial, agricultural, and commercial use. Groundwater is the drinking-water source for about one-half of the nation's population, including almost all residents in rural areas. Information on the quality and quantity of ground water is important because of the nation's increasing population and dependency on this resource. The population dependent on public water systems that used groundwater for drinking water supplies increased during last fifty years. The estimated withdrawal increased about five-fold during last half century. The quality and availability of ground water will continue to be an important environmental issue. Long-term conservation, prudent development and management of this natural resource are critical for preserving and protecting this priceless national asset.

As per the International norms, if per capita water availability is less than 1700 m^3 per year then the country is categorized as water stressed and if it is less than 1000 m^3 per capita per year then the country is classified as water scarce. India is water stressed and is likely to be water scarce by 2050 [1].

Continued research, guidance and regulations by government agencies and pollution abatement programmes are necessary to preserve the Nation's groundwater quality and quantity for future generations. The impact of Industrial effluents is also responsible for the deterioration of the physico-chemical and bio-chemical parameters of groundwater [2]. The environmental impacts on the groundwater contaminations may seriously affect the socio-economic conditions of the country. Knowledge on water chemistry is important to assess the quality of aquatic resources for understanding its suitability for various needs [3]. Information on the status and changing trends in water quality is necessary to formulate suitable guide-

Sponsor by M.N.S.Gold Technologies Madurai, India.

lines and efficient implementation for water quality assessment, water quality monitoring and enforcement of prescribed limits by different regulatory bodies [4]. Various methods discussed in literature on drinking water quality revealed that deterministic approach in decision making by comparing values of parameters of water qua- lity with prescribed limits provided by different regulatory bodies could be used without considering uncertainties involved [5].

There are two areas in which the literature is far from complete and has the gaps which are to be bridged and these are: 1) The decision on the water quality assessm ent (desirable, acceptable or not acceptable) using fuzzy logic and 2) The sets of the monitored data and limits should not be as crisp set, but as fuzzy sets. One way of avoiding the difficulty in uncertainty handling in water quality assessment is to introduce a margin of safety or degree of precaution.

Before applying a single value to drinking water quali ty standards as the same technique was also used by other researchers in the field of environmental science [6-8] Keeping the importance of uncertainty handling in the potable water quality assessment and versatility of the fuzzy set theory in decision-making in the imprecise environment, an attempt has been made to classify the groundwater from Tiruchirappalli City Corporation of Tamilnadu, South India for the potable use [9].

2. Study Area, Materials and Methods

2.1. Study Area

The Base map of Tiruchirappalli city was drawn from Survey of India Topo sheets Nos. 58 J/9, 10, 13 and 14 and satellite imagery (IRS -1C and LISS III) is lies between 10°48'18" North: 78°41'7" East. The general topology of Tiruchirappalli is flat and lies at an altitude of 78 m above sea level. Tiruchirappalli is fed by the rivers Cauvery and Kollidam. There are reserve forests along the river Cauvery. Golden Rock and the Rock Fort are the prominent hills. The southern/south-western part of the district is dotted by several hills which are thought to be an offset of the Western Ghats Mountain range and the soil is considered to be very fertile. For the sample collection, seventy nine bore well locations were identified. These locations were identified in such a way that the bore wells were evenly distributed over the study area and have used for potability.

The water samples were collected for periods between March 2006 and December 2008. The water from these bore wells were used for drinking, house hold utilities and bathing by the residents. The Laboratory tests were conducted on these samples for 16 different physico-chemical potable water quality parameters as per the standard procedure [10-12] criteria were adopted for testing these samples.

2.2. Thematic Maps

The base map data was used for the study included digitized data sets originally developed by Survey of India, and the Tiruchirappalli city corporation. The work maps were prepared from 1:20,000 scale topographic paper maps using AutoCAD, Arc GIS 9.2 and Surfer V.8.

The groundwater hydrochemistry records of the study area were used for the preparation of the maps. These maps are obtained by geostatistical (Kriging) methodology and the results were presented in the form of equal ion concentration lines **[**13].

The groundwater quality data were used as the hidden layer for the preparation of base maps. These features were the boundary lines between mapping units, other linear features (streets, rivers, roads, etc.) and point features (bore well points, etc.). The contours were developed for pH, EC, Cl^-, Na^+, Ca^{2+}, Mg^{2+}, Total Hardness, Alkalinity, F, SO_4^{2-}, Coli form and NO^{3-} for the seasonal conditions of the study period between 2006 and 2008.

The monitoring and sampling program was initiated in 2006 and finalized the year 2008. A total of seventy nine monitoring stations were established of them represented groundwater conditions. The groundwater stations had different depths to groundwater. The sampling locations of all the stations are shown in **Figure 1**. A total of seventy nine separate ground water quality monitoring sessions were realized during the study period during the months of June, August, October and November of the year 2006-2008 and March, June and October of the year 2006-2008.

2.3. Potable Water Quality Maps

The data used for the mapping water quality assessment for potability were developed from the laboratory water quality analysis. Data for these studies were based on the sampling conducted by the first author for groundwater samples collected from predetermined locations of existing bore wells in Tiruchirappalli city. The data were linked to the sampling bore well locations using geodata base creation of Arc GIS 9.2 and Surfer 8 software.

The decision on the water quality assessment for potability gives that the water is desirable, acceptable and not acceptable as per the guidelines from BIS and WHO [9-11] regulatory bodies. But, in the border line cases of water quality parameters, it becomes a Herculean task as different types of uncertainties are involved at various part of experimental and measurement process right from sampling, sample storage, processing and analysis. The sets of the monitored data and limits should not be as crisp set, but as fuzzy sets. One way of avoiding the difficulty in uncertainty handling in water quality assessment is to introduce a margin of safety or degree of precaution before applying a single value to drinking water

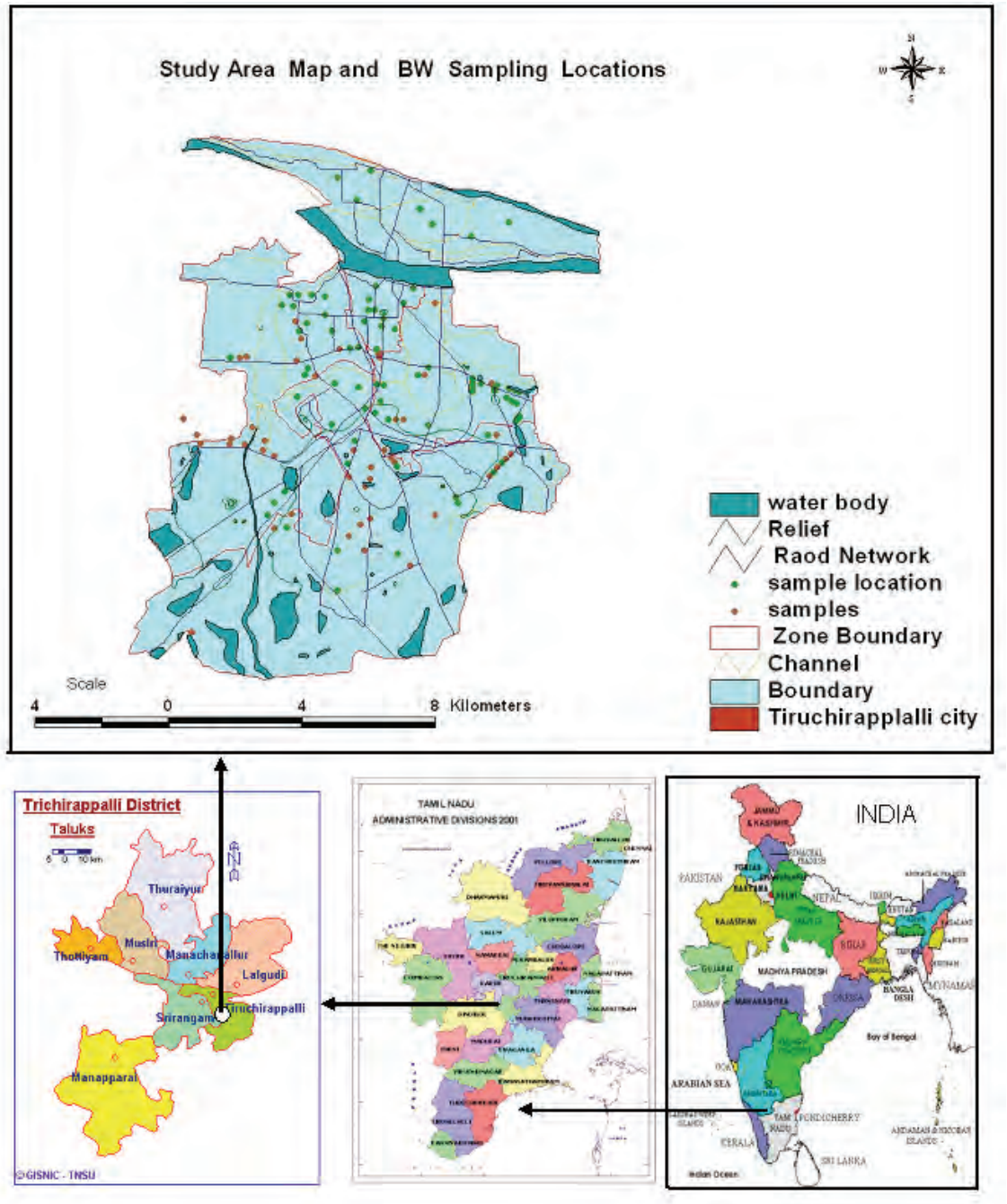

Figure 1. Study area and sampling location map of Tiruchirappalli city.

quality standards as the same technique was also used by other researchers in the field of environmental science [2,5,12-14]. These methodologies based on fuzzy set theory were utilized with real environmental water quality assessment to handle the uncertainties in imprecise environment in decision- making on the potability of water quality can be handled. The concept of a class with unsharp boundaries and marked the beginning of a new direction by providing a basis for a qualitative approach to the analysis of complex systems in which linguistic rather than numerical variables are employed to describe system behavior and performance [15]. Keeping the importance of uncertainty handling in the drinking water quality assessment and versatility of the fuzzy set theory in decision-making. An attempt was made to classify the under ground water from Tiruchirappalli city corporation, South India for the drinking purposes.

3. A Hybrid of Fuzzy Logic Model with GIS

Geographic Information Systems (GIS) have become important tool in efficiently solving many problems in which spatial data are important. Natural re-sources and environmental concerns, including groundwater have benefited greatly from the use of GIS. It is becoming powerful computer tools for varied applications ranging from sophisticated analysis and modeling of spatial data to simple inventory and management. GIS incorporates data that describes population characteristics, socio-economic conditions, landscape and analysis the spatial relationship of these factors. In addition to integrating and analyzing health related data, this technology promotes data sharing through the use of standard formats and act as a highly efficient communication tool. Analysis of spatial and attribute data in a GIS can be classified into five main types of procedures.

1) Data transformation and restructuring
2) Data retrieval, classification and measurement
3) Overlay
4) Neighborhood and statistical measures and
5) Connectivity

The most significant difference between GIS and other information systems, the databases is the spatial nature of the data in a GIS. The analysis functions in a GIS allow manipulation of multiple themes of spatial data to perform overlays, buffering and arithmetic operations on the data with its spatial analysis capabilities, GIS technology can play an important role in human services research there by ensuring better service delivery for clients. Along with other computer applications including word processors, spread sheets, databases, statistical packages and the internet, GIS is thus a versatile tool for human service professionals providing a competitive edge particularly in the areas of planning and evolution and community development. Hence the GIS methodology has been adopted in the presented study and illustrated in **Figure 2**.

Data collected from the study area for various seasons were used as the input for simulation model. The simulation was used for the collected data for all the samples of the studied seasonal variations. Based on expert knowledge [16,17] 66 rules were designed for physico-chemical water quality parameters in Group I **Figure 3**, where as 73 rules were designed for Group II **Figure 4**. Results from group one and two are combined with Group III **Figure 5** to assess the final classification of water. A total of 27 rules were fired for the final assessment of groundwater quality in the fuzzy logic model. The results from all the three groups were aggregated to assess

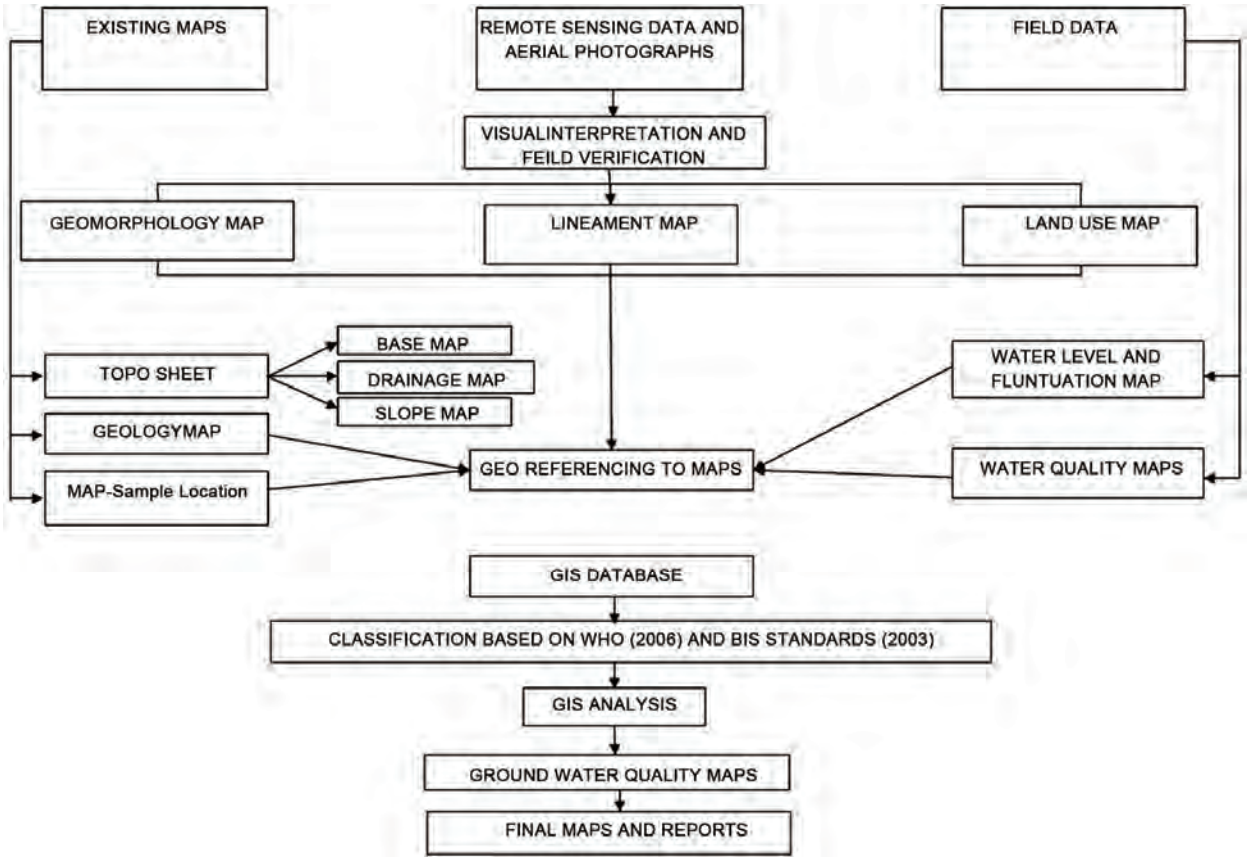

Figure 2. Flow chart showing data flow and analysis of GIS in the present study.

the final classification of water as shown in **Figure 6**. The processes were applied to all the seasonal water samples and the results obtained are as shown in **Figure 7(a), (b)** and **(c).**

The rule based decision on expert's perception has been fired using Mamdani implification of maximum and minimum operator [18]. To assess the drinking water quality of the groundwater samples, 181 rules are fired.

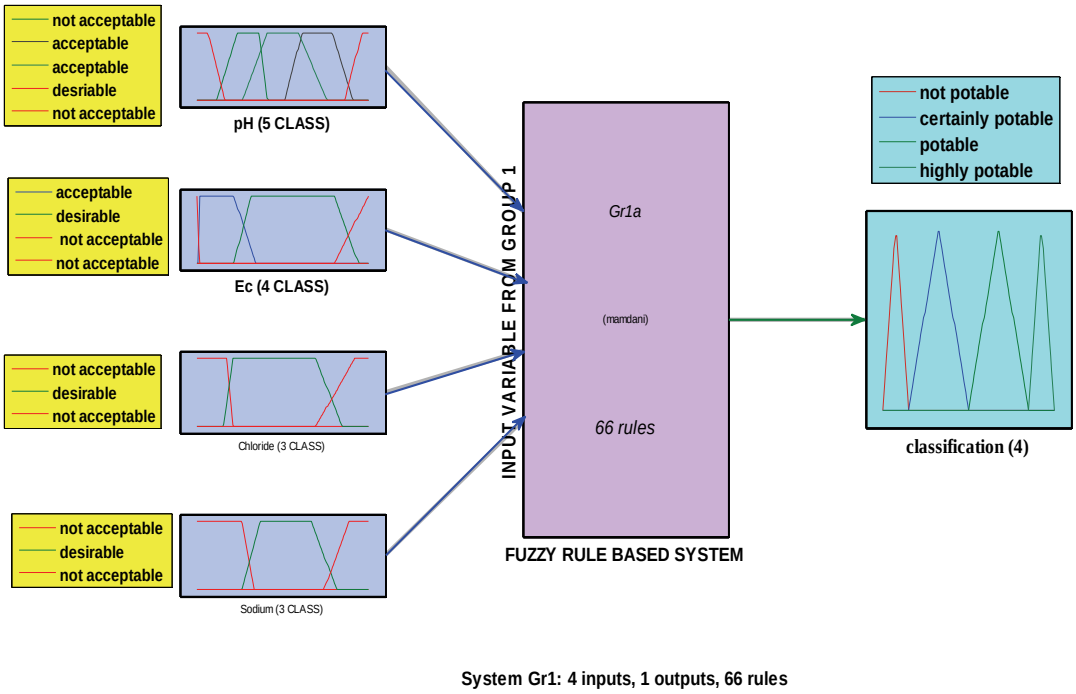

Figure 3. Block diagram for fuzzy logic model for First Group water quality parameters.

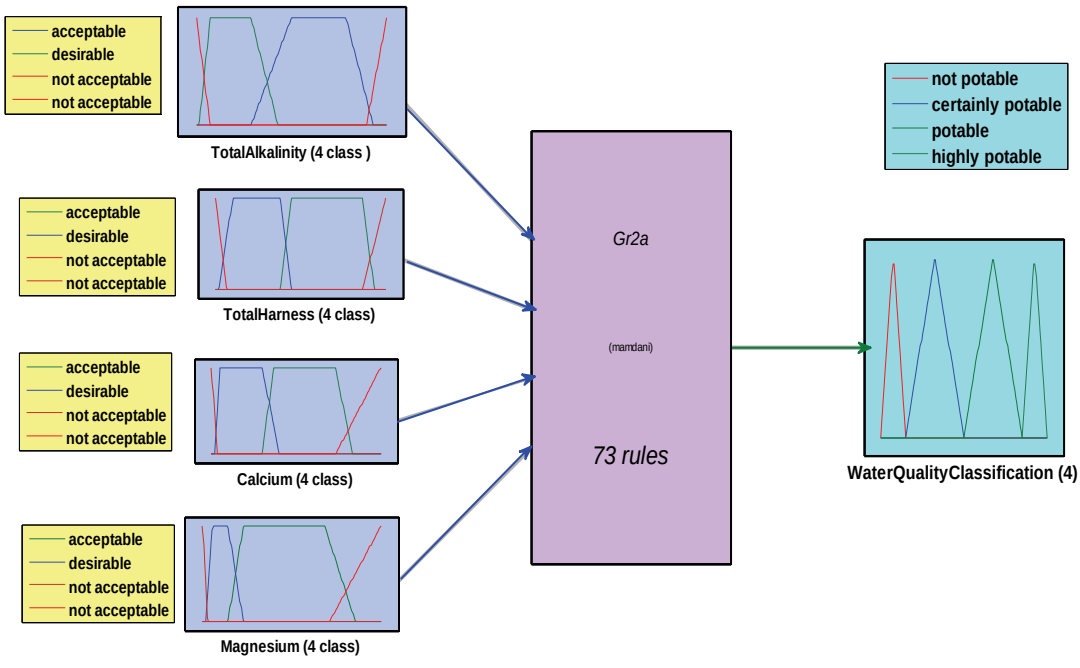

Figure 4. Block diagram for fuzzy logic model for Second Group water quality parameters.

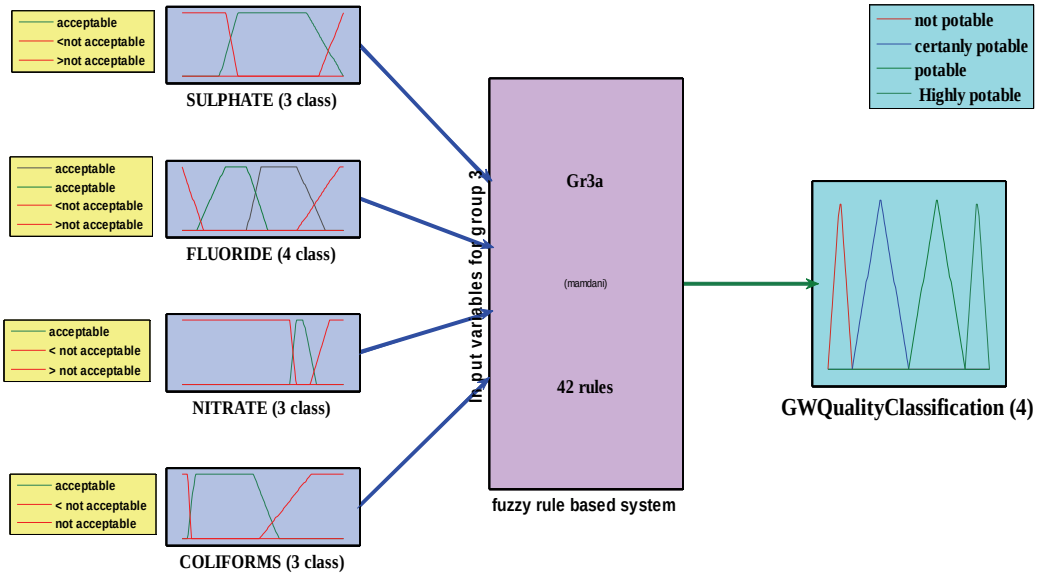

System Gr3a: 4 inputs, 1 outputs, 42 rules

Figure 5. Block diagram for fuzzy logic model for Third Group water quality parameters.

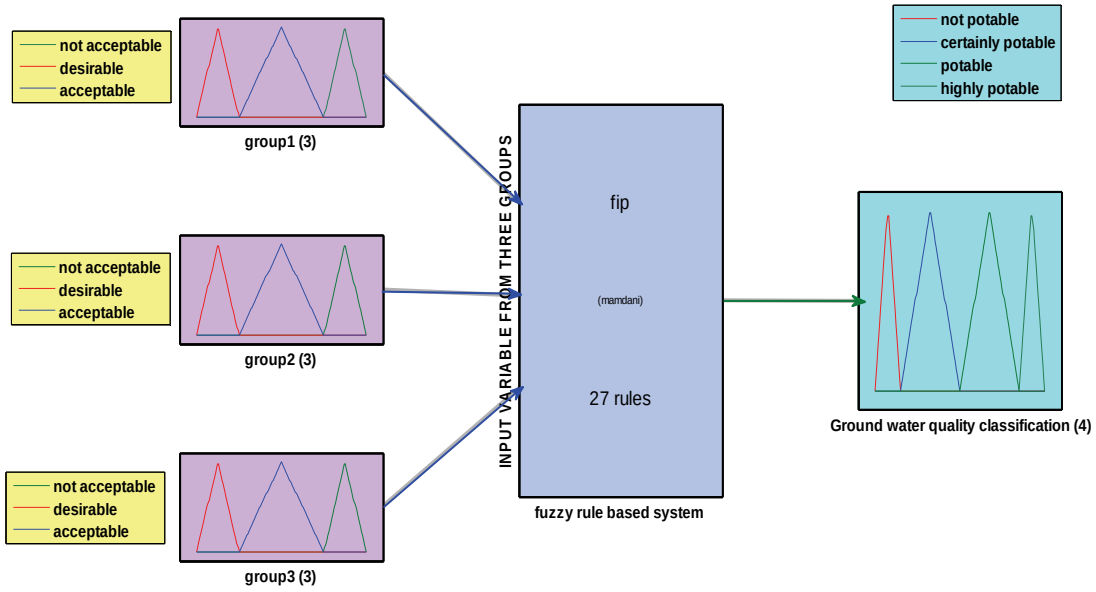

System FIP : 3 inputs, 1 outputs, 27 rules

Figure 6. Block diagram for fuzzy logic model Final groundwater quality assessment.

3.1 Fuzzy Logic and GIS Approach towards Groundwater Classification

A fuzzy rule based system is generated in which users classify the water according to given data in Desirable, Acceptable, Not acceptable, Rejected quality with re spect to different parameters, all connected using AND operator. The user's feedback is also taken with respect to overall quality for different parameters connected by AND operator. For example, one of the feedbacks taken may be like this, If TDS = good AND pH = medium and Sulphate = good then, overall water quality = What ? After this, Delphi's technique is applied to converge the

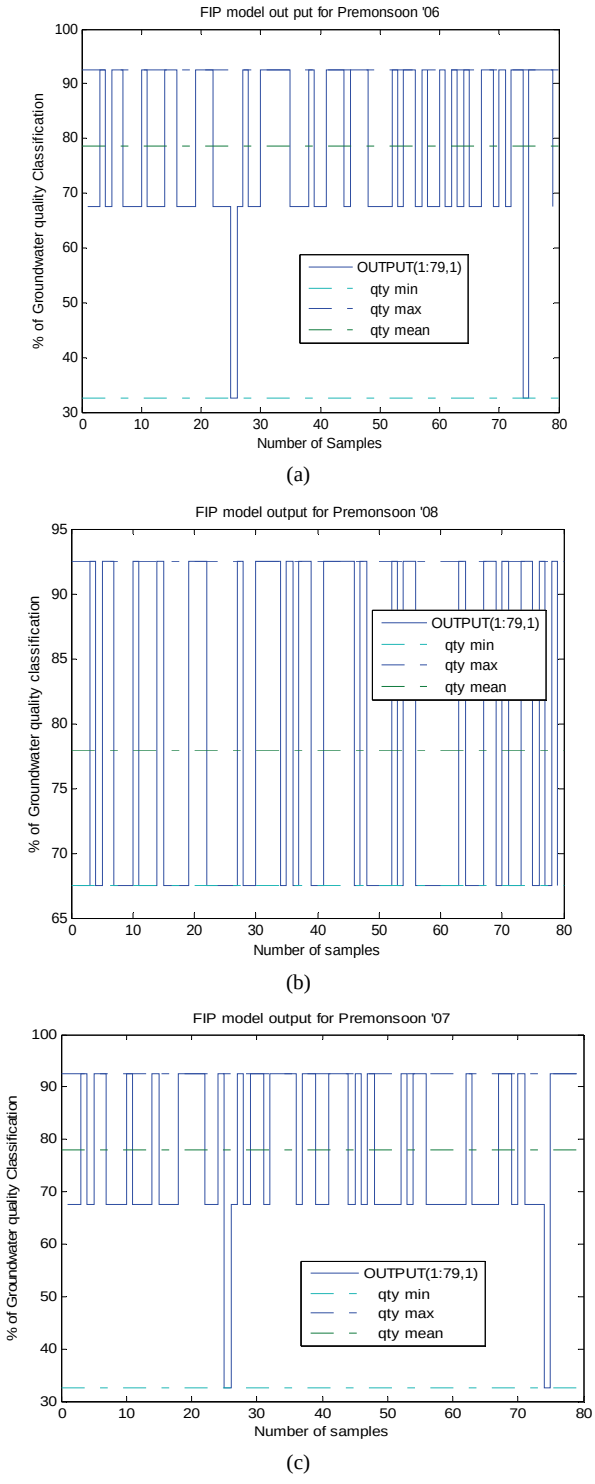

Figure 7. Subsurface water potable frequency during pre-monsoon periods. (a) 2006; (b) 2007; (c) 2008.

feedback of various users to a single value. A degree of match has been computed between the user's perception and field data for different parameters and for every type of water quality viz. good (Desirable) medium (Acceptable) or bad (Not Desirable). The water quality for which degree of match is the highest and was considered to represent the quality of the water sample.

4. Results and Discussions

Physio-chemical groundwater quality assessment by deterministic method for drinking groundwater usage on the basis of einght water quality parameters were compared with the concentration in the water with point value prescribed limits. In case Groundwater quality model approach, these 8 parameters were divided in the four categories on the basis of expert opinion having their importance with respect to drinking water quality criteria.

The hydro chemical analyses revealed that water samples in the study area was characterized by hard to very hard, fresh to brackish and alkaline in nature. The highly turbid water may cause health risk as excessive turbidity can protect pathogenic microorganisms from the effects of disinfectants and also stimulate the growth of bacteria during storage. Characteristic by pH values, most of the water samples were alkaline in nature which are well within permissible limit (6.5-8.5) and some of the samples have been found acceptable for usage and the ranges are between 6.5 and 9.2 meeting with BIS standards of IS: 10500:1991 and WHO (2006) guidelines. Based on Electrical Conductivity (EC) values measured all water samples Zone-I (Srirangam) are desirable (< 1 mS/cm) for potability. Potability maps for the Pre monsoon and post monsoon period is shown **Figures 8(a)**, **8(b)**, **8(c)**, **9(a)**, **9(b)** and **9(c)** for pre monsoon & post monsoon years 2006, 2007 and 2008 respectively.

5. Conclusions

The saying " A picture is worth a thousand words" is true for GIS applications in the field of human services as visual maps on client communities and their needs as an alternative to tables of numbers, charts or anecdotes not only make information easier to grasp but also provide more dimensions to study human service data. Customized maps created using GIS software can help human service professional to gain a better understanding of the client communities they serve, as illustrated by the needs assessment project. Apart from querying information on spatial and non spatial data, print output of the maps at user defined scales and extent, making of an integrated analysis on spatial and non spatial data, performing query on multiple themes simultaneously are some of the features of the health GIS model. It is difficult to understand the issues related to epidemic diffusion simply by groundwater quality analysis as it lacks spatial information. Therefore, combination of both groundwater quality parameters and GIS methods is very useful to researchers

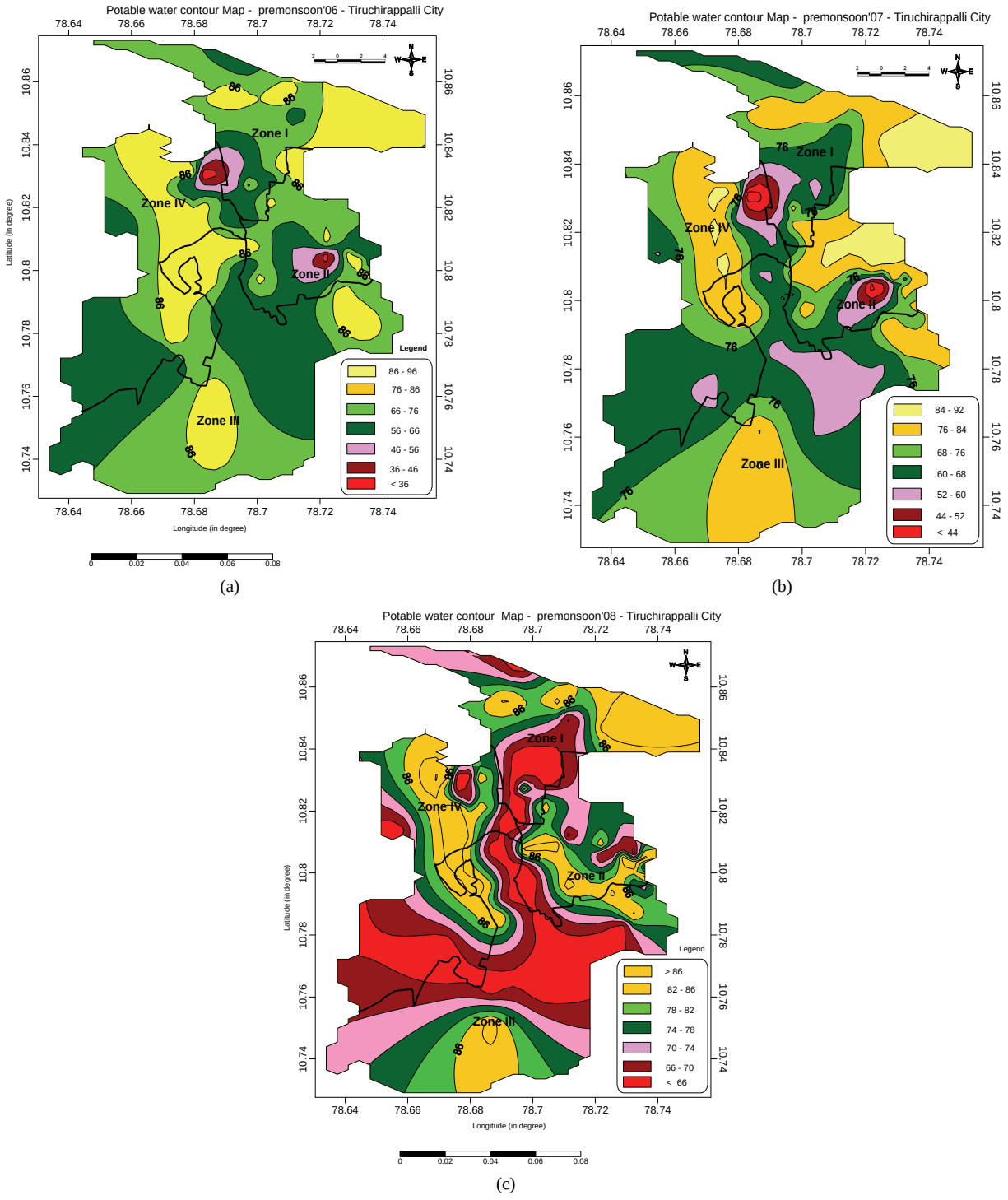

Figure 8. (a) Potability map of pre-monsoon 2006; (b) Potability map of pre-monsoon 2007; (c) Potability map of pre-monsoon 2008.

to model the health related issues as GIS provides efficient capacity to visualize the spatial data [19].

The quality of the groundwater of the Tiruchirappalli city was monitored in 79 sampling wells for 3 years and major recorded data revealed that the concentrations of cations and anions were above the maximum, desirable for human consumption. The Electrical Conductivity was found to be the most significant parameter within input parameters used in the modeling. The developed model enabled well to test the data obtained from 79 samples of

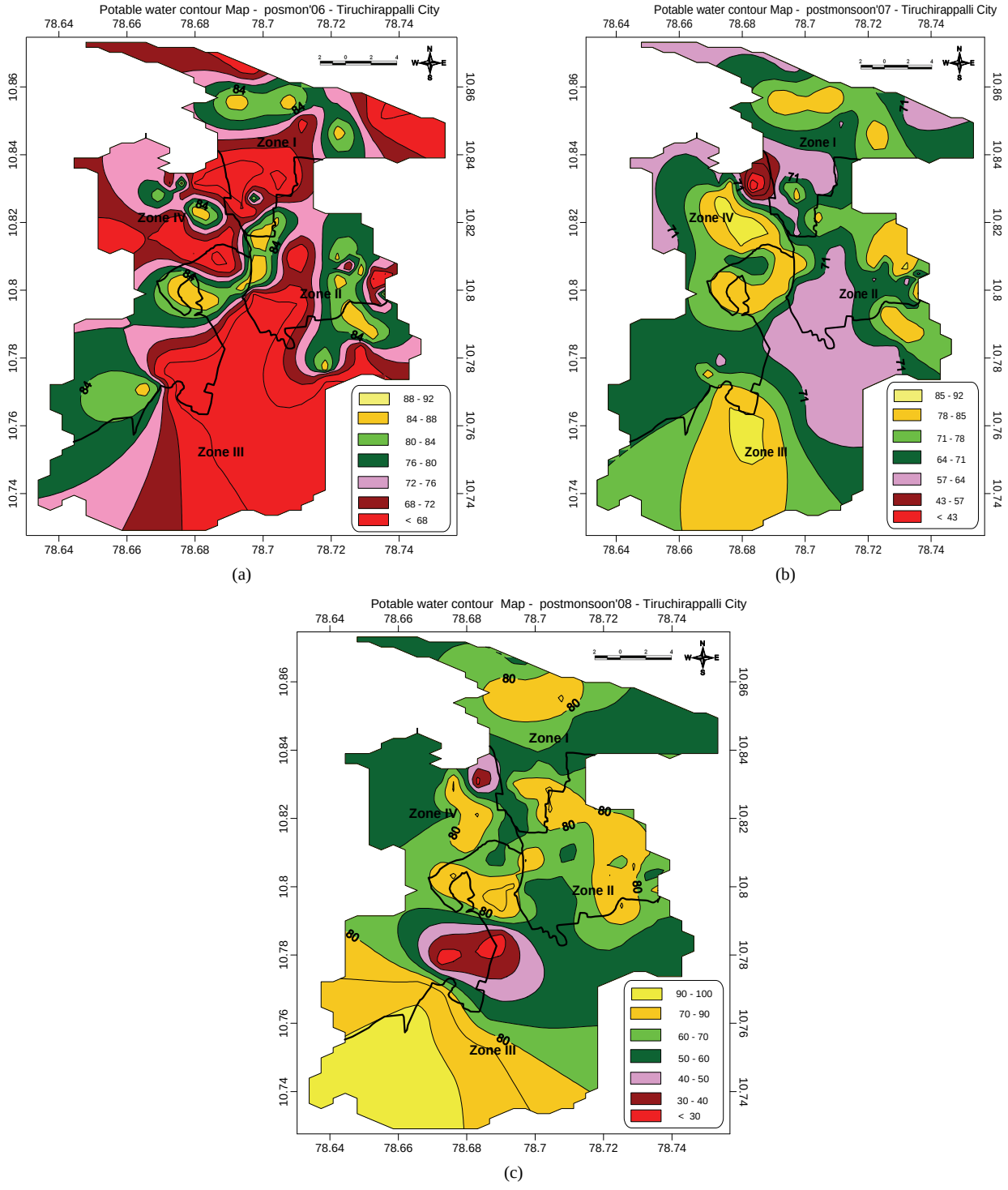

Figure 9. (a) Potability map of post-monsoon 2006; (b) Potability map of post-monsoon 2007; (c) Potability map of post-monsoon 2008.

bore wells of Tiruchirappalli city.

- The groundwater in Tiruchirappalli meets all WHO drinking water standards with in the range of 67.5% to 92.5% for potable during pre monsoon condition of all the sampling durations.
- As the sampling station of 24 and 73 were found in non potable condition due to vicinity of waste-water discharging areas and solid waste dumping sites.
- During post monsoon all the sampling stations

satisfies WHO drinking water standards within in the range of 67.5% to 92.5%.

- At the stations 59, 62 and 72 were reported with non potablity of 32.5% due to unhealthy environmental conditions of wastewater and local waste dumps near by the sampling points.
- Solid wastes including sledges were disposed, and without any pre treatment before dumping and no protection towards the subsurface water for potability.
- In the previous study by the authors the subsurface water quality in Ariyamangalam, Zone Tiruchirappalli City Corporation was seriously under threat by carbonates and sulphates near the sampling points of Ariyamangalam zone. Also contaminated by several pollutants as Ariyamangalam itself was currently polluted due to the waste dumping site and improper waste water vicinity.
- Without immediate response, the subsurface water is currently degrading its consumption quantity and will not be potable in near future if the proper steps have not been taken care.

6. Acknowledgements

The first author gratefully acknowledges the support by Fellowship under TEQIP, MHRD, and Govt. of India for his Doctoral study. The authors wish to express their sincere appreciation to the anonymous reviewers for their valuable comments to enhance the quality of this paper. Special thanks to Jay Krishna Thakur, Institute of Geosciences, Martin Luther University, Halle (Saale), Germany and Sundarambal Palani, Tropical Marine Science Institute, National University of Singapore, Singapore for their constant support in preparation of this manuscript. Special thanks go to M. Kannan (SASTRA) in GIS work, field activities and in the laboratory measurement of this study. Sincere thanks to Prof. K. Palanichamy, Civil Engineering Department, National Institute of Technology, Tiruchirappalli, India for providing constant encouragement throughout his research study. The authors wish to express their sincere thanks to the anonymous reviewers for their valuable comments to enhance the quality of this paper.

7. References

[1] R. D. Deshpande and S. K. Gupta, "Water for India in 2050: First Order Assessment of Available Options," *Current Science*, Vol. 86, No. 9, 2004, pp. 1216-1224.

[2] Z. Chen, G. H. Huan and A. Chakma, "Hybrid Fuzzy-Stochastic Modeling Approach for Assessing Environmental Risks at Contaminated Groundwater Systems," *Journal of Environmental Engineering*, Vol. 129, No. 1, 2003, pp. 79-88.

[3] C. O. Cude, "Water Quality Index: A Tool for Evaluation Water Quality Management Effectiveness," *Journal of the American Water Resources Association*, Vol. 37, No. 1, 2001, pp. 125-137.

[4] S. Dahyia, D. Datta and H. S. Kushwaha, "A Fuzzy Synthetic Evaluation Approach for Assessment of Physio-Chemical Quality of Groundwater for Drinking Purposes," *Environmental Geology*, Vol. 8, No. 1-2, 2005, pp. 158-165.

[5] S. M. Liou, S. L. Lo and S. H. Wang, "Generalized Water Quality Index for Taiwan," *Environmental Monitoring and Assessment*, Vol. 96, No. 1-3, 2004, pp. 35-52. http://www.springerlink.com/content/t425516215118557/

[6] K. Sivasankar and R. Gomathi, "Fluoride and other Quality Parameters in the Groundwater Samples of Pettaivaithalai and Kulithalai Areas of Tamil Nadu, Southern India," *Water Quality Exposure Health*, Vol. 1, 2009, pp. 123-134.

[7] T. Subramani, L. Elango and S. R. Damodarasamy, "Groundwater Quality and its Suitability for Drinking and Agricultural Use in Chithar River Basin, Tamil Nadu, India," *Environmental Geology*, Vol. 47, No. 8, 2005, pp. 1099-1110.

[8] N. V. Kumar, S. Mathew and G. Swaminathan, "Fuzzy Information Processing for Assessment of Groundwater Quality," *International Journal of Soft Computing*, Vol. 4, No. 1, 2009, pp. 1-9. http://www.medwelljjournals.com/fulltext/ijsc/2009/1-9.pdf

[9] American Public Health Association, "Standard Method for Examination of Water and Waste Water," 21st Edition, American Public Health Association, Washington, D.C., 2005.

[10] Bureau of Indian Standard, "Indian Standard Specification for Drinking Water," BIS Publication No. IS: 10501, New Delhi, 1991.

[11] World Health Organization, "Guidelines for Drinking Water Quality Recommendation," 3rd Edition, World Health Organization, Geneva, Vol. 1, 2008.

[12] Z. Sen, "Fuzzy Groundwater Classification Rule Derivation from Quality Maps," *Water Quality Exposure Health*, Vol. 1, No. 1, 2009, 115-112.

[13] S. Liou and S. L. Lo, "A Fuzzy Index Model for Tropic Status Evolution of Reservoir Waters," *Water Research*, Vol. 96, No. 1, 2004, 35-52.

[14] N. Chang, H. W. Chen and S. K. King, "Identification of River Water Quality Using the Fuzzy Synthetic Evaluation Approach," *Journal of Environmental Management*, Vol. 63, No. 3, November 2001, pp. 293-305.

[15] L. Zadeh, "Knowledge Representation in Fuzzy Logic," *IEEE Transactions on Knowledge and Data Engineering*, Vol. 1, No. 1, 1989, pp. 89-100.

[16] M. F. Dahab, Y. W. Lee and I. Bogardi, "A Rule Based Fuzzy-Set Approach to Risk Analysis of Nitrate Contaminated Groundwater," *Water Science and Technology*, Vol. 30, No. 7, 1994, pp. 45-52.

[17] K. Schulz and B. Howe, "Uncertainty and Sensitivity Analysis of Water Transport Modeling in a Layered Soil Profile Using Fuzzy Set Theory," *Journal of Hydro informatics*, Vol. 1, No. 2, 1999, pp. 127-138.

[18] E. M. Mamdani, "Advances in the Linguistic Synthesis of Fuzzy Controllers," *International Journal of Man-Machine Studies*, Vol. 8, No. 6, 1976, pp. 669-678.

[19] N. V. Kumar, S. Mathew and G. Swaminathan, "A Preliminary Investigation for Groundwater Quality and Health Effects—A Case Study," *Asian Journal of Water, Environment and Pollution*, Vol. 5, No. 4, 2008, pp. 99-107.http://iospress.metapress.com/content/a11884502w687x74/.

Journal of Geographic Information System, **2010, 2, 163-168**
doi:10.4236/jgis.2010.23023 Published Online July 2010 (http://www.SciRP.org/journal/jgis)

Contribution of Topographically Explicit Descriptors of Landscape Measures for Application in the Vector Data Environment

Jomaa Ihab[1], Auda Yves[2]
[1]*Remote Sensing Center-National Council for Scientific Research, Riad El Solh, Beirut, Lebanon*
[2]*LMTG, CNRS - Université Paul Sabatier - Observatoire Midi-Pyrénées, Avenue Edouard Belin, Toulouse, France*
E-mail: *ihab@cnrs.edu,Ib, yves.auda@Imtg.obs-mip.fr*
Received February 23, 2010; *revised March* 27, 2010; *accepted April* 5, 2010

Abstract

Digital terrain models (DTMs) are not commonly used to integrate for landscape spatial analysis. Two dimensional patch-corridor-matrix models are prototypes in landscape spatial ecology analysis. Previous studies have motivated ecologists to integrate terrain models in landscape analysis through 1) adjusting areas and distance calculations prior computing landscape indices; 2) designing new indices to capture topography and 3) searching the possible relationship between topographic characteristics and vegetation patterns. This study presents new indices called Relative number of Topographic Faces (RTF) and Simplicity of topographic Faces (STF) that can be easily computed in a GIS environment, capturing topographical features of landscapes. Digital terrain model was first prepared and topographic units were extracted and installed in computing the suggested indices. Mountainous and rugged topography in Lebanon was chosen on a forested landscape for the purpose of this study. The indices were useful in monitoring changes of topographic features on patch and landscape level. Both indices are ecologically useful if integrated in landscape pattern analysis, especially in areas of rugged terrains.

Keywords: Landscape Indices, Topography, Forest, Digital Terrain Model, Patch, Lebanon

1. Introduction

Ecological concern was about quantifying patterns in the spatial heterogeneity of landscapes [1]. Although landscape indices capture important aspects of landscape patterns, one of the main engines of patterning remains poorly or uninstalled into the spatial analysis of landscapes [2-7]. Topographically neutral landscapes remain the backbone of landscape pattern analysis, especially when two dimensional patch-corridor-matrix models are integrated into friendly and easy to use packages of landscape analysis.

Although, ecologists know well the effect of topography on patterns and processes, trials are still rare to integrate topographical characteristics in a landscape spatial analytical approach. Previous proposals on introducing topography to landscape indices include 1) correcting surface areas and distances prior to landscape metric computation, 2) designing new indices that could relate vegetation pattern with topographical characteristics, and 3) use of statistical models relating topography with vegetation patterns. New indices will continue to derive which causes ecologists to face long list metrics [8]. New emerged topographically related landscape metrics are therefore, under prediction, since without topographical analysis and relation to metrics in certain areas will induce misleading final interpretation. Studies still urge scientists for further topographical insertions within metric computations and/or development of simple approaches that could be readily implemented into familiar software packages with regard to ecologists [9,10].

Landscape ecology has started with oversimplification in conceptualizing and analyzing landscapes as mosaic of discrete patches [11,12]. Nowadays, it is being directed toward the utilization of surface metrics together with patch metrics for quantifying landscape patterns [13]. Surface metrics are to be used for continuous representation of spatial heterogeneity but unlike patch metrics they are less accessible for direct computation to the hand of landscape ecologists. A simple easy to use topography related indices remains as a priority.

Developing landscape indices requires deep investigations with trials in order to eliminate redundancy of information [14,15]. Ecological indicators also need to capture the complexities of the ecosystem yet remain simple enough to be easily and routinely monitored [16]. The concept of landscape ecology does not provide well developed and easy to apply methodology for analyzing pattern and dynamics in landscapes with rugged topography.

Topography results variation in community structure, composition and succession pathways [17,18] and influences the frequency, spread, extent, and distribution of natural disturbances [19,20]. Ecosystem dynamics also demonstrated interactions with topography [21]. Relation of topography in forming landscape pattern has not well understood yet.

Topographical analysis is consequently needed for the completion of relating pattern to processes. Accomplishing this concern, a first step is providing ecologists quantifiable topographical information in an easy approach. The present study introduces two landscape indices that account for topography on patch and landscape level of ecological hierarchy. Rugged topography of forest landscapes in Lebanon was chosen for applying such indices.

2. Materials and Methods

2.1. Study Area

Situated on the eastern coast of the Mediterranean Sea, Lebanon occupies the junction between Europe, Asia and Africa, with a surface area of 10,452 km^2 and it is characterized by four main geomorphological units: narrow *Coastal Plain* and two mountain chains (*Mount Lebanon* and *Anti Lebanon*) separated by a fertile and relatively elevated plateau at an elevation of 700 to 1100 m named *Bekaa Plain* (**Figure 1**). The geomorphological units are

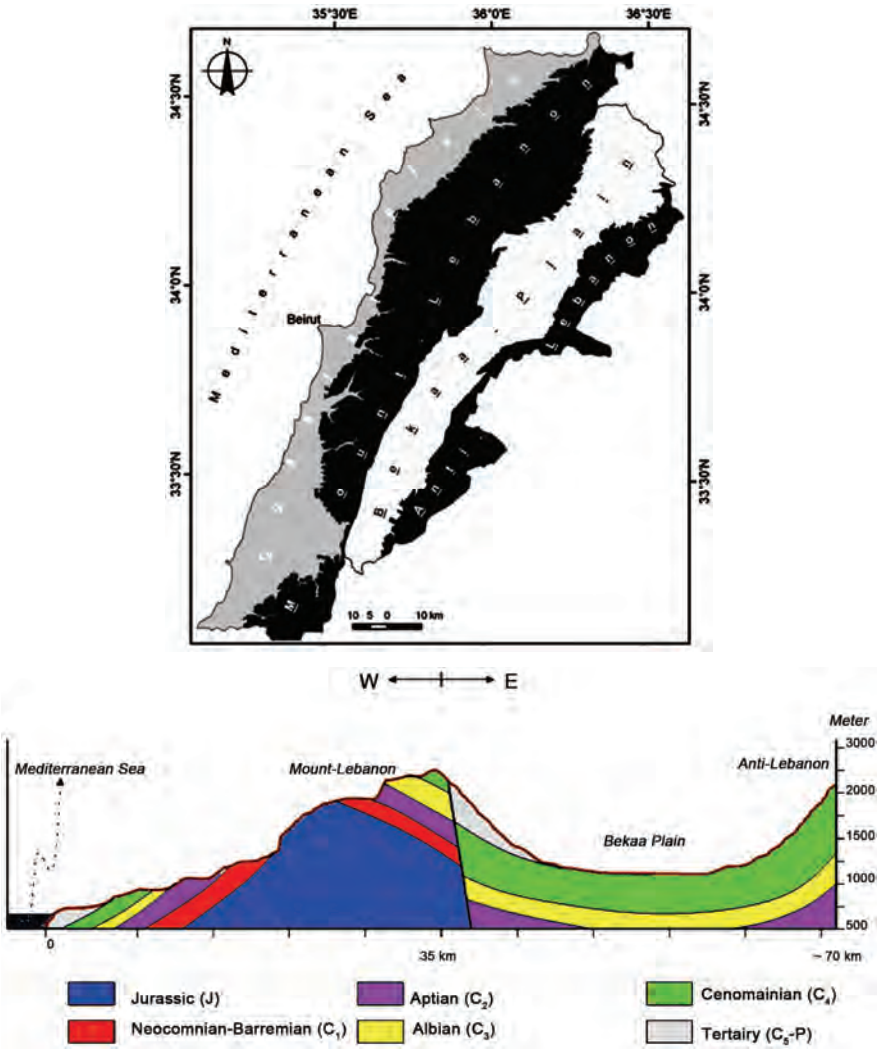

Figure 1. Major geomorphological units of Lebanon (top); East-west cross-section across Lebanon (below).

oriented from northeast to southwest. The two mountain chains are almost of rugged topography due to the dominant hard carbonate rocks, and the occupy about 70% of the total Lebanese territory.

2.2. Preparatory Phase

First, the Triangulated Irregular Network (TIN) of the entire landscape was performed. A TIN is a vector-based representation of physical land surface resulted from the three dimensional coordinates (x, y and z). It is constructed of nodes that are arranged in a network of non-overlapping triangles. The points of a TIN are distributed based on algorithm that uses locations where most necessary to an accurate representation of the terrain. A TIN comprises a triangular network of vertices connected by edges to form a triangular tessellation. Points of triangles are widened in a lower density when terrains have little variations in heights. Conversely, density of points increases in terrains of intense topographic variations. Construction of a TIN requires elevation data of the terrain as points or adapted from contour lines. A TIN is typically based on a Delaunay triangulation that entails points capturing changes in surface forms. Unlike unique sized grid cells, triangles of variable dimensions in a TIN are able to reflect large complexity of relief, providing slope gradient and aspect.

TIN GIS layer was prepared for Lebanon using 50 m equidistance contour lines in the GIS system, using the software ArcGIS 9.2. Forest maps of 1965 [22,23] were overlapped digitally onto the TIN vector layer where topography of each forest patch of both periods was obtained. The geographic space of a patch with triangles (faces or tiles of the TIN) of slope gradients and aspects was dissolved or generalized into contiguous non-overlapping triangles that were first derived from the detailed triangulation of the TIN. For the purpose of this study, triangles of slope gradient were chosen.

2.3. Relative Number of Topographic Faces

Relative number of Topographic Faces (RTF) is one of the suggested new indices that fits within the descriptive modeling of landscape patterns. RTF captures topographical characteristics of vegetation patterns (forest patches) at the level of individual TIN tiles. It is based on computing the number of topographic faces in a forest patch relative to its surface area with a landscape as follows:

$$RTF = \frac{Number\ of\ topographic\ faces}{Area(km^2)}$$

where *Number of topographic faces* is the total variation of landform within a forest patch and *Area* is the spatial extent of the same forest patch in square kilometer.

RTF was computed using GIS facilities of relating each forest patch to other attributable data that were derived from the TIN layer. The number of TIN faces was obtained for each forest patch after overlapping procedures. A one-to-one link was set between GIS tables that hold data about patches surface areas and their number of topographic faces. This database link has enabled the calculation of RTF.

2.4. Topographic Faces Degree of Simplicity

The relative number of topographic faces will reflect one side of a patch topographic feature. The RTF could not perceive the percent area of each topo-face within a patch, which will not completely reflect the topographic characteristics of landscapes. The simplicity of topographic faces (STF) is an added developed index in this study that accounts for percent area of each topo-face within a patch or landscape. STF was computed at the landscape level through the following equation:

$$STF = \frac{\sum_{i=1}^{n} hpp}{N}$$

where *hpp* is the highest percent of area of a topo-face for each patch within the landscape; and *N* is the total number of patches. STF will oscillate between 0 and 100%. Higher STF values is the result of a landscape with larger topo-faces within patches, *i.e*. topographically more homogeneous landscape. Two patches of similar size and equal RTF would probably have completely different STF, which lead us to clearly understand their degree of topographic complexity.

2.5. Application of the Developed Indices

Figure 2 illustrates the different steps followed in the computation of the indices "RTF and STF", starting from contour lines to creation of TIN layer and overlapping forest maps.

Each of the obtained triangles in a forest patch represents a slope gradient and aspect. Within a forest patch, two neighboring triangles of the same slope characteristics were dissolved in a unified larger triangle. Joined triangles or faces have equal slope gradient. These faces were counted within each forest patch.

For the purpose of this work, forest maps of 1965 and 1998 for Lebanon were chosen. Changes in RTF were investigated between different forest patches of both years that explain the trend of forest dynamics, *i.e.*, whether forest patches are moving toward either complex or simple topography.

3. Results

The Relative number of Topographic Faces (RTF) dem-

onstrated sensitivity for variations in patch size and topographic complexity. The total number of topographic faces increases with increasing patch size (**Figure 3(a)**). In Lebanon, it appeared that the increasing trend of topo-faces number is even faster than patch size increase. Topographically complex mountains are what causing such phenomenon; knowing the fact that mountains of Lebanon have intensive rugged topography [24]. In mountainous terrain, forest patches will accumulate topo-faces in accentuated manner as they increase in size. This fact required normalization of RTF to patch size (surface area) in order to buffer out the effect of patch-size-topo-faces relation (**Figure 3(b)**).

The largest patch of the 1965 forest map with an area of 68.6 sqkm has its RTF of 41. This means for each 1 sqkm of an area for this particular patch, 41 facets or topographic faces existed. The topographic complexity or RTF for another patch, half size of the previous one, was 95. The smallest patch size (0.26 sqkm) has RTF of 148. Another example, two patches of almost similar size (0.53 sqkm) have largely different RTF which are 311 and 18. The complexity of the topographic features of a geographic location affects the RTF value of a patch. RTF reflected the degree of ruggedness or topographic complexity of a forest patch.

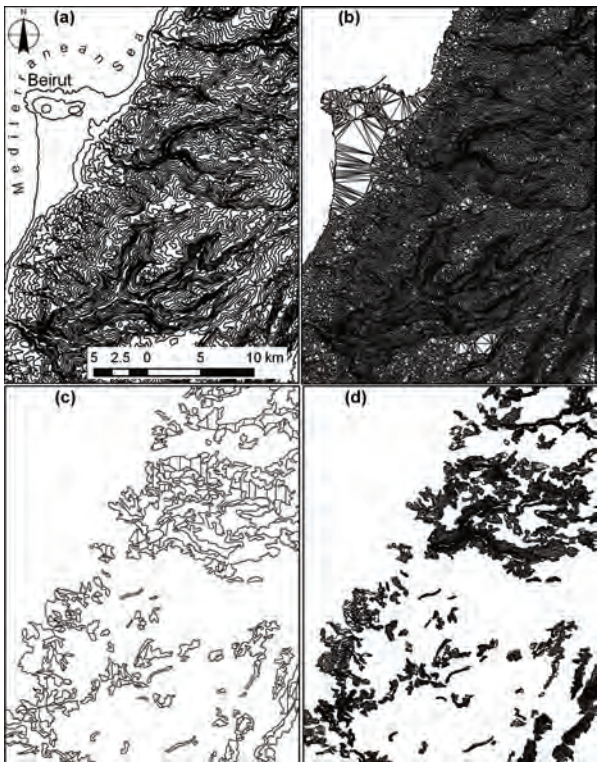

Figure 2. Steps followed to obtain topographic faces of forest patches for the computation of the proposed indices. (a) contour lines of 50 m equidistance; (b) preparation of the TIN; (c) Forest patches; (d) topographic faces within each forest patch.

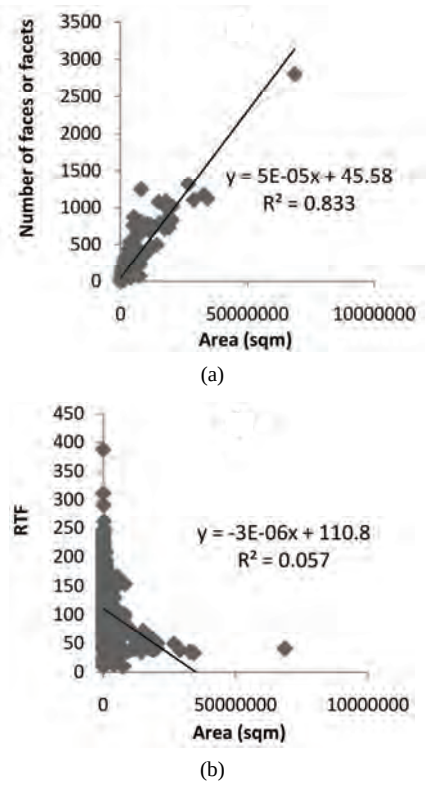

Figure 3. (a) The number of topographic faces with relation to patch area; (b) Relative number of Topographic Faces (RTF) after area normalization.

In addition to the path-based computation of RTF, this index could be computed on landscape level. In 1965, the topographic complexity of the forest patches, entire landscape, was 106, *i.e.*, the mean RTF. The mean RTF demonstrated an important increase, reaching more than double the previous value, *i.e.* 264, in the year 1998. The lowest RTF that characterizes forest of 1965 was 9 and its maximum value was 311 (**Figure 4**). These values have changed to set between 2 and 688 in 1998. Forests have moved toward geographic locations that are characterized by more topographic complexity. Mean forest patch size has decreased from 1.4 sqkm in 1965 to 0.2 sqkm in 1998, *i.e.*, the size of the forest patches decreased by about 75% for both periods. Forests have moved or remained limited in unreachable geographical locations from point of view geomorphology, *i.e.*, moved toward topographically complex places. The simplicity of topographic faces (STF) on landscape level has changed from 32% in 1965 to 12% in 1998. The largest topographic face within a forest patch has decreased by 20% in the entire landscape. This landscape decrease in STF means that each forest patch is being divided into smaller areas of topo-faces.

On patch level, 1965 forests demonstrated a maximum STF of 83% that decreased to 54% in 1998. This largest STF was limited between 20 and 40% of slope gradient

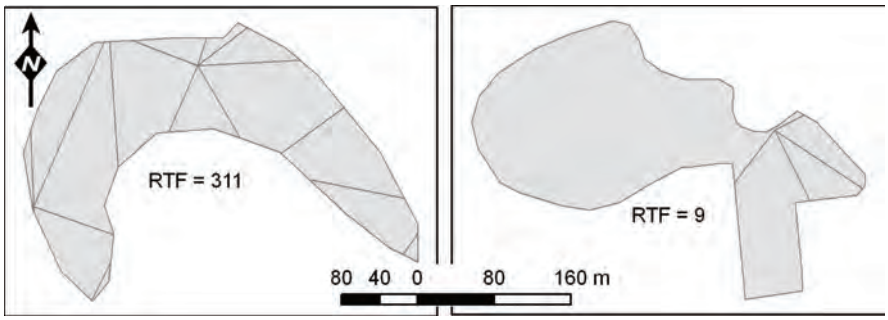

Figure 4. Two different forest patches showing minimum and maximum RTF of 1965 map.

in 1965 and between 27% and 44% of slope gradient in 1998.

4. Discussions and Conclusions

Metrics are still challenging for their ecological applications relating pattern to process. This study gives an insight about how to integrate topography into pattern analysis at the landscape or patch level. New landscape indices were proposed that could be computed in GIS system with automated method. Both indices account directly for topographic characteristics of a patch or landscape. They are designed to assess topographic variation, following detailed topographic segmentation of area through the triangulated irregular network (TIN). Analysis could undergo on any level of subdividing topographic units or faces. Also, a topographic face could remain in the possible smallest subdivision generated through TIN computation or generalization of faces also could be practiced depending on the study purpose. Detailed information of slope gradient or aspect was provided in TIN layer of GIS. The user has to decide whether to establish the analysis on the basis of slope gradient or aspect or on both divisions. Our example uses forests of Lebanon that are characterized by their mountainous habitat. In such rugged mountains, topography play prominent role in patterning the landscape. While landscape indices alone do not account for topographic characteristics of an area, the indices 'RTF and STF', as presented here, integrate topography in a simple manner without the need to pass into complicated transformation of grid computation suggested in previous studies [9]. Through, the computation of RTF and STF, forest patches are separated into different ranges of topographic complexity. Different landscapes could also be analyzed for variations topographic characteristics. The developed indices could also investigate changes of topography through different time periods. In Lebanon, forest patches demonstrated more topographical complexity when comparing forest maps of 1965 and 1998. During this period, such increase in topographic complexity was accompanied with patch size decrease. Some forest patches have moved towards less topographically complex areas while others forest residues remainned in rugged areas. RTF has doubled with 20% decrease in STF and 75% decrease in patch size. This reveals the importance and explains what valuable information could be obtained of computing RTF and STF together with other landscape indices. Previous studies were satisfied in monitoring changes of landscape spatial patterning through the computation of landscape indices that have no relation to topography although the landscapes were mostly of mountainous characteristics. Many landscape indices have limited or no/undiscovered relation to processes. It is therefore, recommended to work on landscape indices basis that are more creditable to answer changes in processes. Processes are largely connected to topography as well as its changes [6]. The presented indices are easy to apply in a GIS system. Their automation is also possible through their future implementation in a landscape spatial analysis software package.

5. References

[1] R. V. O'Neill, J. R. Krummel, R. H. Gardner, G. Sugihara, B. Jackson, D. L. DeAngelis, B. T. Milne, M. G. Turner, B. Zygmunt, S. W. Christensen, V. H. Dale and R. L. Graham, "Indices of Landscape Pattern," *Landscape Ecology*, Vol. 1, No. 3, 1988, pp 153-162.

[2] N. Lele, P. K.Joshi and S. P. Agrawal, "Assessing Forest Fragmentation in Northeastern Region (NER) of India Using Landscape Matrices," *Ecology Indicators*, Vol. 8, No. 5, 2008, pp. 657-663.

[3] I. Jomaa, Y. Auda, B. Abi Saleh, M. Hamze and S. Safi, "Landscape Spatial Dynamics over 38 Years under Natural and Anthropogenic Pressures in Mount Lebanon," *Landscape and Urban Plan*, Vol. 87, No. 1, 2008, pp. 67-75.

[4] M. Li, C. Huang, Z. Zhu, H. Shi, H. Lu and S. Peng, "Assessing Rates of Forest Change and Fragmentation in Alabama, USA, Using the Vegetation Change Tracker Model," *Forest Ecology and Management*, Vol. 257, No. 6, 2009, pp. 1480-1488.

[5] W. Kong, O. J. Sun, W. Xu and Y. Chen, "Changes in Vegetation and Landscape Patterns with Altered River Water-Flow in Arid West China," *Journal of Arid Envi-*

ronments, Vol. 73, No. 3, 2009, pp. 306-313.

[6] M. Sano, A. Miyamoto, N. Furuya and K. Kogi, "Using Landscape Metrics and Topographic Analysis to Examine Forest Management in a Mixed Forest, Hokaido, Japan: Guidelines for Management Interventions and Evaluation of Cover Changes," *Forest Ecology and Management*, Vol. 257, No. 4, 2009, pp. 1208-1218.

[7] I. Jomaa, Y. Auda, M. Hamze, B. Abi Saleh and S. Safi, "Analysis of Eastern Mediterranean Oak Forests over the Period 1965-2003 Using Landscape Indices on a Patch Basis," *Landscape Research*, Vol. 34, No. 1, 2009, pp. 105-124.

[8] E. J. Gustafson, "Quantifying Landscape Spatial Pattern: What is the State of the Art?" Ecosystems, Vol. 1, No. 2, 1998, pp. 143-156.

[9] B. Dorner, K. Lertzman and J. Fall, "Landscape Pattern in Topographically Complex Landscapes: Issues and Techniques for Analysis," *Landscape Ecology*, Vol. 17, No. 8, 2002, pp. 729-743.

[10] S. Hoechstetter, U. Walz, L. H.Dang and N. X. Thinh, "Effects of Topography and Surface Roughness in Analyses of Landscape Structure—A Proposal to Modify the Existing Set of Landscape Metrics," *Landscape Online*, Vol. 3, 2008, pp. 1-14.

[11] R. T. T. Forman, "Land Mosaic: The Ecology of Landscapes and Regions," Cambridge University Press, Cambridge, 1995.

[12] M. G. Turner, R. H. Gardner and R. V. O'Neill, "Landscape Ecology in Theory and Practice: Pattern and Process," Springer, New York, 2001.

[13] K. McGarical, S. Tagil and S. A. Cushman, "Surface Metrics: An Alternative to Patch Metrics for the Quantification of Landscape Structure," *Landscape Ecology*, Vol. 24, No. 3, 2009, pp. 433-450.

[14] B. Traub and C. Kleinn, "Measuring Fragmentation and Structural Diversity," *Forstw Centralblatt*, Vol. 118, 1999, pp. 39-50.

[15] S. A. Cushman, K. McGarigal and M. C. Neel, "Parimony in Landscape Metrics: Strength, Universability, and Consistency," *Ecology Indicators*, Vol. 8, No. 5, 2008, pp. 691-703.

[16] V. H. Dale and S. C. Beyeler, "Challenges in the Development and Use of Ecological Indicators," *Ecology Indicators*, Vol. 1, No. 1, 2001, pp. 3-10.

[17] W. H. McNab, "Terrain Shape Index: Quantifying Effect of Minor Landforms on Tree Height," *Forest Science*, Vol. 35, No. 1, 1989, pp. 91-104.

[18] J. L. Ohmann and T. A. Spies, "Regional Gradient Analysis and Spatial Pattern of Woody Plant Communities of Oregon," *Ecological Monographs*, Vol. 68, No. 2, 1998, pp. 151-182.

[19] W. H. Romme and D. H Knight, "Fire Frequency and Subalpine Forest Succession along a Topographic Gradient in Wyoming," *Ecology*, Vol. 62, No. 2, 1981, pp. 319-326.

[20] M. G. A. Kramer, A. J. Hansen and M. L. Taper, "Abiotic Controls on Long-Term Windthrow Disturbance and Temperate Rain Forest Dynamics in Southeast Alaska," *Ecology*, Vol. 82, No. 10, 2001, pp. 2749-2768.

[21] F. J. Swanson, T. K. Kratz, N. Caine, R. G. Woodmansee, "Landform Effects on Ecosystem Patterns and Processes," *Bio-Science*, Vol. 38, No. 2, 1998, pp. 92-98.

[22] K. El Husseini and R. Baltaxe, "Forest Map of Lebanon at 1/50,000 Scale," Forestry Education, Training and Research Project, Green Plan, Lebanon. United Nations Special Fund/FAO, 1965.

[23] MOA/MoE, "Landcover Map of Lebanon for the Year 1998 (MOS: Mode d'Occupation du Sol)," Prepared by the Lebanese National Council for Scientific Research (CNRS)-Remote Sensing Center with the Collaboration of IAURIF (Institut d'Aménagement et d'Urbanisme de la Région d'Ile de France). LEDO Program, UNDP, Ministry of Agriculture and Ministry of Environment (Lebanon), 2002.

[24] B. Hakim, "Recherches hydrologiques et hydrochimiques sur quelques karst méditerranéennes: Liban, Syrie et Maroc," Publications de L'université Libanaise, Section des études géographiques,Tome 2, 1985, p. 701.

Journal of Geographic Information System, **2010, 2, 169-176**
doi:10.4236/jgis.2010.23024 Published Online July 2010 (http://www.SciRP.org/journal/jgis)

Neotectonic Evidences of Rejuvenation in Kaurik-Chango Fault Zone, Northwestern Himalaya

Moulishree Joshi[1], Girish Chandra Kothyari[2], Arun Ahluvalia[3], Pitambar Datta Pant[1]
[1]*Department of Geology, Kumaun University, Nainital, Uttarakhand, India*
[2]*Institute of Seismological Research, Gandhinagar, Gujarat, India*
[3]*Centre for Advanced Studies in Geology, Panjab University, Chandigarh, India*
E-mail: *kothyarigirish_k@rediffmail.com, moulishreej@yahoo.com*
Received April 28, 2010; *revised May* 30, 2010; *accepted June* 6, 2010

Abstract

Neotectonic investigations using morphotectonic parameters such as basin asymmetry, drainage anomalies, digital data interpretation and geomorphic field evidences were carried out in Satluj river valley downstream of Khab in the Kaurik Chango Fault (KCF) zone. The study reveals the presence of a north-south trending fault which is similar to the KCF. Unpaired, tilted terraces, V shaped valleys, deep gorges and lakes are the manifestations of fault movement in the area. Presence of deformation structures preserved in the palaeolake profile at Morang indicates that the area has also been seismically active in the past. In this paper we present a conceptual model of the formation of lakes in KCF zone. Morphometric analysis was carried out with the help of Digital Elevation Models (DEMs) and field investigations.

Keywords: Neotectonics, Kaurik Chango, Kinnaur, Satluj

1. Introduction

Himalayan mountain range was created as a result of the collision of the Indian and the Asian plate. Ensuing tectonic turmoil is witnessed in the form of intra-continental deformation along major faults and thrusts [1-4]. The Himalayan region is dissected by several NW-SE trending regional thrusts namely Indo Tsangpo Suture Zone, Main Central Thrust and Main Boundary Thrust. These thrust planes and their subsidiary fault systems are the foci of several devastating earthquakes. In the Satluj-Spiti river valleys, a number of N-S trending faults have disturbed the Precambrian-Palaeozoic succession of the Tethys Himalaya [5-8]. Kinnaur lies in the Higher Himalayan region between Main Central Thrust (MCT) and Indo-Tsangpo Suture Zone (ITSZ).

The expression of active tectonism in Kinnaur is reflected in tilted terraces, V shaped valleys, convex slopes, rampant landslides and gorges. Kinnaur is a seismically active segment of the Himalaya. A major earthquake of magnitude > 6.8 occurred in this region in 1975 [9]. The region exhibits diverse deformation including strike-slip, normal and thrust faulting [10]. Kaurik-Chango fault has been studied in detail by several workers [9-13]. Several palaeolake profiles have been reported along the Kaurik Chango fault in the upper Spiti valley [10,12-15]. However, research has not been done in the area between Khab and Akpa. This paper is an attempt to study the neotectonic activity in the area using morphotectonic parameters. The study area lies between 78˚00´ and 79˚00´ E and 31˚25´ to 32˚ N in the rugged Higher Himalayan terrain characterized by barren slopes and steep gradient.

2. Geology of the Area

Satluj River has been studied in detail by a number of workers [7,16-19]. The study area comprises thick succession of medium to high grade metamorphic rocks and their sedimentary cover. The succession is emplaced by granite intrusions of varying ages. Rocks of Vaikrita and Haimanta Groups are exposed in the region **Figure 1(a)**. Vaikrita Group comprises psammatic gneiss with quartzite bands, banded gneiss, granite gneiss, quartz mica gneiss. Haimanta Group comprises grey-purple quartzites, black carbonaceous phyllites and quartz mica schist interbedded with amphibolites and calc schists [19].

Figure 1(b) shows the SRTM image of the study area. River Spiti takes an abrupt southerly turn and flows parallel to the Kaurik-Chango fault near Sumdo. Seven terraces have been observed on the eastern bank [19]. There

is no evidence of terraces on the western bank. This may be due to the shifting of the river westward owing to the uplifted eastern block of the Kaurik Chango fault [20]. Quaternary fluvio-lacustrine deposits occur all along the Satluj valley downstream of Khab. These deposits are well preserved on the eastern bank. Several evidences gathered during the present work between Khab and Akpa indicate that Kaurik-Chango fault extends downward upto Akpa showing an uplifted eastern block. There are indications of tectonic and seismic activity similar to those in the Spiti valley.

In this paper, several morphotectonic indices were used to analyze the tectonic deformation in the area. Digital Elevation Model and satellite data were used to study the landscape evolution of the region. Field investigations were carried out to verify the data generated in the lab.

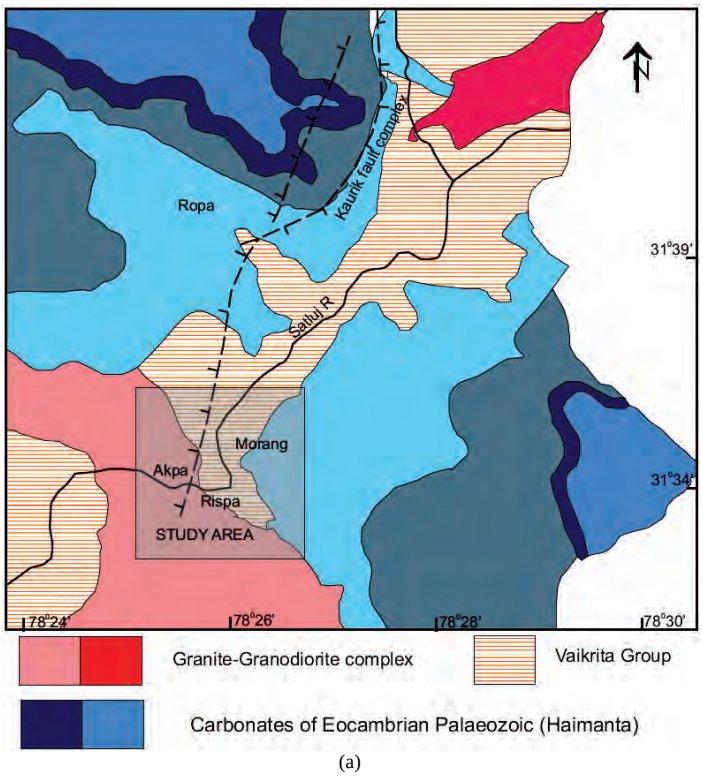

(a)

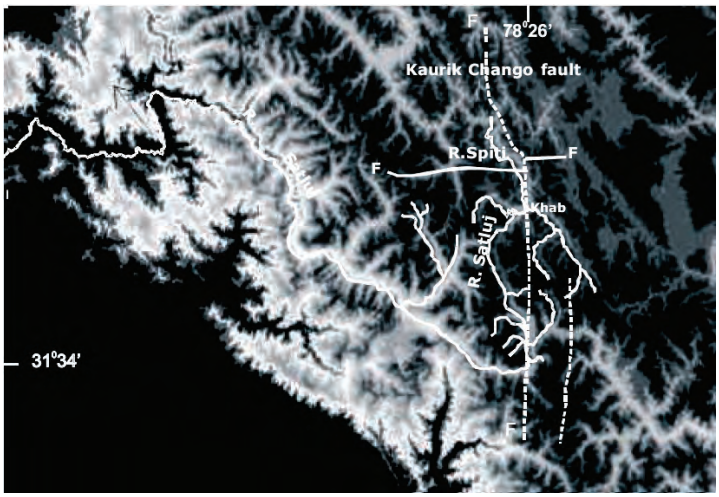

(b)

Figure 1. (a) Geological map of the study area (after Bhargava and Bassi, 1998); (b) SRTM image of Himachal Himalaya showing the location of the study areas. Also marked are the major drainage, thrusts and faults in the study area (image taken from NASA-SRTM program).

3. Methodology

Digital data interpretation was carried out with the help of a 3D Digital Elevation Model (DEM) and 2D topographic map to the scale 1:50,000. The softwares that were used to process the digital data are Surfer 9.6 and Globe Mapper. The Digital Elevation Model (DEM) **Figure 2(a)** of the area indicates significant changes in the topography and development of geomorphic features such as fault facets, abruptly changing river course, meandering and widening of the river, formation of terraces, vertical down cutting and formation of gorges. The uplifted eastern block can be seen clearly in the model. SRTM data of the study area was downloaded from the site (http: //srtm.csi.cgiar.org.). Basin asymmetry was calculated with the help of the SRTM data **Figure 2(b)**. Asymmetry factor AF is defined as AF = 100 (Ar/At) where Ar is the area of the basin to the right (facing downstream)

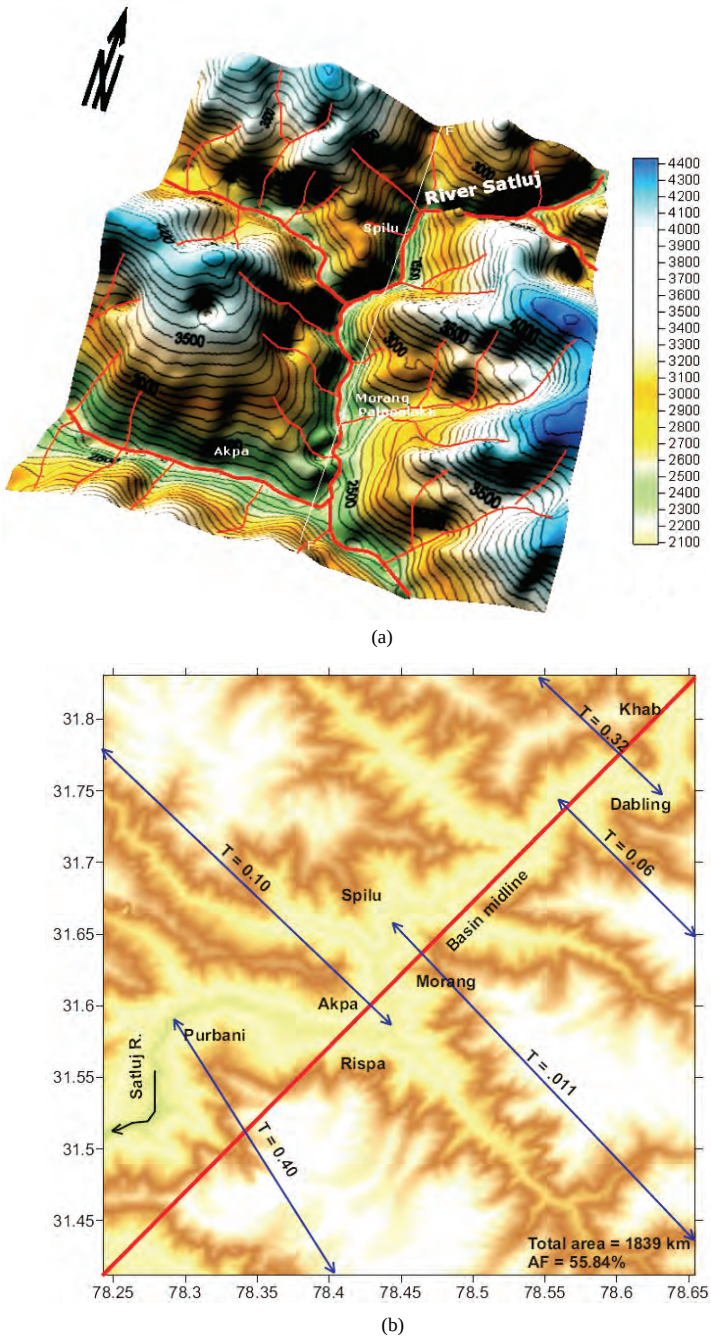

Figure 2. (a) Digital elevation model of the study area; (b) SRTM image of the study area showing basin asymmetry.

of the trunk stream and At is the total area of the drainage basin. In case of tectonic tilting, the value of AF becomes greater than 50 and the tributaries present on the tilted side of the main stream grow longer than those on the other side [21]. Transverse topographic symmetry factor (T) is defined as T = Da/Dd where Da is the distance from midline of the drainage basin to the midline of the active meander belt. Dd is the distance from the basin midline to basin divide. Value of T ranges between 0 to 1. T = 0 implies a perfectly symmetrical basin and T = 1, a perfectly asymmetrical one [20,21].

The landscape morphology of an area is governed by drainage of the rivers and their tributaries. Tectonic deformation has a direct impact on the drainage of that area. Tectonic deformation changes the channel slope which is responsible for variation in the channel morphology [22-27].

Drainage map and stream profiles were prepared with the help of the SRTM data. Valley incision is used to define relative uplift [24,28]. Cross valley profile for the Satluj basin was prepared with the help of SRTM data. A high valley-floor-width to valley-height ratio (seen in a broad valley) indicates tectonic stability. On the other hand, a low valley-floor-width to valley-height ratio (seen in a narrow valley) is associated with recent tectonic movement [29]. Asymmetry Factor calculated for the Satluj river basin is 55.84 indicating that the basin is asymmetrical. Transverse Topographic symmetry factor (T) calculated for the basin is given in **Table 1**. The data clearly shows that the basin is tilted towards the northwest **Figure 2(b)**.

4. Drainage and Stream Profiles

Drainage map of the area shows lower order streams joining the trunk stream at 90˚. The streams on the eastern block are longer and more in number compared to those on the western block. River Satluj flows through a crystalline basement belonging to Vaikrita Group. The area lies in the Kaurik-Chango fault zone. Quaternary reactivation of these faults has lead to bedrock incision by Satluj which flows in a gorge for most of its course in the study area **Figure 3(a)**. Longitudinal profile of Satluj shows a change in elevation near Spilu. Between Spilu and Akpa, the river has carved a deep gorge. This abrupt change in river morphology indicates that the river course in this region is tectonically controlled **Figures 3(b)**–**(c)**. Low valley floor width to height ratio suggests that the river is cutting downwards due to the tectonic activity in the region.

5. Geomorphology

The Satluj river basin under investigation is a rectangular basin with an area of 1839 sq km. The mean height of the basin is 3118.3 m. River Satluj is a 4th order stream as per the Horton–Strahler method of stream ordering. The highest point in the basin is about 4400 m. The total basin relief is 2400 m. The streams on the eastern block flow in escarpments along most of their course. Landslide cones and springs are rampant on the eastern block **Figure 3(e)**. The river flows in a narrow valley for most of its stretch from Spilu to Morang **Figure 4(a)**.

River Satluj has carved three levels of unpaired terraces at Akpa **Figure 4(b)**. The river in this region deflects abruptly towards the west. Tectonic rejuvenation of the N-S fault has also caused the tilting of the terraces **Figure 4(c)**. Landslide cones and springs are rampant along the N-S lineament **Figure 4(d)**.

In Morang, fluvio-lacustrine deposits are exposed for about 1 km **Figure 4(e)**. These deposits are 60-70 m thick. The sedimentary succession is represented by laminated clay-silty clay and horizontally bedded sands. Laminated sediments dominate the lake section. Presence of lacustrine deposits also suggests that neotectonic movements along the N-S fault were responsible for blocking the river and forming a lake. The uplifted eastern block led to the damming of the rivulet, Khokpa nala. Ensuing landslides facilitated the formation of a lake on the footwall

Table 1. Morphometric characters of Satluj river showing active nature.

River Basin	Basin Area Total (Km^2)	Basin Asymmetry (AF)	Topographic symmetry factor (T)	Valley Floor width Ratio (Vf)	Mean Height
Satluj River	1839	55.84	0.32	1.2	3118.3 m
			0.06		
			0.011	2.3	
			0.10		
			0.40	0.60	

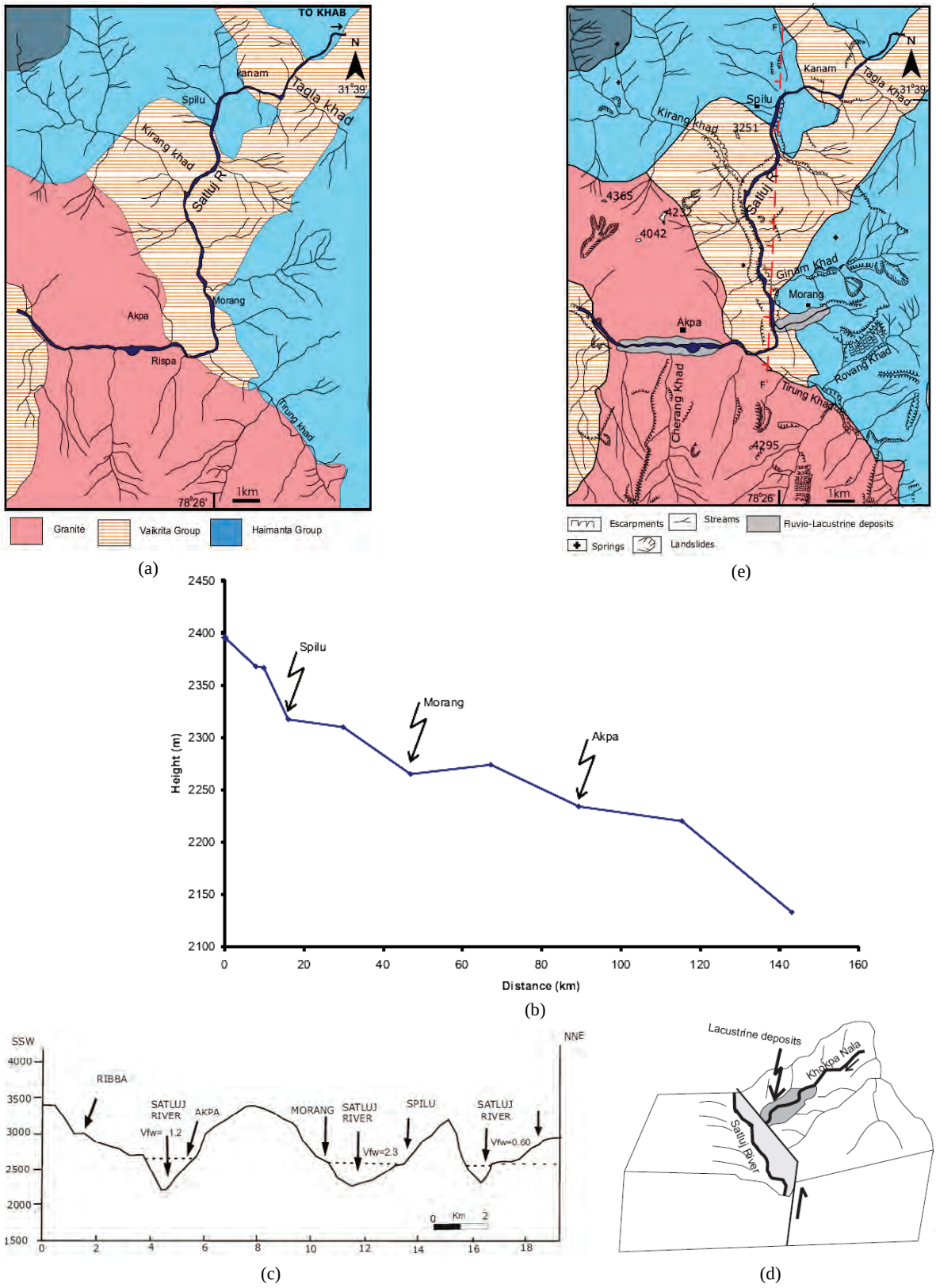

Figure 3. (a) Drainage map of the study area; (b) longitudinal profile of river Satluj in the study area; (c) cross valley profile of river Satluj in the study area; (d) hypothetical model showing lake formation in KCF zone; (e) geomorphological map of the study area.

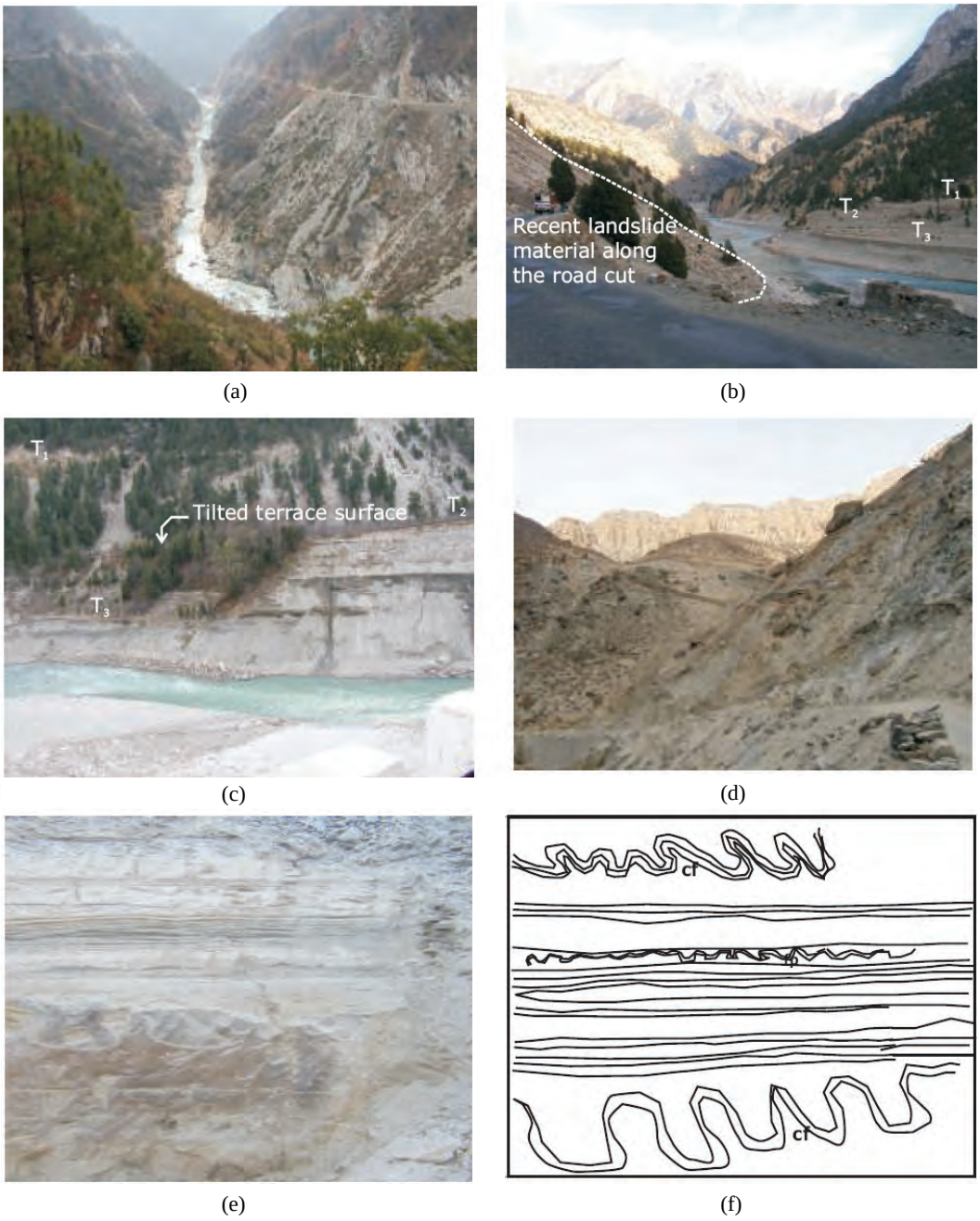

(a) (b) (c) (d) (e) (f)

Figure 4. (a) River Satluj flowing in a narrow valley from Spilu to Morang; (b)-(c) three levels of unpaired terraces formed by the river at Akpa, showing tilted surface; (d) recent landslide material; (e) fluvio lacustrine deposits at Morang; (f) sketch of deformation structure in the lacustrine profile.

block **Figure 3(d)**. At least five levels of deformation structures are exposed in the palaeolake profile at Morang **Figure 4(f)**.

6. Discussion

Kinnaur and Lahaul Spiti districts of Himachal Pradesh were severely rocked by a major earthquake of magnitude > 6.8 in 1975. The earthquake was associated with movements along a subvertical N-S trending normal fault named Kaurik-Chango fault. Luminescence chronology of seismites in Sumdo suggests that activation of Kaurik-Chango fault and seismic activity dates back to Late Pleistocene [15].

In the present area of investigation, a N-S lineament was observed along which river Satluj flows for a consi-

derable distance before getting deflected near Akpa. A number of neotectonic evidences which were gathered during the study testify to its active nature. Morphotectonic parameters such as Asymmetry Factor (AF) and Transverse topographic symmetry factor (T) as well as the field evidences suggest that the Satluj river basin is tilted. DEM of the area also shows the difference in elevation of the two blocks. Drainage analysis clearly displays the effect of tectonic rejuvenation. Blocking of Khokpa nala, a small rivulet took place due to fault movement leading to the formation of Morang palaeolake on the eastern block. Several levels of deformation structures have been observed in the fluvio-lacustrine profile at Morang. Similar structures are seen near Kaurik Chango fault in Sumdo and Leo. Presence of deformation structures in the Morang fluvio-lacustrine profile indicate that the area lies in the tectonically and seismically active zone and has experienced several pulses of intense seismic activity. Neotectonic indicators such as the uplifted terrain, unpaired terraces, fluvio-lacustrine deposits, deformation structures, alignment of springs and landslides in the fault zone are strong evidences of the active nature of the N-S fault in the study area.

7. Acknowledgements

The first and second authors are grateful to CSIR, New Delhi for providing financial support in the form of Research Associateship (9/428 (57) 2004-EMR-I) and Senior Research Fellowship (9.429(61)2K6-EMR1). Department of Geology, Kumaun University Nainital is acknowledged for providing facilities.

8. References

[1] A. Gansser, "The Geology of Himalaya," Wily Interscience, London, 1964, p. 289.

[2] T. Nakata, "Geomorphic History and Crustal Movements of the Himalayas," Institute of Geography Tohoku University, Sendai, 1972, p. 77.

[3] T. Nakata, O. Kenshiro and S. H. Khan, "Active Faults, Stress Field and Plate Motion along the Indo-Eurasian Plate Boundary," *Tectonophysics*, Vol. 181, No. 1-4, 1990, pp. 83-95.

[4] J. C. Atchinson, J. R. Ali and A. M. Davis, "When and Where did India and Asia Collide?" *Journal of Geophysical Research*, Vol. 112, 2007, pp. 1-19.

[5] H. H. Hayden, "The Geology of Spiti with Parts of Bushahr and Rupshu," *Geological Survey of India Memoir*, Vol. 6, 1904, pp. 1-121.

[6] V. J. Gupta and N. S. Virdi, "Geological Aspects of Kinnaur Earthquake, Himachal Pradesh," *Journal of Geological Society India*, Vol. 16, No. 4, 1975, pp. 512-514.

[7] O. N. Bhargava and U. K. Bassi, "Geology of Spiti-Kinnaur Himachal Himalaya," *Memoir Geological Survey of India*, Vol. 124, 1998, p. 212.

[8] O. N. Bhargava, R. N. Srivastava and S. K. Gadhoke, "The Proterozoic-Palaeozoic Spiti Sedimentary Basin," In: S. K. Tandon, C. Pant and S. M. Casshyon, Eds., *Sedimentary Basins of India*: *Tectonic Context*, Gyanodaya Prakashan, Nainital, 1991, pp. 236-260.

[9] K. N. Khattri, K. Rai, A. K. Jain, H. Sinvhal, V. K. Gaur and R. S. Mithal, "The Kinnaur Earthquake, Himachal Pradesh, India of 19th January 1975," *Tectonophysics*, Vol. 49, No. 1-2, 1978, pp. 1-21.

[10] S. Singh and A. K. Jain "Paleosiesmicity: Geological Evidences along the Kaurik-Chango Fault Zone and Other Related Areas in Lahaul-Spiti and Ladakh Himalaya," In: O. P. Varma, Ed., *Highlights in Earth Sciences DST's Spl. Vol.* 2 *on Seismicity*, International Geological Congress, 2001, pp. 205-225.

[11] O. N. Bhargava, S. S. Ameta, R. K. Gaur, S. Kumar, A. N. Agarawal, P. M. Jalote and M. L. Sadhu, "The Kinnaur (H.P., India) Earthquake of 19 January, 1975: Summary of Geoseismological Observations," *Bulletin of the Indian Geological Association*, Vol. 11, No. 1, 1978, pp. 39-53.

[12] T. N. Bagati, "Lithostratigraphy and Facies Variation in the Spiti Basin (Tethys), Himachal Pradesh," *Journal of Himalayan Geology*, Vol. 1, No. 1, 1990, pp. 35-47.

[13] A. K Jain and S. Singh, "Palaeoearthquakes along the Kaurik-Chango Fault Zone, Satluj-Spiti Valleys, Himachal Pradesh, India: Geological Evidence. Extended Abstract of Indo-US Workshop on Palaeoseismicity," WIHG, Dehradun, 1997, pp. 62-67.

[14] R. Mohindra and T. N. Bagati "Seismically Induced Soft Sediment Deformation Structures (Seismites) around Sumdo in the Lower Spiti Valley (Tethys Himalaya)," *Sedimentary Geology*, Vol. 101, No. 1, 1996, pp. 69-83.

[15] D. Banerjee, A. K. Singhvi, T. N. Bagati and R. Mohindra, "Luminescence Chronology of Seismites at Sumdo (Spiti Valley) Near Kaurik-Chango Fault, Northwestern Himalaya," *Current Science*, Vol. 73, No. 3, 1997, pp. 276-281.

[16] V. P. Sharma, "Geology of the Kullu-Rampur Belt, Himachal Pradesh," *Memoir Geological Survey of India*, Vol. 106, No. 2, 1976, pp. 235-403.

[17] A. P. Tiwari, R. K. Gaur and S. S. A. Ameta, "Note on the Geology of a Part of Kinnaur District, Himachal Pradesh. Him," *Geology*, Vol. 8, No. 1, 1978, pp. 574-582.

[18] U. K. Bassi and S. A. Chopra, "Contribution to the Geology of Kinnaur Himalaya, Himachal Pradesh," *International Journal of Earth Sciences*, Vol. 10, No. 1, 1983, pp. 96-99.

[19] S Srikantia and O. N. Bhargava, "Geology of Himachal Pradesh," *Geological Society of India*, 1998, p. 406.

[20] S. S. Ameta, "Some Observations on Geomorphology of Spiti Valley, Lahaul and Spiti distt. Himachal Pradesh," *Himalayan Geology*, Vol. 9, No. 2, 1997, pp. 646-656.

[21] C. A. Keller and N. Pinter, "Active Tectonics: Earthquake, Uplift and Landscape," Prentice Hall, New Jersey, 1996, p. 338.

[22] N. S. Virdi, G. Philip and S. Bhattacharya, "Neotectonic Activity in the Markanda and Bata River Basins, Himachal Pradesh, NW Himalaya: A morphotectonic Approach," *International Journal of Remote Sensing*, Vol. 27, No. 10, 2006, pp. 2093-2099.

[23] A. W. Burnett and S. A. Schumm, "Alluvial River Response to Teotectonic Deformation in Louisiana and Mississippi," *Science*, Vol. 222, No. 4619, 1983, pp. 49-50.

[24] S. Ouchi, "Response of Alluvial Rivers to Slow Active Tectonic Movement," *Geological Society of America Bulletin*, Vol. 96, No. 4, 1985, pp. 504- 515.

[25] D. I. Gregory and S. A. Schumm, "The Effect of Active Tectonics on Alluvial River Morphology," In: K. S. Richards, Ed., *River Channels*: *Environment and Process*, Blackwells, London, 1987, pp. 41-68.

[26] S. A. Schumm, J. F. Dumont and J. M. Holbrook, "Active Tectonics and Alluvial Rivers," Cambridge University Press, New York, 2000, p. 276.

[27] V. Jain and R. Shina, "Response of Active Tectonics on the Alluvial Bagmati River, Himalayan Foreland Basin, Eastern India," *Geomorphology*, Vol. 70, 2005, pp. 339-356.

[28] W. B. Bull and L. D. Mc. Fadden, "Tectonic Geomorphology North and South of Garlock Fault California," In: D. O. Doehring, Ed., *Geomorpholoy in Arid Regions*, *Proceedings of* 8th *Annual Geomorphology Symposium*, University of New York, Binghampton, 1977, pp. 115-137.

[29] L. Mayer, "Tectonic Geomorphology of Escarpments and Mountain Fronts," In: R. E. Wallace, Ed., *Active Tectonics*, National Research Council, Washington, D.C., 1985, pp. 125-135.

Journal of Geographic Information System, **2010, 2, 177-184**
doi:10.4236/jgis.2010.23025 Published Online July 2010 (http://www.SciRP.org/journal/jgis)

Geospatial Mapping of Singhbhum Shear Zone (SSZ) with Respect to Mineral Prospecting

Bijay Singh, Jimly Dowerah
University Department of Geology, Ranchi University, Ranchi, India
E-mail: *bsingh*6029*@gmail.com, jdowerah@gmail.com*
Received January 19, 2010; *revised February* 25, 2010; *accepted March* 2, 2010

Abstract

Singhbhum Shear Zone is a highly mineralized zone having variety of minerals, predominantly those of uranium, copper and some sulphide minerals. From Remote Sensing data it is possible to decipher the regional lithology, tectonic fabric and also the geomorphic details of a terrain which aid precisely in targeting of metals and minerals. Mapping of mineralized zones can be done using Geospatial Technology in a GIS platform. The present study includes creation of various maps like lithological map, geomorphological map, contours and slope map using satellite data like IRS LISS-IV and ASTER DEM which can be used to interprete and correlate the various mineral prospective zones in the study area. Even the alterations of the prevalent mineral zones can be mapped for further utilization strategies. The present work is based on the investigations being carried under ISRO-SAC Respond Project (Dept. of Space, Govt. of India SAC Code: OGP62, ISRO Code: 10/4/556).

Keywords: Singhbhum Shear Zone, Geospatial Mapping, Mineral Prospecting, Alterations, Sulphide Ores

1. Introduction

Mineral Exploration is not only highly imaginative and creative but a very costly activity as well. Much information about potential areas for mineral exploration can be provided by interpretation of surface features on aerial photographs and satellite images (Lilesand et al, 2007). From Remote Sensing data it is possible to decipher the regional lithology, tectonic fabric and also the geomorphic details of a terrain which aid precisely in targeting of metals and minerals. Usage of Geospatial Technology has enhanced the study of mineral exploration as geological maps can be easily integrated with other important details like geomorphology, structure, geophysical data etc.

Multispectral image analysis technique in the field of Geologic remote sensing has proved to be a potential technique for the information extraction process. Number of image analysis techniques are evolved and applied for optimization of information extraction process.

SSZ represents one of the most spectacular tectonic features is occurring in the Singhbhum Craton spread over Jharkhand and adjoining areas, marks the boundary between the two Archaean Cratons of Singhbhum Granite Batholith and the Iron Ore Group and the Proterozoic Mobile Belt in the north. SSZ is an arcuate belt of 200 km length and width varying between 1-25 kms. It is one of the most well known mineral abundant zones in the country and extensive mineral exploration has been carried out in this zone since a long time. The Central Indian Suture or the Satpura Mobile Belt continues across the Mahanadi fault to form the Northern Boundary of the Singhbhum craton. The mobile belt bends around the craton to merge with the Eastern Ghats Mobile Belt in the south. The latter overthrusts the Singhbhum craton at the Sukhinda thrust.

The study area falls in the SSZ and is extended between Tatanagar (22° 50' N: 86° 10' E) and Bahragora (22° 16' N: 86° 43' E) in the south east falling mostly in the Survey of India Toposheet no. J/2, 6, 7, 10 and 11, confined in the East Singhbhum of Jharkhand (**Figure 1**). The present work involves geospatial mapping of the study area on a GIS platform by interpreting multispectral satellite imagery.

2. Geological Setting

SSZ is a unique arcuate structure extending from Bahragora in east to Porahat in west. At the extreme west end it grades into high angle fault and extends upto the western margin of Bonai granite. Satellite imagery study sho-

ws that beyond Bahragora in east, the arcuate southern continuation of the shear zone extends through Mayurbhanj to Sukinda thrust (Ramakrishnan and Vaidyanathan, 2008). The shear zone is characterized by extreme ductile shearing, multiple metasomatism, migmatisation and prominent mineralization of copper, uranium, tungsten and phosphate. The bulk of the shear zone material is made up of pelites and volcanic clastics, probably generated during the Dhanjori and Koira depositional cycles. The shear zone is also characterized by abundance of ultramafic intrusions such as hornblende schists, talc schists, serpentinite and synkinematic body of serpentinised lherzolite with pyroxinite relics. The deformational history of this shear zone is highly complex marked by repeated phases of folding, mylonitisation and rotation of fabric (**Figure 2**).

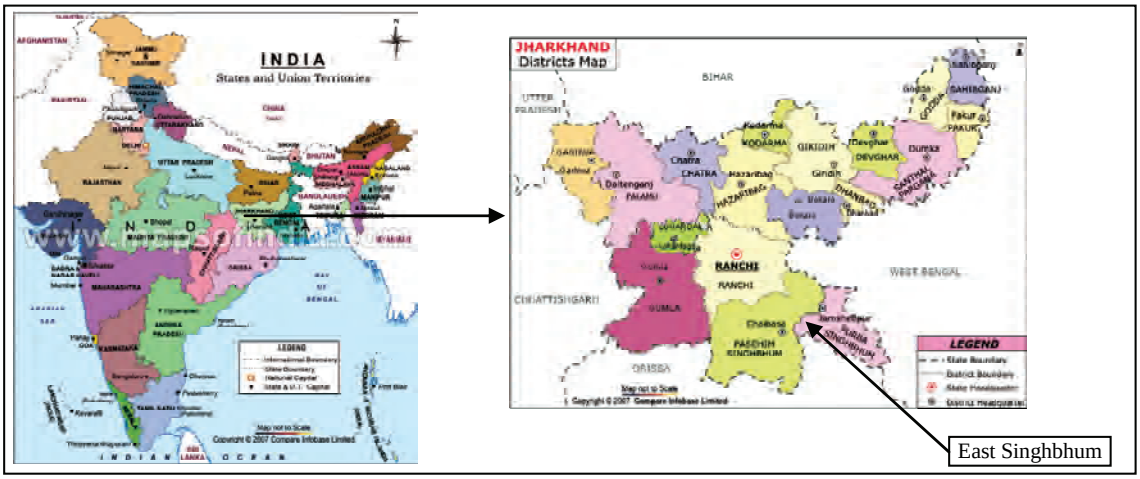

Figure 1. Location map.

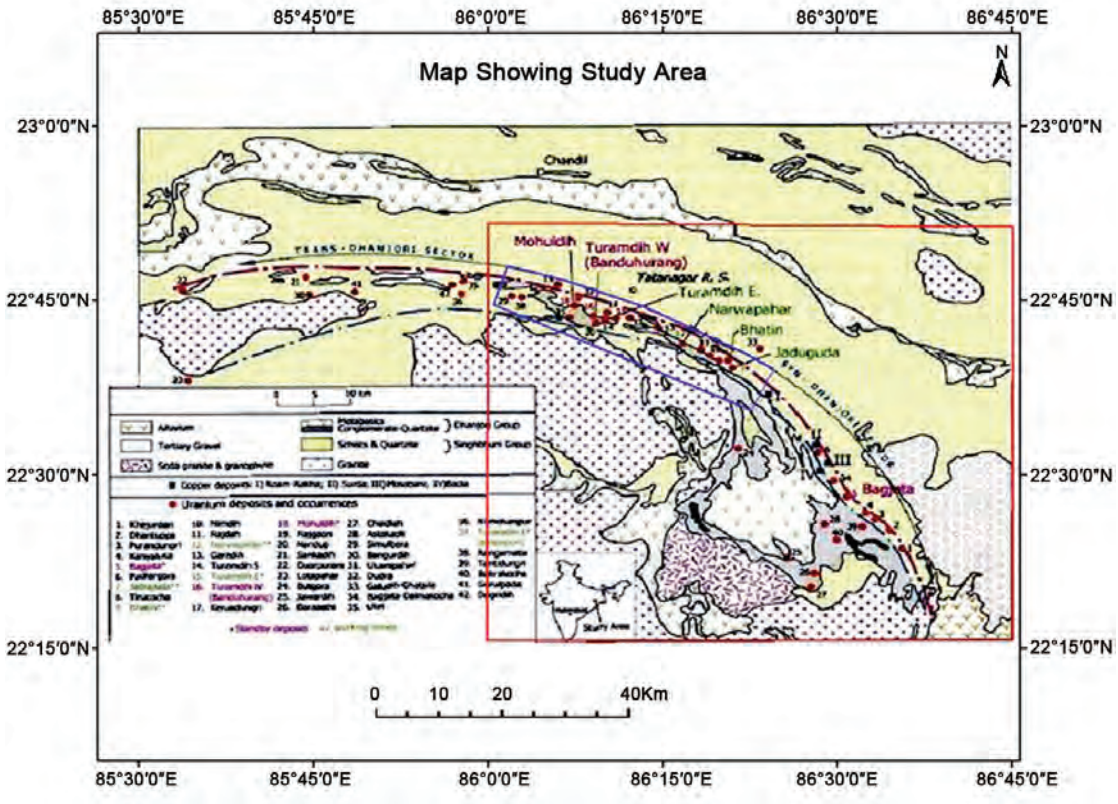

Figure 2. Geological map of Singhbhum shear zone (source: www.dae.gov.in/amd/regions).

3. Materials and Methods

Data used: (see **Table 1**)

1) IRS LISS IV
2) ASTER DEM
3) Survey of India Toposheets

Software used:

1) ERDAS IMAGINE
2) Arc GIS 9.3

The methodology used in the present study in shown in the following Flow **Figure 3**.

Table 1. Specifications of LISS IV.

Ground Resolution	5.8 m
Steerability	Yes
Swath	23.5 km (MX),70 km (MONO)
Spectral Bands	B_2(green, 520-570 nm), B_3(red, 630-700 nm), B_4(NIR, 700 nm-1400 nm)
Radiometric Resolution(Bits)	7 bits selected out of 10
IGFOV	5.8 m
SNR@Saturation	>128
SWR@Nyquist	>20 all bands
Off Nadir Viewing	+/–26°

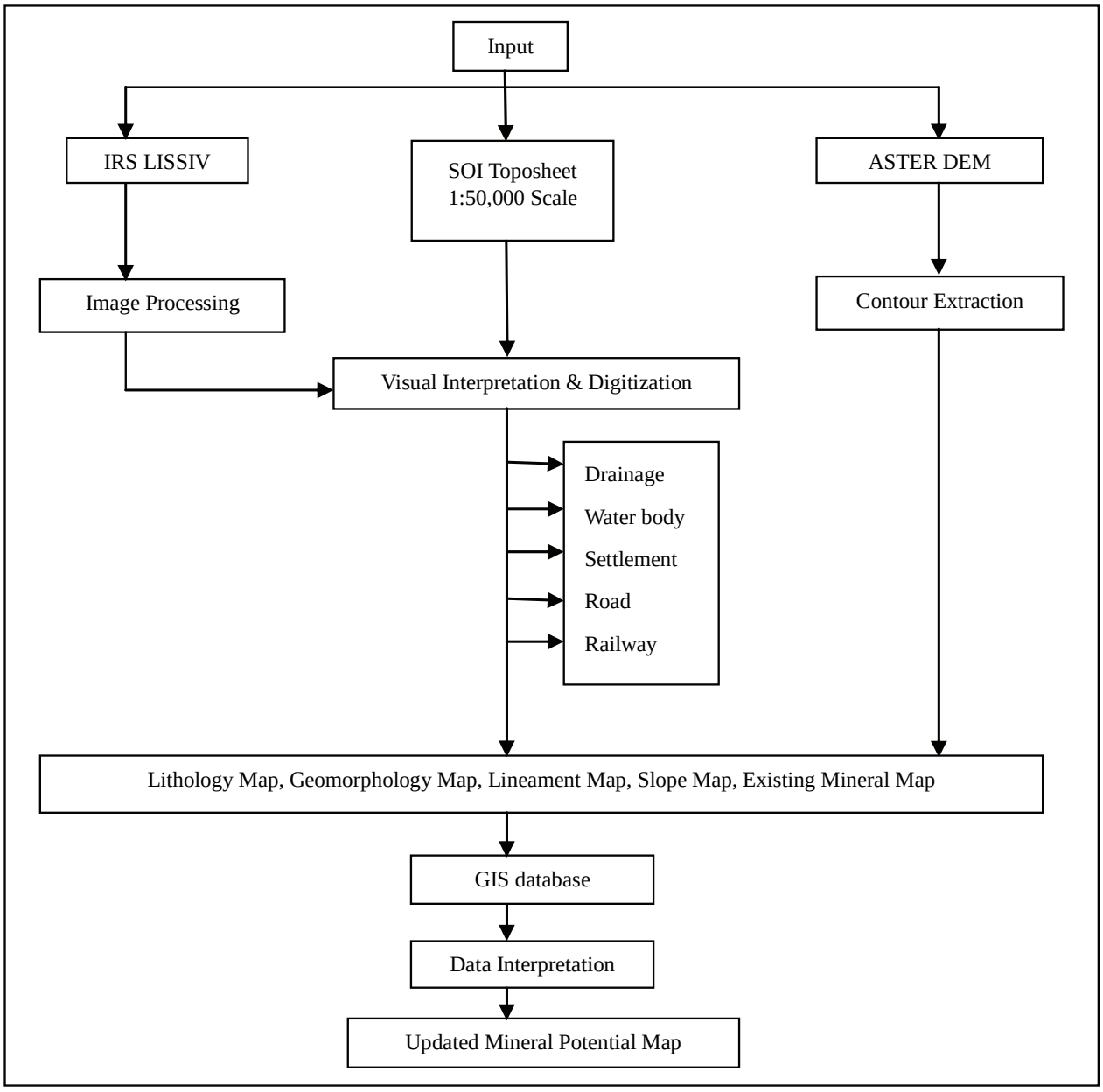

Figure 3. Flowchart showing methodology.

4. Generation of Maps

The capability of GIS to manipulate classified spatial information through amalgamated layers makes it a unique tool for delineating potential locales. Flexibility of experimenting with spatial data followed by visualization of its effect immediately gives GIS a cutting edge over other contemporary techniques for modeling mineral deposits. For the preparation of GIS map, the data sets are grouped into polygon, line and point features depending upon the geographic distribution. The areas having aerial extent are taken as polygon layers; line features are digitized as line coverages.

In the present study, apart from the base map of the study area, Drainage map was prepared with the help of the LISS IV data (**Figure 4**). The contour lines at 50 m intervals were extracted from the ASTER DEM and the slope map (**Figure 7**) of the area was generated from it. The Geomorphological units were interpreted from the LISS IV imagery after processing the imagery and then with the help of the image interpretation keys like tone, texture, pattern, association and by relating to the lithology and height information of that particular area..

5. Geomorphology

Geomorphology serves as an excellent tool in economic geological point of view and aim in search of mineral deposits, the topographic expression gives clue to the geologic structure which is favourable for mineral deposits and indirect inference of geomorphic details of an area. It includes surface expression of the ore bodies like ridges, plateaus or some elevated position, which are indications of gossans and residual mineral occurring in weathering surface. Geomorphology not only gives the pattern and the spatial distribution of various landforms but also gives information on the natural resource potential. Such maps are graphic representation of landforms of an area. For mineral exploration, the geomorphic features are important in prospecting; the deposits formed by residual

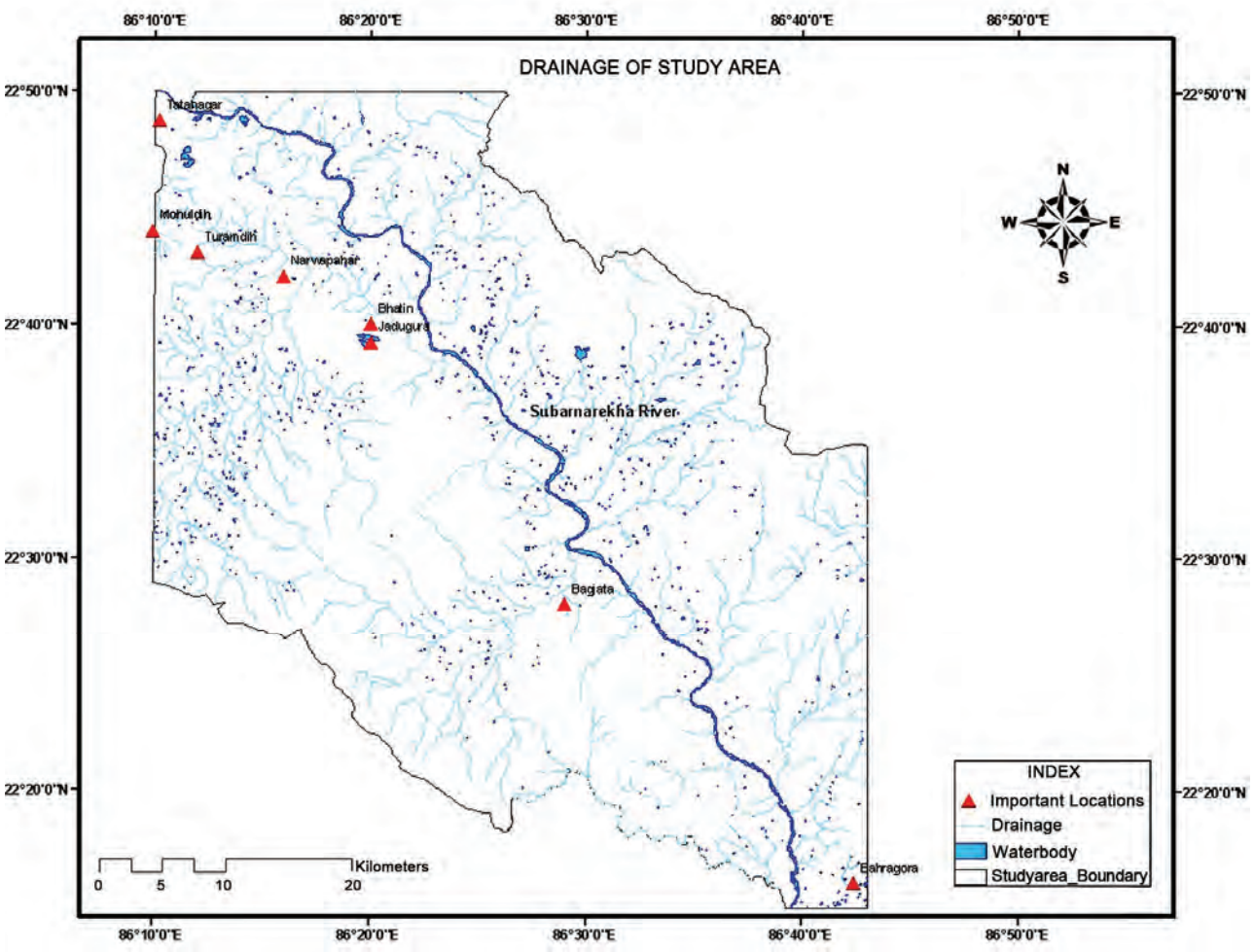

Figure 4. Drainage map of the study area.

and supergene enrichment can be indicated. (E.g. hill slopes, ridges, plateaus and valleys etc) Alluvial plain, denudational hill, intermontane valley, pediment-inselberg complex, pediplain, pediment, undissected plateau, residual hill, structural hill, valley fill, water body and river sand make up the geomorphology of the study area. Pediplain covers 49.51% *i.e.* the majority of the area whereas least area is covered by undissected plateau (0.28%). The Shear Zone is mainly covered by structural hill with intermontane valley in between and pediment and pediplain adjacent to it (**Figure 5**).

6. Lithology

Lithological maps can be easily integrated with other important details like geomorphology, structure, etc. This kind of data integration facilitates for the better identification of mineralized zones. The lithology of the study area is made up of talc-chlorite schists, phyllite, granite, quartzite, migmatite, mica-schist, laterite, hornblende schist, dolerite, epidiorite, gabbro anthracite, sandstone and alluvium. Mica/ Hornblende Schist with Phyllite bands occupy the largest area with 15.34% whereas sand/silt dominant alluvium covers the least area with 0.36%.The lithology in the Shear Zone is mainly of Quartzite and Mica schist with phyllite adjacent to it (**Figure 6**).

7. DEM

DEM is created and the same is wrapped with digital FCC data. It gives a 3D view (**Figure 8**) of the landscape from which precise mapping can be interpreted perfectly. DEM wrapped various thematic layers can be used to prepare probable mineralized zones.

8. Identification of Potential Mineralized Zones

Mineral Resource Potential Mapping is a very complex analytical procedure which requires simultaneous consideration of a number of spatial evidences-geological, geomorphological, structural etc. In the present study, geomorphology and lithology has been mapped and observations have been made based on it. As quartzite dominates the lithology of the Shear Zone, it can be said that the area contains zircon, rutile as minerals. Zircon is known to contain uranium and rutile is mainly composed of titanium. Natural rutile also contains significant amount of niobium and tantalum. The presence of phyllite in the shear zone indicates quartz, sericite content. Sericite is a common alteration mineral of orthoclase or plagioclase feldspars in areas that have been subjected to hydrothermal alteration typically associated with copper, tin, or other hydrothermal ore deposits.

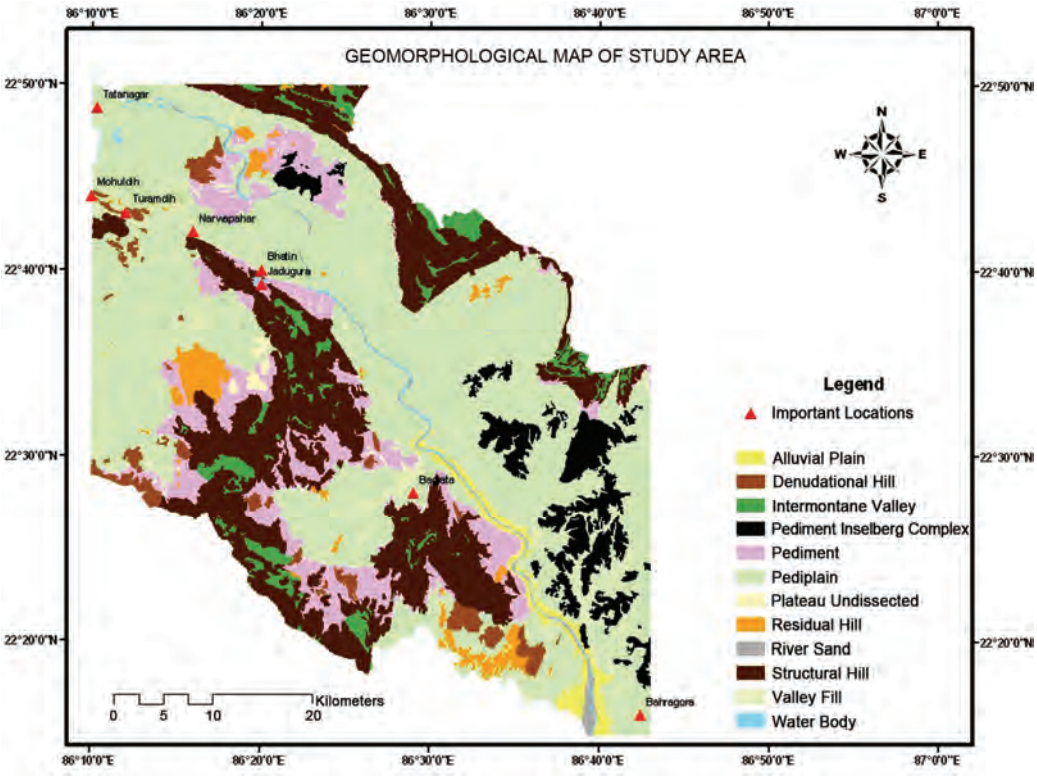

Figure 5. Geomorphological map of the study area.

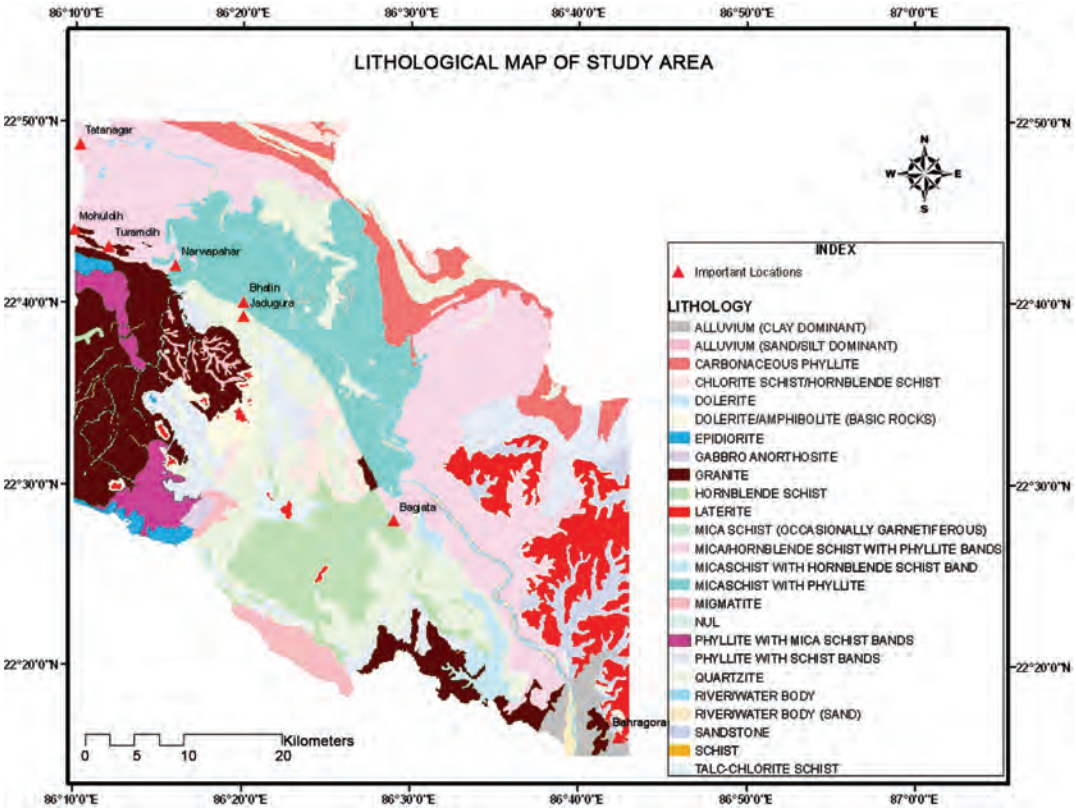

Figure 6. Lithological map of study area,

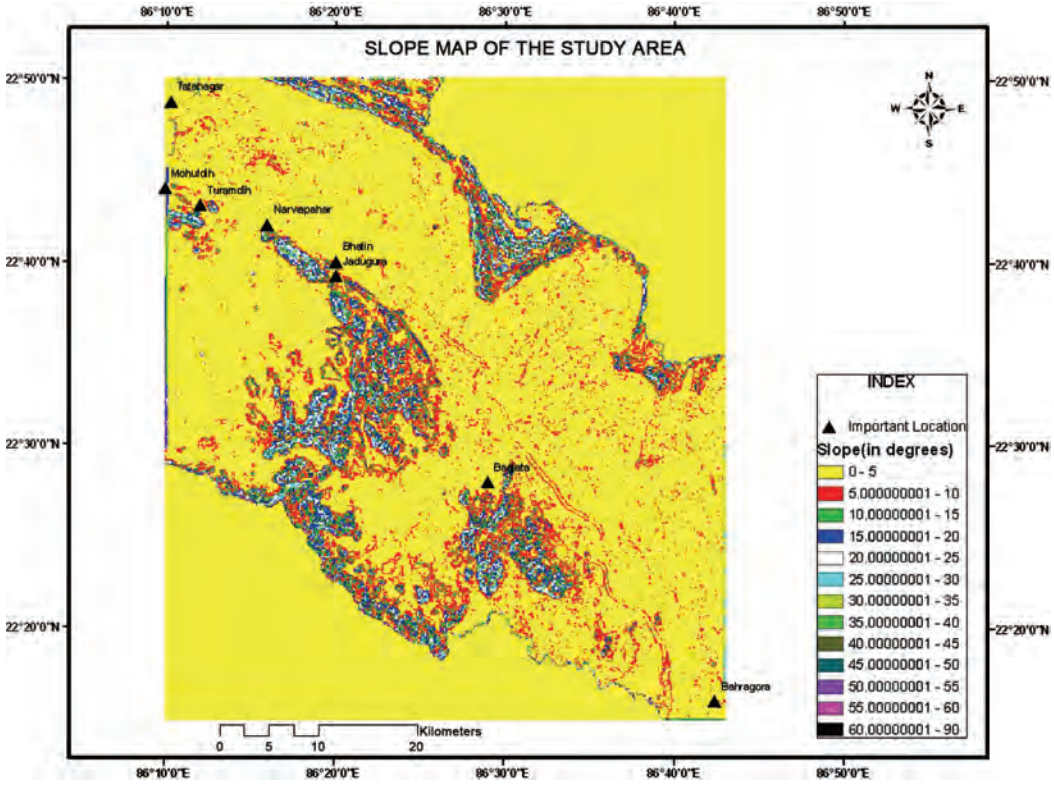

Figure 7. Slope map of the study area.

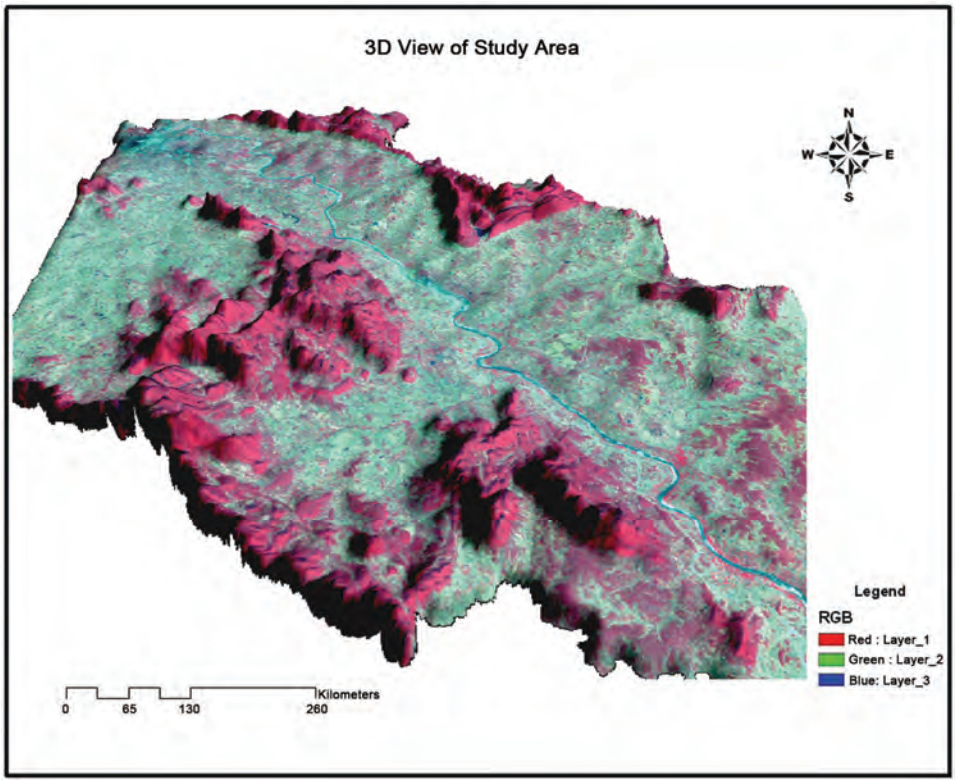

Figure 8. 3D view of study area.

The probability of occurrence of minerals as mentioned above is based on the lithology and related geomorphology. Further studies based on alteration zone, lineament mapping will make it more specific as lineaments can help to spot the location of mineral abundance and so can alteration zones.

9. Summary and Conclusions

Geospatial Mapping for complex regions like Singhbhum Shear Zone is an important activity since it involves a detailed information database through the satellite based studies. These informations have to be generated for an integrated regional development approach for this strategic location. Presently the LISS-IV imagery has been utilized to prepare an updated host of geological maps like geomorphology, slope, drainage, base map. The drainage pattern of the area provides clue about the bedrock lithology, topography and the types of landform present. In the present area, the drainage pattern is seen to be dendritic. The delineation of geomorphological units suggest that the landform class in the study region is that of landform developed on folded strata whereas the adjacent areas have a fluvial landform (after landform classification by Rasher and Weaver, 1990). Due to a hostile and inaccessible area these maps are highly useful for further investigations and interpretations to be used by the mining industries especially Uranium Corporation of India Limited (UCIL), Indian Copper Complex (ICC) for their optimum utilization and the Government and NGOs to take advantage for their need based planning and programmes. The various geomorphological units and their features are attempted to delineate the adjacent viable mining areas and their potential estimation. The factors responsible for contamination of the local water bodies with the radiogenic environment and their side effects are also being investigated on the basis of these maps.

10. Acknowledgements

The authors wish to acknowledge the Head of the Dept. of Geology, Ranchi University for his support and motivation. Dr. A. T. Jeyaseelan, Director, JSAC is sincerely acknowledged for his kind permission to avail the lab facilities at JSAC under his guidance. The Focal Person of the ISRO-SAC RESPOND Project (SAC code: 0GP62, ISRO code: 10/4/556) is also gratefully acknowledged for his motivation and academic comments.

11. References

[1] T. S. Balakrishnan, P. Unnikrishnan and A. V. S. Murty, "The Tectonic Map of India and Contiguous Areas,"

Journal of the Geological Society of India, Vol. 74, 2009, pp. 158-170.

[2] T. K. Bhattacharya, A. V. Sankaran and S. R. Shivananda, "Observations on Uranium Mineralization in Jaduguda and Other Places of Singhbhum Thrust Belt," *Symposium on Uranium Prospect in India*, Jaduguda Mines Project, Bihar, 1996, pp. 78-88.

[3] J. A. Dunn, "The Geology of North Singhbhum including Parts of Ranchi and Manbhum Districts," *Memoir Geological Survey of India*, Vol. 54, No. 2, 1929, pp. 1-166.

[4] J. A. Dunn and A. K. Dey, "Geology and Petrology of Eastern Singhbhum and Surrounding Areas," *Memoir Geological Survey of India*, Vol. 69, No. 2, 1942, pp. 281-456.

[5] T. M. Lillesand and R. W. Kiefer, "Remote Sensing and Image Interpretation," 6th Edition, John Wiley & Sons, New York, 2007, pp.10-15.

[6] S. Mishra, "Precambrian Chronostratigraphic Growth of Singhbhum Orissa Craton, Eastern Indian Shield: An Alternative Model," *Journal of the Geological Society of India*, Vol. 67, 2006, pp. 356-378

[7] B. Mukhopadhyay, N. Hazra, S. R. Sengupta and S. K. Das, "Mineral Potential Map by Knowledge Driven GIS Modeling: An Example from Singhbhum Copper Belt, Jharkhand". http://www.gisdevelopment.net/Application/Geology

[8] D. Mukhopadhyay and G. K. Deb, "Structural and Textural Development in Singhbhum Shear Zone, Eastern India," *Proceedings of the Indian Academy of Sciences*, Vol. 104, No. 3, 1995, pp. 385-408.

[9] S. Rajendran, *et al*. (Eds.) "Mineral Exploration: Recent Strategies," New India Publishing Agency, New Delhi, 2007, pp. 49-61.

[10] M. Ramakrishnan and R. Vaidyanathan, "Geology of India," Geological Society of India, Bangalore, Vol. 1, 2008, pp. 232-233.

[11] B. Singh and J. Dowerah, "RS-GIS Based Strategies for Mineral Targetting in Parts of Singhbhum Shear Zone, Jharkhand," Vistas in Geological Research U. U. Spl. Publ. in Geology Vol. 8, 2009, pp. 81-86.

[12] K. K. Sinha, N. K. Rao, V. L. Saha and T. S. Sunilkumar, "Stratigraphic Succession of Precambrian of Singhbhum: Evidence from Quartz-Pebble-Conglomerate," *Journal of the Geological Society of India*, Vol. 49, 1997, pp. 577-588.

Journal of Geographic Information System (JGIS)

ISSN 2151-1950 (print) ISSN 2151-1969 (online)

http://www.scirp.org/journal/jgis/

Journal of Geographic Information System (JGIS) is a comprehensive international academic theory journal associated published by Zondy Cyber Group and SRP (Scientific Research Publishing) Inc.
The goal of this journal is to provide an international platform for engineers and academicians all over the world to promote, share, and discuss various new issues and developments in relevant GIS fields.

Subject Coverage

- Cartography and Geodesy
- Computational Geometry
- Computer Vision Applications in GIS
- Distributed, Parallel, and GPU algorithms for GIS
- Earth Observation
- Geographic Information Retrieval
- Human Computer Interaction and Visualization
- Image and Video Understanding
- Location-based Services
- Location Privacy, Data Sharing and Security
- Performance Evaluation
- Photogrammetry
- Similarity Searching
- Spatial Analysis and Integration
- Spatial and Spatio-temporal Information Acquisition
- Spatial Data Mining and Knowledge Discovery
- Spatial Data Quality and Uncertainty
- Spatial Data Structures and Algorithms
- Spatial Data Warehousing, OLAP, and Decision Support
- Spatial Information and Society
- Spatial Modeling and Reasoning
- Spatial Query Processing and Optimization
- Spatio-temporal Data Handling
- Spatio-temporal Sensor Networks
- Spatio-temporal Stream Processing
- Spatio-textual Searching
- Standardization and Interoperability for GIS
- Storage and Indexing
- Systems, Architectures and Middleware for GIS
- Traffic Telematics
- Transportation
- Urban and Environmental Planning
- Visual Languages and Querying
- Wireless, Web, and Real-time Applications

Notes for Intending Authors

Submitted papers should not have been previously published nor be currently under consideration for publication elsewhere. Paper submission will be handled electronically through the JGIS online system.
All papers are refereed through a peer review process.
For more details about the submissions, please access the website.

Website and E-Mail

Website: **http://www.scirp.org/journal/jgis** E-Mail: **jgis@scirp.org**

Journal of Geographic Information System, **2010, 2, 129-184**
Published Online July 2010 in SciRes (http://www.scirp.org/journal/jgis).

TABLE OF CONTENTS

Volume 2 Number 3 July 2010

ISSN: 2151-1950